NEUROFIBROMIN, NERVE GROWTH FACTOR AND RAS: THEIR ROLES IN CONTROLLING THE EXCITABILITY OF MOUSE SENSORY NEURONS

Yue Wang

Submitted to the faculty of the University Graduate School
in partial fulfillment of the requirements
for the degree
Doctor of Philosophy
in the Department of Pharmacology and Toxicology,
Indiana University

December 2006

Accepted by the Faculty of Indiana University, in partial
fulfillment of the requirements for the degree of Doctor of Philosophy.

Grant D. Nicol, Ph.D, Chair

Michael R. Vasko, Ph.D.

Doctoral Committee

D. Wade Clapp, M.D.

October 9, 2006

Theodore R. Cummins, Ph.D.

DEDICATION

To my parents, Yashan Xing and Honghe Wang, and my husband, Yunlong Liu,

for their unconditional love and support throughout all the years.

ACKNOWLEDGEMENTS

I would like to express my gratitude to all those who gave me the possibility to complete this thesis.

I am greatly indebted to my supervisor, Dr. Grant D. Nicol, for his help, guidance, stimulating suggestions and encouragement, as well as always steering me in the right direction without being too pushing…throughout my research and writing of this thesis. Thank you for showing the way how to become an independent scientist and to learn from "an unfortunate event" for future success. There is no way to return the gift you have given to me. The only thing I can do is to pass them on…

I would like to thank Dr. Michael R. Vasko, Theodore R. Cummins and D. Wade Clapp for their time as members of my graduate committee and for their advices throughout the course of my study. In particular, I would like to thank Dr. Cynthia Hingtgen, who has been crucial to my research as well as scientific writing. Her dedication and support are indescribable.

I would like to acknowledge Dr. Xianxuan Chi, Yihong Zhang and Shannon Roy, who are currently working in Dr. Nicol's or Dr. Hingtgen's laboratory, for all their help, support and valuable comments.

I want to thank Amy Lawson and Lisa King in the Department of Pharmacology and Toxicology for coordinating my Ph.D. studies and preparing for this thesis.

I am deeply grateful to my parents for their unconditional love, caring and support. They are always a source of strength in all moments of need.

To my husband, thank you for being my happiness and sunshine everyday. Without your love, encouragement and unconditional support, I could not have come this far.

ABSTRACT

Yue Wang

Neurofibromin, nerve growth factor and Ras: their roles in controlling the excitability of mouse sensory neurons

Neurofibromin, the product of the *Nf1* gene, is a guanosine triphosphatase activating protein (GAP) for p21ras (Ras) that accelerates the conversion of active Ras-GTP to inactive Ras-GDP. It is likely that sensory neurons with reduced levels of neurofibromin have augmented Ras-GTP activity. In a mouse model with a heterozygous mutation of the *Nf1* gene (*Nf1*+/-), the patch-clamp recording technique is used to investigate the role of neurofibromin in controlling the state of neuronal excitability. Sensory neurons isolated from adult *Nf1*+/- mice generate more APs in response to a ramp of depolarizing current compared to *Nf1*+/+ mice. In order to elucidate whether the activation of Ras underlies this augmented excitability, sensory neurons are exposed to nerve growth factor (NGF) that activates Ras. In *Nf1*+/+ neurons, exposure to NGF increases the production of APs. To examine whether activation of Ras contributes to the NGF-induced sensitization in *Nf1*+/+ neurons, an antibody that neutralizes Ras activity is internally perfused into neurons. The NGF-mediated augmentation of excitability is suppressed by the Ras-blocking antibody in *Nf1*+/+ neurons, suggesting the NGF-induced sensitization in *Nf1*+/+ neurons depends on the activation of Ras. Surprisingly, the excitability of *Nf1*+/- neurons is not altered by the blocking antibody, suggesting that this enhanced excitability may depend on

previous activation of downstream effectors of Ras. To determine the mechanism giving rise to augmented excitability of *Nf1+/-* neurons, isolated membrane currents are examined. Consistent with the enhanced excitability of *Nf1+/-* neurons, the peak current density of tetrodotoxin-resistant (TTX-R) and TTX-sensitive (TTX-S) sodium currents (INa) are significantly larger than in *Nf1+/+* neurons. Although the voltage for half-maximal activation ($V_{0.5}$) is not different, there is a significant depolarizing shift in the $V_{0.5}$ for steady-state inactivation of INa in *Nf1+/-* neurons. In summary, these results demonstrate that the enhanced production of APs in *Nf1+/-* neurons results from a larger current amplitude and a depolarized voltage dependence of steady-state inactivation of INa that leads to more sodium channels being available for the subsequent firing of APs. My investigation supports the idea that regulation of channels by the Ras cascade is an important determinant of neuronal excitability.

Grant D. Nicol, Ph.D, Chair

TABLE OF CONTENTS

LIST OF TABLES

LIST OF FIGURES

LIST OF ABBREVIATIONS

ANOVA	Analysis Of Variance
AP	AP
BDNF	Brain-Derived Neurotrophic Factor
CGRP	Calcitonin Gene-Related Peptide
DRG	Dorsal Root Ganglion
DAG	diacylglycerol
ERK1/2	Extracellular signal-Regulated protein Kinase
GAP	Guanosine triphosphatase Activating Protein
EPSP	excitatory post-synaptic potentials
IB4	plant lectin Isolectin B4
Ikir	Inward-rectifying potassium currents
IP3	inositol 1,4,5-trisphosphate
IK	Potassium currents
INa	Sodium currents
JNK/SAPK	c-Jun N-terminal Kinase/Stress-Activated Protein Kinase
MAPK	Mitogen-Activated Protein Kinase
MEK	Mitogen-Activated Protein Kinase Kinase
MPL	Methyl-2-Pyrrolidinone
NF1	Neurofibromatosis type 1
NGF	Nerve Growth Factor
NMG	N-Methyl-Glucamine
p75 NTR, p75	p75 Neurotrophin Receptor
PDK-1	3'-Phosphoinositide-Dependent Kinase-1
PDK-2	3'-Phosphoinositide-Dependent Kinase-2
PI-3K	Phosphatidylinositol 3-Kinase
PIP2	phosphatidylinositol-4,5-bisphosphate
PKA	Protein Kinase A
PKC	Protein Kinase C
PLC	phosphoinositide-specific phospholipase C
Ras	p21Ras
REM	Resting Membrane Potential
S1P	Sphingosine-1-Phospate
SCF	Stem Cell Factors
SEM	Standard Error of the Mean
SM	Sphingomyelin
SMase	Sphingomyelinase
SNL	Spinal Nerve Ligation
SP	Substance P

Sph	Sphingosine
TEA	tetraethylammonium
TNF	Tumor Necrosis Factor
TRPV1	Vanilloid Receptor Type 1
TTX	Tetrodotoxin

I. INTRODUCTION

Overview

Neurofibromatosis type 1 (NF1) is a common genetic disorder characterized by formation of tumors (Lakkis and Tennekoon, 2000). Many people with NF1 exhibit an exaggerated painful response to stimuli that elicit only slight discomfort in normal people (Creange et al., 1999; Wolkenstein et al., 2001). The origins of this painful sensation are not understood, and there is no effective treatment. The perception of pain starts from the activation of the peripheral endings of special nerve cells, known as nociceptors (specific sensory neurons that initiate the signaling pathway that leads to the perception of pain). The peripheral activation of these nociceptors generates action potentials (APs) and the subsequent release of neurotransmitters, such as glutamate, substance P (SP) and calcitonin gene-related peptide (CGRP). These released neurotransmitters generate excitatory post-synaptic potentials (EPSP) in the dorsal horn neurons by which the pain signals are relayed to the thalamus and cerebrum where the pain is localized and fully realized. Under some pathological conditions, such as inflammation and neuropathic pain, there is an increase of pain perception (hyperalgesia) that is caused, at least in part, by a reduction of the threshold for activation of nociceptors (peripheral sensitization). The abnormal painful sensation in people with NF1 may suggest an enhanced sensitivity of sensory neurons in the dorsal root ganglion (DRG). The work presented in this thesis mainly focuses on sensory neurons and to examine the alterations in the firing of APs of neurons with a heterozygous mutation of the *Nf1*

gene (*Nf1+/-*) isolated from a mouse model of NF1. NF1 results from a heterozygous mutation (*NF1+/-*) in the *NF1* gene. Because *NF1+/-* neurons have only one functional copy the *NF1* gene, the protein product of the *NF1* gene, neurofibromin, should be lower. Neurofibromin increases the intrinsic GTPase activity of Ras (Ras-GTP, active form), thereby accelerates the hydrolysis of GTP from active Ras (Martin et al., 1990). A decrease in the level of neurofibromin frequently results in an increase of Ras-GTP level (Guha et al., 1996; Ingram et al., 2001; Klesse and Parada, 1998). Therefore, in *Nf1+/-* neurons, the level of Ras-GTP could be higher than in wild-type (*Nf1+/+)* neurons.

One of the principle aims in this thesis is to determine whether *Nf1+/-* neurons have enhanced neuronal firing and support the idea that the augmentation of intracellular Ras-GTP level correlates with increased neuronal excitability (neurons have enhanced ability to generate APs, and transmits much stronger signals of pain to the brain). The basic understanding of these mechanisms underlying the sensitization of nociceptors could lead to more effective treatment of the exaggerated painful condition associated with NF1 or other chronic painful conditions that arise from other ailments.

A. Sensory neurons and ion channels

Peripheral sensory neurons are nerve cells responsible for converting external stimuli, such as mechanical, thermal and chemical noxious information, into internal electrical signals like APs. In complex organisms, when APs travel to the presynaptic membrane of DRG fibers in spinal cord, the rapid

depolarization of the membrane potential opens voltage-gated calcium channels and facilitates the influx of calcium ions that stimulate the release of neurotransmitters from the nerve terminal (Hawkins et al., 1983). These released neurotransmitters generate EPSP in the dorsal horn neurons by which the pain signals are relayed to the thalamus and cerebrum where the pain is localized and fully realized. These sensory neurons vary in size, specialization of endings, the degree of myelination around the axon, as well as the expression of different channels and receptors in the neuronal membrane. These variations enable sensory neurons to propagate APs at various conduction velocities and detect multiple environmental stimuli.

Neuronal sensitization is defined as a process of enhanced responses of a neuron to a given stimulation. These responses include a decrease of the firing threshold for generating an AP, an increase of the numbers of APs in response to the same electrical stimuli and/or an increase in the release of neuronal transmitters, such as substance P (SP) and calcitonin gene-related peptide (CGRP) from sensory neurons. A major focus of our laboratory has been to elucidate the electrical events and signaling pathways involved in neuronal sensitization, especially on the subset of sensory neurons thought to be involved in the transmission for signals of pain to the brain. This subset of neurons is smaller in size, extends axons that are either lightly myelinated (Aδ) or unmyelinated (C), and has lower conduction velocities (the conduction velocity of Aδ fiber is 2.2-8.0 m/s, whereas the conduction velocity of C fiber is less than 1.4 m/s) (Harper and Lawson, 1985).

The generation of APs by sensory neurons relies on the activity of ion channels, the pore-forming proteins, located across the neuronal membrane. Based on their properties of activation, ion channels can be classified as voltage-gated, ligand-gated, or stretch-gated channels. Channels can either open or close upon changing of the membrane voltage (voltage-gated channels), the binding of a specific ligand (ligand-gated channels), mechanical forces (stretch-gated channels) as well as temperature (heat or cold responsive channels). The opening of ion channels allows the passage of specific ions and thereby changes the transmembrane potential and underlies the generation of APs. An AP can be roughly divided into three separate phases, the rising phase (depolarization), the falling phase (repolarization) and the recovery phase. During the rising phase of the AP, the sodium channels open, which allows positively-charged sodium ions to enter cells and depolarize the membrane potential. After the depolarization of membrane potential reaches its peak, sodium channels are inactivated and potassium channels are open. Both the closing of the sodium channels and the opening of potassium channels lead to the repolarization of membrane potential back to the resting membrane potential (REM). The propagation of APs along the cell membrane carries fast internal messages that trigger many downstream cellular activities, such as the secretion of hormones from glands and the release of neurotransmitters. Since APs are such an essential feature in life, the regulation of channel activity that is critical in generating APs, such as potassium channels and sodium channels, has a significant influence on neuronal excitability and many other physiological functions of the cell.

1. Voltage-gated potassium channels in sensory neurons and their influence on neuronal excitability

Voltage-gated potassium channels (Kv channels) are widely expressed in most cells. They form potassium-selective pores that span cell membranes and play an essential role in controlling neuronal excitability (figure 1A). In sensory neurons and many other types of excitable cells, potassium currents provide the outward currents that repolarize the membrane potential during the falling phase of APs. Therefore, the properties of Kv channels, such as density, trafficking and the kinetics of activation and inactivation could all influence the firing patterns of sensory neurons. Although more than 200 genes encoding a variety of potassium channels have been identified (Shieh et al., 2000), all potassium channels have common features: all potassium channels have: 1. a water-filled pore that allows potassium ions to flow across the cell membrane; 2. a highly selective filter to establish the ionic selectivity; 3. a sensor to control the opening and closing of the channel (Long et al., 2005; MacKinnon, 1991b). Based on the primary amino acid sequence of the pore-containing subunit (α subunit), Kv channels can be divided into five subfamilies: Shaker (Kv1.1-1.7), Shab (Kv2.1-2.2), Shaw (Kv3.1-3.4), Shal (Kv4.1-4.3) and ether-*a-go-go* (HERG) (Chandy and Gutman, 1993). Kv channels are tetrameric assemblies of four identical or different pore-forming α-subunits containing six transmembrane regions (Christie et al., 1990; Isacoff et al., 1990; MacKinnon, 1991a). Some Kv channels may have an auxiliary β subunit binding to the N-terminus of the α-subunit (Shieh et al., 2000). The pore-forming structure (the region between fifth and sixth

transmembrane domains, the p domain) forms the specific pathway for potassium ions to flow through (MacKinnon, 1991b), whereas the positively charged residues within the fourth putative transmembrane segments (S4) are thought to be the major component of the voltage sensor (Liman et al., 1991; Tytgat et al., 1993).

The large diversity of the primary amino acid sequence of the pore-containing subunits serves as an important mechanism for the heterogeneity of voltage-gated potassium channels, and underlies the variety of potassium currents (IK) with distinct kinetics and pharmacological properties (Stuhmer et al., 1989; Wei et al., 1990). Therefore, it is difficult to characterize the phenotypes of IK in DRG sensory neurons. For example, Kostyuk et al., (1981) report that there are two major potassium currents on DRG sensory neurons. In contrast, Gold et al., (1996b) demonstrate that there are six different voltage-gated potassium currents in adult rat DRG neurons. It is highly possible that the large diversity of the phenotypes of potassium current observed in these published studies resulted from the expression of multiple Kv subtypes in sensory neurons. In addition, the different conditions to culture these cells, such as the enzyme used to dissociate tissues, different percentage of CO_2 in the incubator, different salt and nutrients in the culture media as well as the time of cells in culture may contribute to the differential expression of the potassium currents.

It is well established that potassium currents are critical to determine neuronal excitability. The outflow of potassium ions from inside to the outside of

the cell draws the membrane potential closer to the equilibrium potential of potassium (E_K). Under my experimental condition with 140 mM potassium ion ($[K]_i$) in the pipette solution, 5 mM potassium ion in the extracellular solution ($[K]_o$) and at room temperature of 20 °C, E_k is calculated to be -84 mV based on the Nernst equation ($E_K=2.303\frac{RT}{F}\log_{10}\frac{[K]_o}{[K]_i}$ where R is the gas constant, T is the absolute temperature and F is Faraday's constant. At room temperature of 20 °C, RT/F=25.26 mV; Hille, 2001). The opening of potassium channels hyperpolarizes the resting membrane potential (REM, around -50 to -70 mV in isolated sensory neurons in culture), decreases the frequency of neuronal firing and increases the rheobase currents (the minimum currents required to evoke an AP). Although the roles of almost all potassium channels are to "stabilize" membrane potential, different potassium currents have a distinct function during the process of neuronal firing. In sensory neurons, both the fast inactivating IA types (IA) and the slow inactivating delayed-rectifier types of IK (IKd) are identified by previous studies (Gold et al., 1996b; McFarlane and Cooper, 1991). The suppression of both types of current could result in augmentation of neuronal excitability. Activation of IA modulates neuronal excitability by decreasing the frequency of neuronal firing (Connor and Stevens, 1971). During the depolarization of membrane potential (the rising phase of an AP), most channels conducting IA are inactivated. These channels can be reprimed (channels are recovered from inactivation and ready to open upon stimulation) during a period of hyperpolarization (most likely occurred during the phase for after-hyperpolarization of the AP), IA can be activated again as the membrane

potential depolarizes. The transient outward IA could cancel the inward INa during the depolarization of membrane potential. Consequently, the membrane potential does not change. The membrane potential will continue to approach the firing threshold as IA inactivates (Connor, 1978). Therefore, IA is a key factor to determine the interspike interval, the time between the successive APs. The suppression of IA results in a faster depolarization of membrane potential and shortens the interspike intervals. IKd is another major type of potassium current that is critical to neuronal excitability by repolarizing membrane potentials and regulating the duration of the AP. The high potassium permeability during repolarization decreases the duration of APs, thereby facilitates the quick recovery of neurons from a given stimuli. A suppression of IKd produces a longer duration of the AP. As a consequence, more calcium ions enter cells and facilitate the release of neurotransmitters from sensory neurons (Hawkins et al., 1983).

Since potassium channels have such significant roles in modulating firing patterns and other neuronal functions, such as the release of neurotransmitters, it is not surprising that potassium channels regulate neuronal excitability during inflammation and in neuropathic pain (Cherkas et al., 2004; Gold and Flake, 2005; Katz and Gold, 2006; Liu et al., 2001). Therefore, we asked whether potassium currents were suppressed in *Nf1*+/- neurons. By using voltage-clamp technique, experiments were performed to determine the amplitude, the levels of steady-state inactivation as well as the voltage for half maximum activation and inactivation ($V_{0.5}$) of potassium currents in both genotypes.

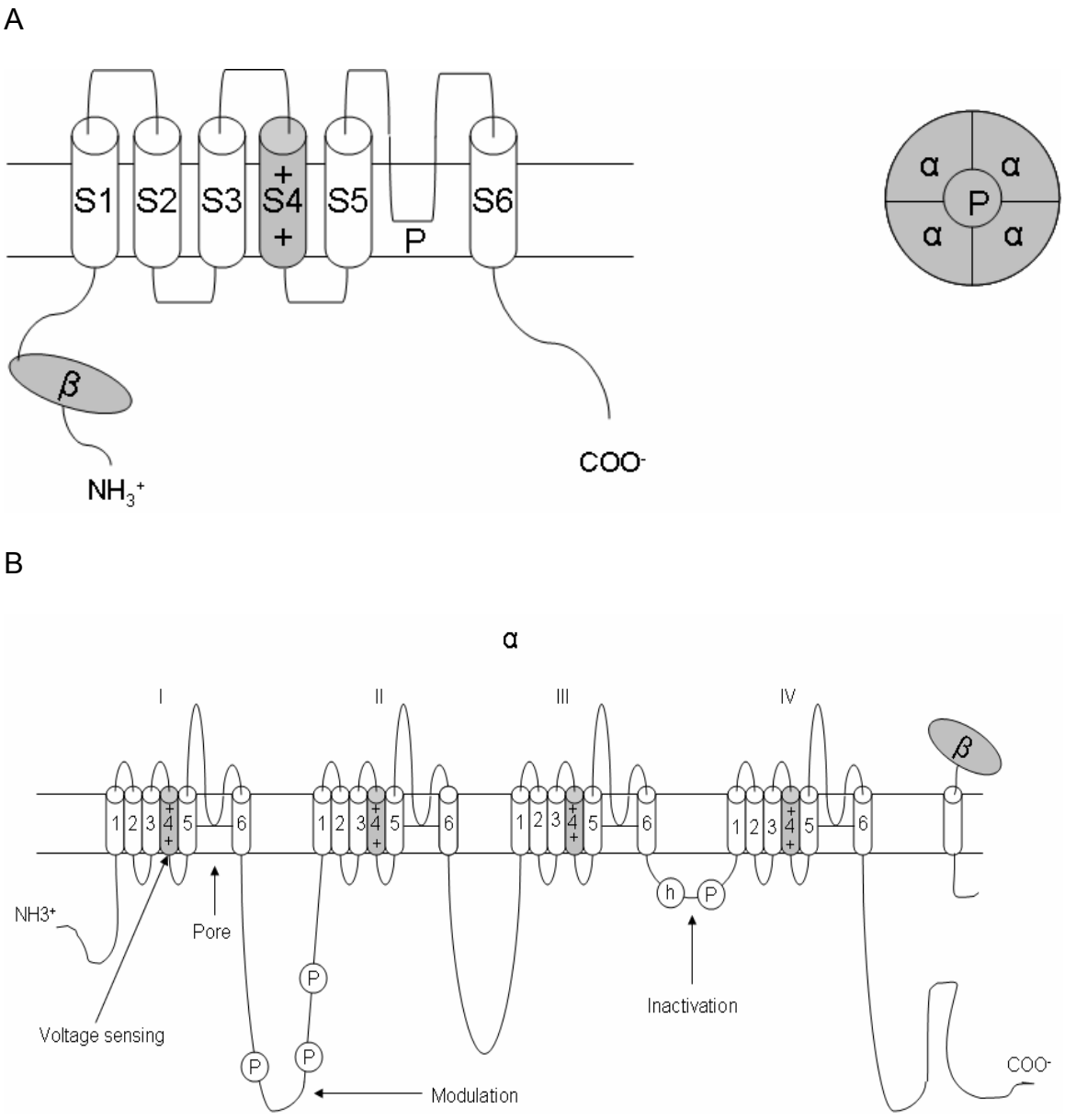

Figure 1. Schematic picture of the structure of voltage-gated potassium channels (A) and sodium channels (B). A is modified from Shieh et al., (2000). The voltage-gated potassium channels (Kv) are transmembrane proteins that consist of four α subunits containing six transmembrane regions (S1-S6), a pore forming structure (P) between S5 and S6 and a voltage sensor (S4). Some of Kv channels may have auxiliary β subunits binding to the N-terminus of the α-subunit. B is modified from Yu and Catterall, (2003). The core of a voltage-gated sodium channel is composed of one α-subunit, which has 4 repeat domains, named from I to IV. Each domain contains six transmembrane regions. The structure between S5 and S6 is the pore-forming region, whereas the highly conserved S4 segments act as the voltage sensor. The α subunits can assemble with one or more β subunits (β1-β4).

2. Voltage-gated sodium channels in sensory neurons and their influence on neuronal excitability

Sodium channels are integral membrane proteins forming sodium-selective pores that span the plasma membrane. Like potassium channels, sodium channels play an essential role in controlling neuronal excitability. In sensory neurons and many other types of excitable cells, upon changing of membrane potential, the opening of sodium channels allows sodium ions to flow rapidly down their electrochemical gradient and generate the upstroke of an AP (Hodgkin, 1949). Thus, the properties of sodium channels, such as distribution, density, trafficking as well as the threshold of activation and inactivation could all influence the firing patterns of sensory neurons.

Voltage-gated sodium channels have several known subunits: the α-subunit that forms the sodium-selective aqueous pores and one or more smaller β subunits (β1-β4) which regulate the function of the α-subunit (Catterall, 2000; Isom, 2001; Yu and Catterall, 2003). A functional sodium channel is composed of one α-subunit that can assemble with one or more β subunits (Yu and Catterall, 2003). The α-subunit has four repeat transmembrane domains, named from I to IV. Each domain contains six transmembrane regions (S1-S6; Guy and Seetharamulu, 1986; Noda et al., 1984). The S4 segments, which have positively charged arginines at every third residue and are thought to be the voltage sensor of voltage-gated sodium channels (Guy and Seetharamulu, 1986). When stimulated by a depolarization of the transmembrane potential, the

positively charged S4 segments within the pore move to the extracellular side, allowing the channel to become permeable to sodium ions (Leuchtag, 1994; Yang and Horn, 1995). Without this movement, the positively charged S4 segments block the entry of positive-charged sodium ions.

Although voltage-gated sodium channels are less diverse than potassium channels, they clearly have functional diversifications (Neumcke, 1990). Based on the primary amino acid sequence of the α-subunits, a family of nine isoforms of sodium channels has been identified: $Na_v1.1$, $Na_v1.2$, $Na_v1.3$, $Na_v1.4$, $Na_v1.5$, $Na_v1.6$, $Na_v1.7$, $Na_v1.8$ and $Na_v1.9$ (Wood et al., 2004). Based on the sensitivity to tetrodotoxin (TTX, a paralytic toxin isolated from puffer fish that blocks one type of sodium channels), two general classes of voltage-gated INa has been identified in sensory neurons: TTX-sensitive (TTX-S) INa and TTX-resistant (TTX-R) INa (Elliott and Elliott, 1993; Kostyuk et al., 1981; Roy and Narahashi, 1992). In contrast to TTX-S INa, which is blocked by TTX at nanomolar concentrations (IC_{50}=0.3 nM), TTX-R INa can only be suppressed by micromolar TTX (IC_{50}=100 μM) (Roy and Narahashi, 1992). The $Na_v1.1$-1.4 and $Na_v1.6$-1.7 are TTX-S sodium channels, whereas $Na_v1.5$, $Na_v1.8$ and $Na_v1.9$ are recognized as TTX-R sodium channels. TTX-S INa and TTX-R INa differ in their activation and inactivation kinetics. The peak of the I-V relationship, the $V_{0.5}$ for activation and steady-state inactivation of TTX-R INa are more depolarized in sensory neurons compared to TTX-S INa (Elliott and Elliott, 1993; Roy and Narahashi, 1992). As the membrane potential is held at -67 mV, TTX-R INa is recovered from inactivation within 5 ms, which is much faster when compared to TTX-S INa

(over 50 ms) (Elliott and Elliott, 1993). This rapid recovery of TTX-R INa from inactivation could enable sensory neurons with a larger proportion of TTX-R INa to fire at a higher frequency than the neurons with more TTX-S INa (less sodium channels are available to generate the upstroke of an AP because of the slow recovery of TTX-S INa from inactivation).

A number of studies indicate that the alteration of INa is an important underlying mechanism for a variety of painful disorders, such as inflammation (Black et al., 2004; Li et al., 2006; Tanaka et al., 1998), neuropathic pain (Dib-Hajj et al., 1999; Lai et al., 2002), a painful inherited neuropathy called erythermalgia (Cummins et al., 2004), experimental ulcers (Bielefeldt et al., 2002) and nerve injury (Black et al., 1999; Dib-Hajj et al., 1996; Rizzo et al., 1995; Sleeper et al., 2000). Both TTX-R and TTX-S INa are reported to have strong links with the development of inflammatory and neuropathic pain (in which the excitability of nociceptive neurons is enhanced) (Waxman et al., 1999). For example, following peripheral inflammation, the TTX-R INa is enhanced in nociceptive neuronal cells in DRG (Tanaka et al., 1998). In addition, inflammatory mediators like NGF, prostaglandin E_2 (PGE_2) and bradykinin enhance neuronal excitability in vitro, through an increase in the amplitude of TTX-R INa (England et al., 1996; Gold, 1999; Gold et al., 1996a; Gold et al., 2002; Jeftinija, 1994; Rush and Waxman, 2004; Zhang et al., 2002). As to TTX-S sodium channels, it is reported that axotomy and other forms of nerve damage led to the reexpression of an embryonic form of TTX-S sodium channel, $Na_v1.3$, in adult rat DRG neurons (Waxman et al., 1994). The expression of another

TTX-S channel, Nav 1.7, was increased in DRG neurons after caraggeenan-induced inflammation (Black et al., 2004). A parallel increase of TTX-S INa is often observed as a consequence of the transcriptional change of TTX-S sodium channels. All of these publications are consistent with the idea that the modulation of both TTX-R and TTX-S INa by multiple inflammatory mediators contributes to neuronal sensitization during inflammation or nerve injury.

Evidence indicates that the sensory neurons with a heterozygous mutation of the *Nf1* gene are sensitized because these cells release more CGRP upon the stimulation of capsaicin (Hingtgen et al., 2006). Capsaicin is a compound found in hot peppers. This compound selectively activates small-diameter sensory neurons involved in nociception (Holzer, 1991). Hingtgen's work indicates a significant neuronal sensitization in nociceptive sensory neurons with the heterozygous mutation. Because INa is often regulated during neuronal sensitization, the next question to be examined in this work is whether INa in *Nf1+/-* neurons is altered, and could underlie the neuronal sensitization of *Nf1+/-* neurons.

B. Multiple inflammatory mediators sensitize DRG sensory neurons via modulating ion channel activity

Multiple inflammatory mediators, such as prostaglandins, bradykinin and NGF are known to sensitize sensory neurons to given stimuli, resulting in a condition of enhanced neuronal sensitivity. Prostaglandins, the metabolites of essential fatty acids, such as gamma-linolenic acid (GLA), arachidonic acid (AA) and eicosapentaenoic acid (EPA), are found in almost all tissues and organs. Once AA, GLA or EPA are oxidized by cyclooxygenases (COX), prostaglandins are produced (Bergstroem et al., 1964; Samuelsson, 1972). Prostaglandins regulate a number of normal physiological functions, such as the constriction of smooth muscle or the aggregation/disaggregation of platelets. In addition, prostaglandins closely correlate with inflammation. The level of one form of prostaglandins most associated with inflammation, PGE2, is elevated significantly during inflammation and serves as an important mediator that causes redness, swelling and hyperalgesia (Ferreira et al., 1978; Willis and Cornelsen, 1973). At the behavioral level, repeated injection of PGE_2 in rat paws reduced the threshold for the withdrawal response to mechanical and thermal stimuli (Willis and Cornelsen, 1973). PGE_2 also directly sensitizes sensory neurons as demonstrated by the studies using electrophysiological methods. PGE_2 was demonstrated to enhance the number of APs elicited by a ramp of depolarizing current in embryonic rat sensory neurons and suppressed a voltage-gated potassium current (Nicol and Cui, 1994; Nicol et al., 1997). The direct sensitizing effect of PGE_2 is further confirmed by the studies using

radioimmunoassay, such as the observation that PGE_2 augments the release of neuropeptides, SP and CGRP, from sensory neurons (Hingtgen and Vasko, 1994). These two neuronal peptides are widely expressed in the primary DRG sensory neurons (Lee et al., 1985; McCarthy and Lawson, 1990). Evidence indicates that the release of these two neuropeptides participates in nociceptive transmission, such as the observation that the mechanical and thermal hyperalgesia (the enhanced sensitivity to a painful stimulus) induced by carrageenan was attenuated by an intrathecal administration of anti-CGRP antiserum (Kawamura et al., 1989). In addition, the Intrathecal injection of SP produced a significant mechanical hyperalgesia (Kawamura et al., 1989). The release of these two neuronal peptides from the central and peripheral terminal of Aσ or C type fibers is a critical event in modulating pain perception and in initiating neurogenic inflammation (Cuello, 1987). The increase of the release of the two neuronal peptides, therefore, indicates a significant enhancement of the sensitivity of neurons to noxious stimuli and facilitates the onset of hyperalgesia.

Evidence suggests that the sensitizing effect of PGE_2 may result from its capacity to modulate the activity of ion channels. Linhart et al., (2003) reported that the enhancement of intracellular calcium concentration by PGE_2 was abolished in calcium-free solution, suggesting that PGE_2 activates ion channels permeable to calcium ions. These channels could be vanilloid receptor type 1 (TRPV1) or related ion channels because Lopshire and Nicol (1998) reported that PGE_2 augmented the inward currents elicited by the vanilloid, capsaicin, in embryonic rat sensory neurons. In addition, PGE_2 was reported to enhance TTX-

R INa in DRG neurons (England et al., 1996; Gold et al., 2002; Rush and Waxman, 2004). Furthermore, Nicol et al., (1997) and Evans et al., (1999) demonstrated that PGE_2 suppressed outward potassium currents. These studies are consistent with the notion that PGE_2 sensitizes sensory neurons via modulation of ion channels.

NGF is another important inflammatory mediator that sensitizes sensory neurons. NGF was discovered by Rita Levi-Montalcini in the 1950's (Levi-Montalcini, 1952; Levi-Montalcini and Hamburger, 1951) and recognized to be an important factor in the survival, development and maintenance of sensory and sympathetic neurons (Eichler and Rich, 1989; Johnson et al., 1989; Kirstein and Farinas, 2002; Marzella and Gillespie, 2002). However, it is clear that NGF also regulates the sensitivity of sensory neurons to noxious stimulation. NGF was reported to be a potent causative agent in producing both thermal and mechanical hyperalgesia (Lewin et al., 1993). In addition, approaches that blocked increased levels of NGF reduced the inflammatory pain. By using an NGF neutralizing antibody, the elevated sensitivity to painful stimuli was attenuated in a rat model of inflammation induced by complete Freund's adjuvant (Woolf et al., 1994). Likewise, the hyperalgesia in carrageenan-induced inflammation was blocked by using a synthetic protein, TrkA-IgG, that abolished the biological effect of any free NGF (McMahon et al., 1995). These studies suggest that an increase in NGF concentration is critical for the generation of inflammatory pain. The effect of NGF in inflammatory hyperalgesia is on neurons because treatment of sensory neurons with NGF for two weeks increases the

basal and stimulus-evoked release of substance P (SP) and calcitonin gene-related peptide (CGRP), from these neurons (Malcangio et al., 1997). Similarly, NGF was shown to enhance neuronal excitability by increasing the frequency of AP firing elicited by a ramp of depolarizing current (Zhang et al., 2002). Interestingly, evidence also supports the idea that NGF or its downstream effectors sensitizes sensory neurons by modulating ion channels. NGF was reported to enhance the inward currents elicited by capsaicin in small-diameter sensory neurons, indicating that NGF could be important in sensitizing nociceptive neurons to thermal stimuli (Lewin et al., 1993; Shu and Mendell, 1999). Moreover, NGF augmented the excitability of small diameter sensory neurons by increasing a TTX-resistant sodium current and suppressing a voltage-gated potassium current (Zhang et al., 2002).

To date, investigators have recognized that NGF activates two kinds of receptors on the membrane of sensory neurons. One is TrkA ($p140_{trkA}$), the high affinity receptor ($K_d = 10^{-11}$ M), and the other is p75, the low affinity receptor ($K_d = 10^{-9}$ M) (Meakin and Shooter, 1992). The stimulation of TrkA or p75 by NGF can lead to the activation of multiple intracellular cascades, such as the Ras cascade (Blochl et al., 2004; Corbett and Alber, 2001; Huang and Reichardt, 2003; Susen et al., 1999), mitogen-activated protein kinase (MAPK) pathway (Ji et al., 2002), phosphatidylinositol 3-kinase (PI-3K) pathway (Salvarezza et al., 2003), phospholipase C_γ (PLC) pathway (Kim et al., 1991; Vetter et al., 1991) as well as sphingolipid pathway (see figure 2 for a summary). However, which pathway modulates the sensitizing effect of NGF remains largely unclear.

C. Intracellular signaling pathways that may be involved in neuronal sensitization by NGF

1. Ras-MEK-MAPK pathway

Ras belongs to the superfamily of small GTP-binding proteins that function as “switches” in many intracellular signaling cascades. Ras was the first member to be identified in this family of small GTP-binding proteins by analyzing the genome of cell lines transformed by Kirsten and Harvey sarcoma viruses (Chien et al., 1979). Upon binding growth factors, such as NGF, epidermal growth factor and fibroblast growth factor, to their receptors on the cell membrane, the autophosphorylation of the receptors is initiated. This autophosphorylation of specific tyrosine residues allows the subsequent binding of adaptor proteins, such as Shc, Grb2. The activated Grb2 activates the guanine nucleotide exchange factor, Son of sevenless (SOS), which in turn stimulates the release of GDP from Ras and allows the subsequent binding of GTP. This switches the complex to the active form, Ras-GTP (Schlessinger, 1993). Active Ras-GTP will recruit the kinase, Raf, to the cell membrane. The activated Raf stimulates a cascade of downstream effectors, such as mitogen-activated protein kinase kinase (MEK), which culminates in activation of a serine/threonine kinase, called mitogen-activated protein kinase (MAPK). The MAPK family includes extracellular signal-regulated protein kinase (ERK1/2), p38, c-Jun N-terminal kinase/stress-activated protein kinase (JNK/SAPK), and ERK5 (Marshall, 1995).

The Ras-MEK-MAPK pathway has many functions in neurons, including synaptic plasticity, long-term potentiation, and survival (Grewal et al., 1999).

Recently, several investigations have reported that the activation of MAPK is involved in the sensitization of nociceptors. Zhuang et al., (2005) reported that phosphorylated ERK (P-ERK, the active form of ERK) was detected both in spinal cord and DRG after spinal nerve ligation (SNL). Likewise, injecting NGF into the peripheral tissue increased P-ERK labeling in TrkA-containing neurons in DRG (Averill et al., 2001). Moreover, p38 was activated in nociceptive sensory neurons located in the DRG after inflammation (Beloeil et al., 2006; Ji et al., 2002). All these observations indicate that the activation of MAPK may underlie the augmented painful sensation during inflammation or neuropathic pain. In support of this idea, Zhuang et al., (2005) reported that the SNL-induced mechanical allodynia was suppressed by the Intrathecal injection of the MEK inhibitor, PD98059, which suggests that the activation of MAPK contributes to mechanical allodynia. One possible mechanism for MAPK in hyperalgesia and allodynia could be the activation of phospholipase A2, the enzyme that liberates arachidonic acid, which then serves as the substrate for the generation of prostaglandins, leukotrienes and other proinflammatory agents. These compounds could contribute to the abnormal painful sensation associated with inflammation (Higgs et al., 1984). For example, leukotriene B_4 was shown to directly activate TRPV1, the capsaicin receptor on isolated membrane patches of small-diameter sensory neurons (Hwang et al., 2000). These observations are consistent with the idea that the activation of Ras-MEK-MAPK pathway serves as

an important component in numerous painful conditions, such as inflammation and nerve injury.

2. Phosphoinositide-3-kinase (PI-3K) pathway

Phosphoinositide-3-kinase (PI-3K) pathway is the major survival-promoting cascade in neurons (Philpott et al., 1997). It can be activated by binding to the activated TrkA receptor, or by Ras-GTP (Rodriguez-Viciana et al., 1996; Yuan and Yankner, 2000). The activation of PI-3K stimulates 3'-phosphoinositide-dependent kinase-1 (PDK-1) and 3'-phosphoinositide-dependent kinase-2 (PDK-2), both of which can, in turn, activate a serine/threonine kinase, Akt. Akt may suppress apoptosis by inhibiting the activities of Forkhead and Bad, proapoptotic members of the Bcl-2 family or attenuates apoptotic activities of GSK-3, thus increase the level of the anti-apoptosis proteins, like IAP, Bcl-2 or Bcl-XL (Datta et al., 1997; Yuan and Yankner, 2000). Akt might also promote neuronal survival by blocking the JUK-p53-Bax pathway, the primary apoptotic cascade in neurons (Kaplan and Stephens, 1994).

Evidence shows that PI-3K pathway is involved with neuronal sensitization induced by NGF. By mutating the tyrosine residue Y760 on TrkA that is critical in activation of PI-3K, the NGF-induced phosphorylation of TRPV1 was completely abolished (Zhang et al., 2005). Additionally, the potentiation of NGF for the capsaicin-evoked TRPV1 currents was completely blocked by PI-3K inhibitors (Zhuang et al., 2004), indicating the activation of PI-3K could modulate TRPV1

channels, thereby enhancing the inward currents elicited by capsaicin or noxious heat and contributes to the heat hyperalgesia that occurs during inflammation.

PI-3K can lead to the activation of other downstream protein kinases such as protein kinase A (PKA) and protein kinase C (PKC) via PDK-1 (Le Good et al., 1998). The activation of both kinases can initiate hyperalgesia (Aley and Levine, 1999; Cesare et al., 1999; Souza et al., 2002; Zhou et al., 2001). PI-3K was also reported to activate ERK (Zhuang et al., 2004), which is another possible factor that contributes to neuronal sensitization (Aley et al., 2001; Dai et al., 2002). These studies indicate that PI-3K is involved in neuronal sensitization either by directly modulating TRPV1 channels or by activating other intracellular cascades, whose activation leads to the sensitization of sensory neurons, and underlies the hypersensitivity of pain during inflammation.

3. The Phospholipase C (PLC) Pathway

The phosphoinositide-specific phospholipase C (PLC) is an enzyme that hydrolyzes phosphatidylinositol-4,5-bisphosphate (PIP2) to liberate inositol 1,4,5-trisphosphate (IP3) and diacylglycerol (DAG). PLCs can be divided into three types: $PLC_{\beta,}$ PLC_{γ} and PLC_{δ} (Lee and Rhee, 1995). The activation of PLC_{γ} by NGF has been demonstrated in previous studies (Rhee and Choi, 1992). Evidence indicates that NGF-induced sensitization of DRG cells is through PLC. Using an inhibitor of PLC, U73211, the effect of NGF to reverse the tachyphylaxis (the inward current in response to the second of two heat pulses is significantly smaller than the current elicited by the first heat pulses) was abolished in small-

diameter DRG neurons (Galoyan et al., 2003). Consistent with their findings, Chuang et al., (2001) demonstrated that the NGF-induced potentiation of the proton-evoked TRPV1 currents was abrogated in a heterologous system expressed mutant TrkA which is unable to interact with PLC. Although these studies mainly focus on the potentiation of NGF on the TRPV1 currents, they do not rule out the possibility that the activation of PLC by NGF is an integral step of NGF-induced augmentation of neuronal firing in sensory neurons.

4. The p75 pathway

The p75 neurotrophin receptor (p75 NTR, p75) is a member of the tumor necrosis factor (TNF) receptor superfamily. It is a pan-neurotrophin receptor that can be activated by NGF, brain-derived neurotrophic factor (BDNF), NT-3 and NT4/5 with equal affinities. The intracellular domain of p75 is similar to the "death domain" found in the cytoplasmic regions of members in the tumor necrosis factor receptor family, whose activation is thought to induce apoptosis in certain cell types (Smith et al., 1994). Although there is no inherent enzymatic activity in the cytoplasmic domain of the receptor, p75 has been shown to activate many intracellular signaling pathways. The activation of p75 stimulates stress-activated protein kinase (JUNK) pathway in PC12 cells and activates NFκB in Schwann cells and oligodendrocytes (Becker et al., 2004; Carter et al., 1996; Yoon et al., 1998). The activation of JUNK and NFκB mainly leads to the apoptosis of non-neuronal cells. However, in sensory neurons, evidence suggests that the activation of p75 leads to neuronal sensitization. The activation of p75 by NGF stimulates sphingomyelinase (SMase), the enzyme that

hydrolyzes sphingomyelin (SM) to liberate ceramide (Dobrowsky et al., 1994), which is also a key player to modulate the excitability of nociceptive sensory neurons (Zhang et al., 2002; Zhang et al., 2006b). Ceramide can be metabolized by ceramidase to sphingosine (Sph), which can be further converted to sphingosine-1-phospate (S1P). Both Sph and S1P were shown to augment the excitability of sensory neurons isolated from adult rats. Internal perfusion with Sph and S1P augments AP numbers evoked by a standard amount of current (Zhang et al., 2006b). This augmented neuronal excitability may result from the direct modulation of ion channels by Sph/S1P or by the downstream signaling molecules activated by Sph/S1P. Interestingly, external perfusion with S1P also augments neuronal excitability (Zhang et al., 2006a). The external S1P may act via EDG receptors, the G-protein-coupled receptors, to augment neuronal excitability by activating various downstream signaling cascades, such as PLC, PKC and MAPK pathway. S1P may modulate neuronal excitability in two ways: one is via a paracrine manner, in which S1P is released and bound to the EDG receptors of nearby neurons and thereby augments neuronal firing; second, via activation by NGF, S1P can act as internal second messenger to regulate membrane excitability.

Interestingly, p75 also links to the activation of Ras-MEK-MAPK pathway, the possible contributor in the elevated sensitivity of sensory neurons to noxious stimuli during inflammation or nerve injury (Aley et al., 2001; Dai et al., 2002). Through activation of the p75 receptor, NGF stimulates the Ras and MAPK transduction cascade in expression systems and neuronal cells that do not

express TrkA (Blochl et al., 2004; Susen et al., 1999). Additionally, Hida et al., (1998) demonstrated that ceramide activated Ras in cultured oligodendrocytes. Based on these observations, it is reasonable to speculate that the activation of p75 stimulates MAPK pathway and leads to neuronal sensitization.

p75 was originally thought to cooperate with TrkA based on the observation that the activation of p75 enhances the number of high affinity binding sites for NGF in PC-12 cells. Surprisingly, this effect of p75 does not require the extracellular domain, suggesting the transmembrane domain and cytoplasmic domain of p75 are responsible for the formation of high affinity binding sites for NGF (Esposito et al., 2001). This enhancement of NGF binding with TrkA may result from the conformational change of TrkA by interacting with p75, and thereby generate the high affinity binding sites (Esposito et al., 2001). However, it is also possible that p75 enhances the potency of TrkA via the downstream effectors. A recent study by Epa et al., (2004) showed that p75 binds to and enhances the phosphorylation of Shc, a signaling molecule interacting with TrkA and leading to the activation of both MAPK and PI-3K pathway. In addition, the phosphorylation of Akt is diminished by using an antisense molecule to reduce the expression of p75, suggesting the activation of Akt, the downstream effectors of TrkA, depends on the activation of p75 (Epa et al., 2004). Based on these studies, it is reasonable to speculate that there could be a redundancy or synergy of the signaling cascades activated by TrkA and p75.

However, the pathways downstream of TrkA may also inhibit the pathways activated by p75, or the pathway activated by p75 may be suppressed by stimulating of TrkA. Indeed, the stimulation of TrkA attenuates the “death signal”, i.e., the activation of JUNK and NFκB following the activation of p75 in cultured oligodendrocytes (Yoon et al., 1998). In addition, in PC12 cells expressing both TrkA and p75, the activation of TrkA inhibits p75-dependent sphingomyelin (SM) hydrolysis (Bilderback et al., 2001). The different ratio for the expression of NGF receptors in distinct systems could also contribute to the complexity of NGF signaling (Twiss et al., 1998).

We are just beginning to understand the complex system of NGF signaling. The intricate aspect in investigating these pathways lies in the heterologous expression systems used to perform those studies. The events happening in native cells may not actually occur in those artificial systems. For example, in PC12 cells, the inhibition of PIP2 by using a monoclonal antibody augments TRPV1 currents (Chuang et al., 2001). Such inhibition has not been observed in sensory neurons. Another disadvantage of using heterologous expression systems is that, after growing for a period in different culture environments, the characteristics of these cells may become quite different compared to those found in their ascendant population, probably because the adaptation for different culture environments, such as temperature, pH, nutrients as well as concentration of salt. Thus, the results from those studies using cell lines must be interpreted with great caution.

D. The intracellular transduction pathways activated by NGF modulate ion channels

Numerous reports demonstrated that the downstream effectors following the activation of TrkA and p75 regulated channel activity. For example, Fitzgerald and Dolphin (1997) demonstrated that the microinjection of K-Ras (an isoform of Ras) enhanced a voltage-gated calcium current in DRG neurons isolated from neonatal rats. In addition, the overexpression of dominant active Ras mimicked the effect of NGF to augment the expression of the noxious heat-sensing protein, TRPV1 in rat DRG neurons (Bron et al., 2003). Moreover, activation of Ras decreased inward rectifier types of potassium currents in the heterologous expression of HEK 293 cells (Giovannardi et al., 2002). MEK and MAPK, the downstream effectors of Ras, also regulate membrane currents like TTX-R INa (Jin and Gereau, 2006), A-type potassium currents (Karim et al., 2006) and voltage-gated calcium currents (Fitzgerald, 2000). As to the signaling cascades activated by p75, SMase pathway, modulates membrane currents such as TTX-R INa and delayed-rectifier types of IK (Zhang et al., 2006a; Zhang et al., 2002; Zhang et al., 2006b). Taken together, these observations suggest that the binding of NGF to its receptors, TrkA and p75, leads to the activation of multiple intracellular signaling cascades that may sensitize sensory neurons by modulating membrane currents. However, it remains to be clarified which cellular mechanism(s) underlies the augmented neuronal firing by NGF. In this thesis work, two approaches are used to determine whether Ras is an important step in this NGF-induced augmentation of neuronal firing. The first is to examine

whether the NGF-induced sensitization in *Nf1*+/+ mouse sensory neurons can be attenuated by using a neutralizing antibody to block the intracellular Ras activity. Second, to investigate whether NGF can sensitize *Nf1*+/- sensory neurons that supposedly have augmented intracellular level of Ras-GTP (see next section for detailed description; Guha et al., 1996). If the stimulation of Ras is important in NGF-induced augmentation of neuronal firing, then it is not surprising that NGF loses its effect on neurons with previous activation of this cascade. These works indicate whether Ras contributes to the augmented neuronal firing induced by NGF.

E. Neurofibromatosis and sensory neurons with *Nf1* heterozygous mutation

Neurofibromatosis type 1 (NF1) is a common genetic disease in humans. It is an autosomal dominant disease with an incidence of 1 in 3,500 people (Lakkis and Tennekoon, 2000). It is characterized by numerous abnormalities including neurofibromas (complex tumors composed of axonal processes, Schwann cells, and mast cells), as well as malignant tumors such as neurofibrosarcomas, malignant astrocytomas and myeloid leukemias. In addition to the tumor formation, some people with NF1 also experience much more intense painful sensations to stimuli, such as minor injuries, that elicit only slight discomfort in normal people (Creange et al., 1999; Wolkenstein et al., 2001). Although the mechanism by which the NF1 causes the enhanced painful sensation has not been elucidated, it is likely that these abnormal painful states

involve the sensitization of small diameter nociceptive sensory neurons, cells that are known mediate the transmission of pain and itch.

NF1 results from a heterozygous mutation of the *NF1* gene (*NF1+/-*). Currently, investigators have developed two mouse models for NF1. One is a mouse with a heterozygous mutation of the *Nf1* gene (*Nf1+/-*; developed by Jacks et al., 1994). Another is a mouse with a homozygous mutation of the *Nf1* gene (*Nf1-/-* ; developed by Largaespada et al., 1996). Because *Nf1-/-* mice die at embryonic day 14, I use adult *Nf1+/-* mice in my study. Although the disrupted *Nf1* gene in these *Nf1+/-* mice can still be transcribed into mRNA containing an open reading frame, the protein product of the mutant mRNA is unstable and does not accumulate in cells (Jacks et al., 1994). Therefore, the protein products of the *Nf1* gene, neurofibromin, could be lower in cells with only one functional copy of the *Nf1* gene. Neurofibromin is expressed most abundantly in the nervous system, such as neurons, Schwann cells and oligodendrocytes in adult animals (Daston et al., 1992). The high incidence of developmental retardation, learning difficulties as well as exaggerated painful response of those people with NF1 (Creange et al., 1999; Trovo-Marqui et al., 2005) indicates that the single active NF1 allele does not generate enough neurofibromin to fulfill the normal biological function in the nervous system. Neurofibromin helps to switch the active form of Ras (Ras-GTP) to its inactive form (Ras-GDP) by serving as a GTPase activating protein (GAP). The decrease of neurofibromin levels frequently results in both basal and cytokine-stimulated Ras activity in many cell types. Investigators have shown that the level of Ras-GTP is elevated in NF1

neurofibrosarcomas and neurofibromas (Guha et al., 1996), in *Nf1+/-* mast cells (Ingram et al., 2001), in *Nf1-/-*Schwann cells (Sherman et al., 2000) and in *Nf1-/-* sensory neurons (Klesse and Parada, 1998; Vogel et al., 2000). Based on the published studies, it is reasonable to speculate that the level of Ras-GTP is higher in adult sensory neurons with a heterozygous mutation of the *NF1* gene (*NF1+/-* or *Nf1+/-*) than that of wild-type cells. The augmentation of Ras-GTP alters the function of many cell types. It is reported that neurons, mast cells, fibroblasts and Schwann cells from *Nf1+/-* and *Nf1-/-* mice exhibit abnormal characteristics compared to wild types. The *Nf1* mutation increased mast cell proliferation, survival and colony formation in response to the steel factor, which is a ligand for c-kit (the receptor for stem cell factors; Ingram et al., 2001). In addition, embryonic sensory neurons with the *Nf1* mutation do not require NGF for survival (Vogel et al., 1995; Vogel et al., 2000), indicating the importance of the Ras transduction cascade in the survival of embryonic sensory neurons, and the *Nf1* mutation eliminated their dependency for NGF.

Ras can be activated by many growth factors. Among the growth factors that activate the Ras cascade, NGF has been explored extensively by researchers who study neuronal sensitization in inflammation or nerve injury. It is clear that NGF regulates the sensitivity of sensory neurons to noxious stimulation because NGF in culture media for over 2 weeks increases the basal and stimulus-evoked release of SP and CGRP from these neurons (Malcangio et al., 1997). NGF also enhances neuronal excitability by increasing the frequency of firing APs elicited by a ramp of depolarizing current (Zhang et al., 2002). It is

possible that the enhanced Ras-GTP levels in nociceptive sensory neurons serves as a common mechanism either in the painful sensations experienced by people with NF1 or in the NGF-induced neuronal sensitization.

Given the information that Ras modulates membrane currents that underlie the generation of APs (Bron et al., 2003; Fitzgerald, 2000; Fitzgerald and Dolphin, 1997; Giovannardi et al., 2002), it is logical to infer that enhanced Ras-GTP levels in sensory neurons confers a change in channel activity that leads to increased neuronal excitability and underlies the onset of enhanced painful sensation in people with NF1 as well as NGF-induced neuronal sensitization.

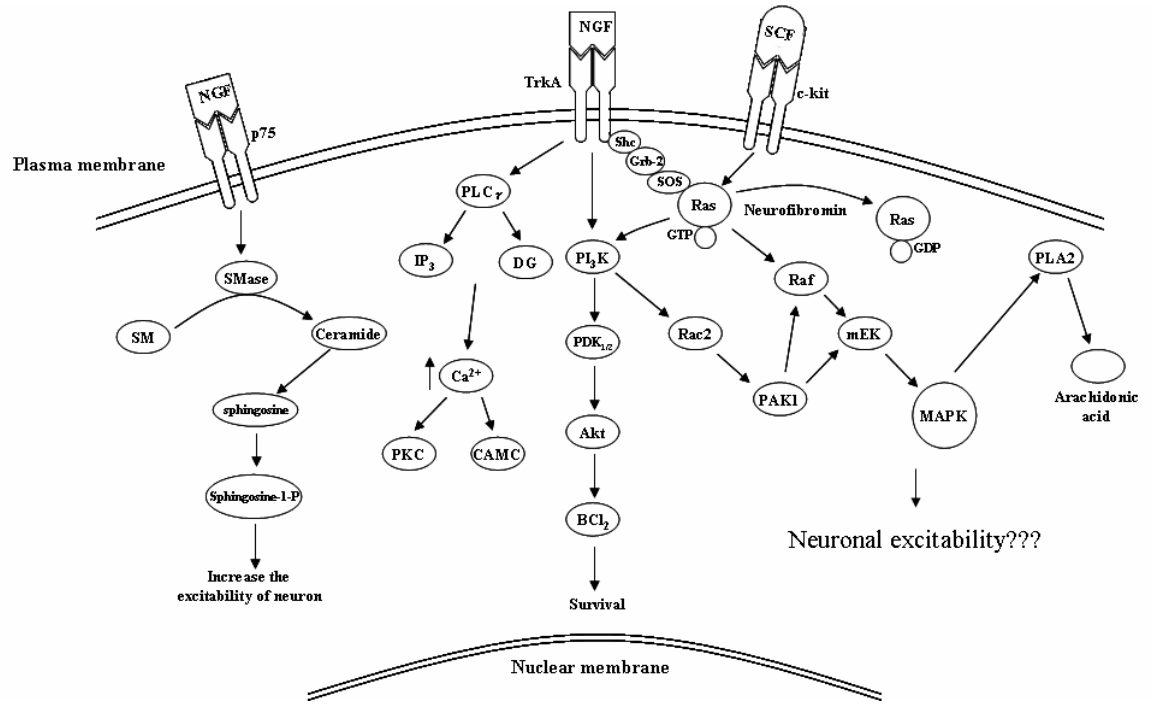

Figure 2. Intracellular signaling cascades that may contribute to the sensitization of DRG neurons.

F. Hypothesis and specific aims

Specific Aims

Based on the above introduction, my hypothesis is: ***enhanced Ras-GTP levels in sensory neurons changes the activity of ion channels that leads to an increased neuronal excitability.*** In the studies outlined in this thesis, sensory neurons isolated from *Nf1+/-* mice, a mouse model for neurofibromatosis, are used to investigate the actions of the Ras transduction cascade on the neuronal excitability. The electrophysiological properties of these neurons are examined with the patch-clamp recording technique. This technique allows measurement of membrane voltage or currents arising from a single neuron. Since the recording pipette has direct access to the cytoplasmic space, the intracellular signal transduction pathways can be manipulated in a physiologically characterized neuron. To those ends, the specific aims are as follows:

Specific aim 1 determines whether the excitability of sensory neurons is enhanced in *Nf1*+/- mice compared to wild types. Since *Nf1+/-* neurons have augmented Ras activity, these studies investigate whether the activation of Ras enhances the excitability of sensory neurons.

Specific aim 2 examines the sensitizing effect of NGF on wild-type neurons and *Nf1+/-* neurons. Because *Nf1+/-* neurons have augmented Ras activity, the studies that compared the NGF-induced sensitization on wild-type and *Nf1+/-*

neurons determine whether Ras had a significant role in neuronal sensitization induced by NGF.

Specific aim 3 by using an antibody that neutralizes intracellular Ras activity, this aim will investigate whether the suppression of Ras activity in *Nf1*+/- neurons decreases the excitability to the levels observed in *Nf1*+/+ neurons.

Specific aim 4 examines which membrane currents are altered in *Nf1*+/- neurons and may contribute to the augmented neuronal excitability of *Nf1*+/- neurons.

II. MATERIALS AND METHODS

A. Animals

Adult mice heterozygous for the *Nf1* mutation on a background of C57BL/6J were originally developed by Tyler Jacks (MIT). Animals were housed and bred in the Laboratory Animal Care Resource Center (LARC) in accordance with protocols approved by the Indiana University Animal Care and Use Committee. The mice used in this study served as a model for humans with NF1. The experiments used both *Nf1+/+* and *Nf1+/-* mice as a source for acutely dissociated sensory neurons.

The Laboratory Animal Resource Center, Indiana University School of Medicine, is in compliance with State and Federal regulations and is operated according to the “Guide for Care and Use of Laboratory Animals”. The Director and Assistant Director are both veterinarians. The animal care technicians are at various stages of AALAS certification. A letter of assurance is on file with the Office of Protection from Research Risks. Animals were housed in individual or group cages in the LARC facility until used for experiments. In all experiments, animals were sacrificed by CO_2 prior to tissue harvesting. Those procedures are approved by the Indiana University Animal Care and Use committee.

B. Materials

Horse serum, F-12 medium, L-glutamine, and penicillin/streptomycin were purchased from Invitrogen (Carlsbad, CA). NGF was purchased from Harlan Bioproducts for Science (Indianapolis, IN). Papain was purchased from Worthington Biochemical, and dispase was obtained from Roche (Indianapolis, IN). Collagenase, poly-D-lysine, laminin, 5'-fluoro-2'-deoxyuridine, uridine, and standard laboratory chemicals were from Sigma-Aldrich (St Louis, MO). Capsaicin was first dissolved in 1-methyl-2-pyrrolidinone (MPL) to obtain a 1 mg/ml stock solution. The stock solution was diluted with normal Ringer's solution to yield final concentration, 100 ng/ml capsaicin. Anti-v-H-Ras, a monoclonal antibody that neutralizes the biological and biochemical activities of H-, K-, and N-Ras of vertebrates by binding to residues Glu-63, Ser-65, Ala-66, Met-67, Gln-70, and Arg-73 (Sigal et al., 1986), was obtained from Calbiochem (San Diego, CA). Lyophilized solid antibody was reconstituted in normal pipette solution (see below for composition), then stored in aliquots at -20°C for long term storage.

C. Isolation and culture of adult mouse sensory neurons

Isolation of sensory neurons from adult mice used the procedure developed by Lindsay (1988) with slight modification. Briefly, male adult animals were killed by placing them in CO_2 chamber. The isolated spinal column was dissected, the spinal cord was removed, and the dorsal root ganglia were collected in a culture dish filled with sterilized Pucks solution composed of (in

mM): 171 NaCl, 6.7 KCl, 1.6 Na_2HPO_4, 0.5 KH_2PO_4, 6 D-glucose, and 0.01% phenol red, pH 7.3. The ganglia were transferred to a conical tube with Pucks solution containing 10 ng/ml papain. After 10-15 min incubation at 37°C, the ganglia were transferred to another conical tube with F-12 medium containing 1mg/ml collagenase 1A and 2.5 mg/ml dispase. After 10-15 min incubation at 37 °C, the tube was centrifuged for 30 s at 3000 rpm before the enzyme-containing supernatant was removed. The pellet was resuspended in F-12 medium either without NGF or with various concentrations of NGF (1, 30, 100 ng/ml) and mechanically dissociated with fire-polished pipettes until all obvious chunks of tissue were gone. Isolated cells were plated onto plastic cover slips that were previously coated with poly-D-lysine and laminin. The cells were maintained in F-12 medium that was supplemented with 10% horse serum, 2 mM glutamine, 100 µg/ml normocin, 50 µg/ml penicillin and streptomycin, 50 µM 5-fluoro-2'-deoxyuridine, 150 µM uridine at 37 °C and 3% CO_2 and used within 4-12 hour for electrophysiological recordings. All procedures had been approved by the Animal Use and Care Committee of the Indiana University School of Medicine.

D. Whole-cell patch-clamp recording

Recordings were made using the whole-cell patch-clamp technique. This technique was originally developed by Erwin Neher and Bert Sakmann in the 1970s. Detailed description of this technique can be found in many sources, such as the Axon Guide (Axon instruments, Foster City, CA, USA) and other highly cited papers (Hamill et al., 1981; Neher and Sakmann, 1976).

1. Instruments

The patch-clamp recording system can be divided in three parts: electronics, optical system and mechanical components. The accessories, such as perfusion system, Agar bridge, recording pipette puller and polisher are outlined below.

1). Electronics

Two different patch-clamp systems were utilized in this study. One was composed of an EPC-7 amplifier (List Electronics, Darmstadt, Germany); a customized amplifier built by Dr. Grant Nicol; an analog to digital (A-D) converter (Model TL-1, Axon instruments, Foster City, CA, USA), an oscilloscope (Model 5113, Tektronix Inc., Beaverton, Oregon) and a personal computer (Dell, Round Rock, TX). The other was composed of an Axopatch 200B amplifier (Axon Instruments, Foster City, CA, USA); an A-D converter (DigiData 1322A, Axon Instruments, Foster City, CA, USA); an oscilloscope (Model 5113, Tektronix Inc., Beaverton, Oregon) and a personal computer (Dell, Round Rock, TX).

Briefly, command signals, either holding voltages or stimulating currents, were designed by using pCLAMP 6.0.3 or pClamp 9 software to evoke APs or activate/inactivate certain types of ion channels. The digital signals generated by the computer were converted to analog signals by a digital to analogue (D-A) converter. The analog signals then were sent to sensory neurons via the amplifier and headstage, to evoke a response from the sensory neurons. The

electrical response of the sensory neuron, either membrane voltage or currents, were recorded by the headstage. After amplification and filtration, the signals were sent to an oscilloscope for monitoring and to an A-D converter to be digitized. The digitized signals were stored and analyzed in the computer by utilizing pCLAMP 6.0.3 or pCLAMP9 software (Axon Instruments, Foster City, CA, USA). A schematic of the configuration for patch-clamp recording is provided in Fig 3.

2). Optics and mechanical components

During experiments, the sensory neurons were visualized by using an inverted microscope (Model IMT-2, Olympus Corp. Tokyo, Japan) with 200× magnification. One hydraulic micromanipulator was mounted on the microscope and held the amplifier headstage. For all electrophysiological experiments, the microscope was placed on an anti-vibration table (Technical Manufacturing Corporation, Peabody, MA) with 50-60 psi maintained air pressure. A Faraday cage was placed on the air table in order to shield the experimental signal from other noises. A central ground point that connected to the water pipe located in the ceiling of the laboratory was built on the wall of the Faraday cage. The microscope and all the cables in the cage were connected to the central ground point.

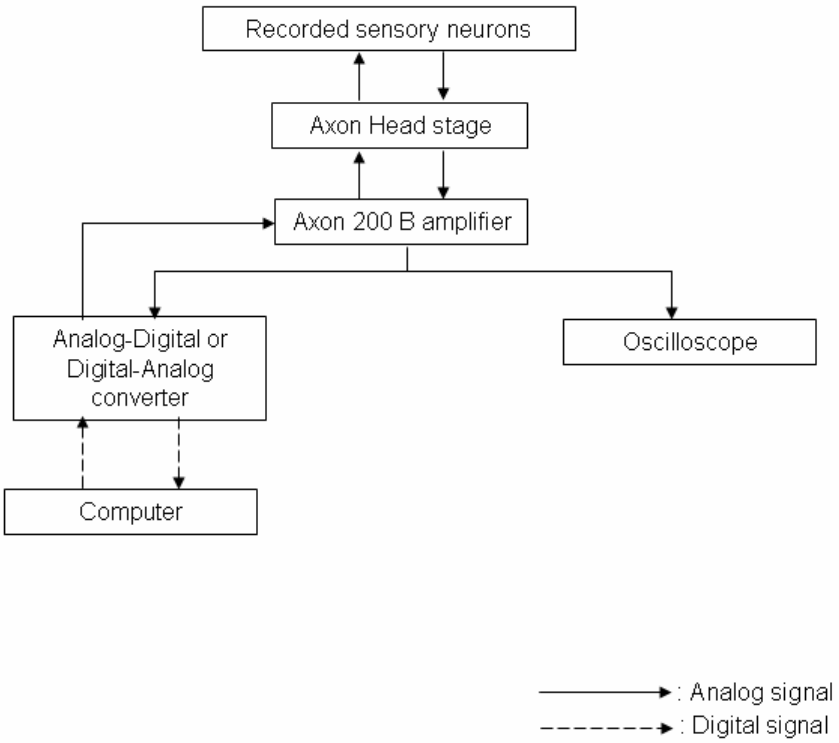

Figure 3. Schematic draft of the Patch-clamp device.

3). Superfusion system and recording chamber

During all electrophysiological experiments, a VC-8 Eight Channel Perfusion Valve Control Systems (Warner Instruments, Hamden, CT,USA) was used. The VC-8 Valve Controller was configured to control up to eight valves. Each valve was individually accessed by a manual switch for selecting perfusion solutions. During experiments, eight (or less) 60 ml reservoirs were filled with different solutions. The eight reservoirs fed into one polyethylene inflow tube connected to the recording chamber. The superfusate was aspirated from the recording chamber by a polyethylene tube connected to a collection flask. In most experiments, the solution flow was terminated during recording in order to reduce noise levels.

The recording chamber was built on a 3” × 1” glass microscope slide. The walls of the chamber were made of silicone epoxy sealant. A 1-2 mm dam, made of fast drying epoxy glue, divided the chamber into two parts, the inflow chamber and the outflow chamber. The inflow and outflow polyethylene tubing were connected to the inflow and the outflow chamber, respectively. During perfusion, the solution passed over the epoxy dam and was drawn from the recording chamber to a connected flask. The diameter of the inflow and outflow polyethylene tubing, the height of the silicone sealant wall and the epoxy dam were carefully adjusted to prevent the inflow chamber from drying. In all experiments, the recording chamber was placed in a grooved opening of an aluminum platform and stabilized with tape.

4). Agar bridge, recording pipette, pipette puller and polisher.

For all experiments, an agar bridge which served as reference electrode was placed in the recording chamber. The agar bridge was constructed from #205 polyethylene tubing filed with 2% agar dissolved in normal Ringer's solution (see below for composition). The agar bridge was connected to a Ag-AgCl electrode that was contained in an electrode holder. During experiments, the electrode holder was filled with normal Ringer's solution, and was connected to the reference input of the amplifier headstage. This electrode holder was permanently fixed to the aluminum platform that held the recording chamber.

The recording pipette for whole-cell recordings was prepared from custom 8520 glass micropipette (Warner Instruments, Hamden, CT) using a micropipette puller (Model P-87, Sutter Instruments, San Rafael, CA). The tips of the recording pipette were polished using a microforge (MF-830, Narishige, Japan). Once filled with normal pipette solution (see below for composition), the recording pipette typically had a resistance between 1-2 MΩ.

2. Solutions

1). Normal Ringer's solution

Normal Ringer's solution was the standard bath solution. During all current and voltage clamp experiments, the whole-cell configuration was established in normal Ringer's solution. The composition of the normal Ringer's solution was as follows (in mM): 140 NaCl, 5 KCl, 2 $CaCl_2$, 1 $MgCl_2$, 10 HEPES

and 10 glucose, pH adjusted to 7.4 with NaOH. To test for the sensitivity to capsaicin, 10 µl of capsaicin stock solution (1 mM, in methyl-2-pyrrolidinone, MPL) was dissolved in 100 ml of normal Ringer's solution to yield a final concentration of 100 nM.

2). N-methyl-glucamine (NMG) Ringer's solution

In order to isolate the potassium currents, the INa was eliminated by replacing NaCl in normal Ringer's solution with an equimolar impermeant cation, NMG chloride. The composition of NMG Ringer's solution was as follows (in mM): 140 NMG chloride, 5 KCl, 2 $CaCl_2$, 1 $MgCl_2$, 10 HEPES and 10 glucose, pH adjusted to 7.4 with KOH.

3). Ringer's solution for INa recording (INa Ringer's solution)

Two INa Ringer's solutions were used in this study. The sodium concentration of one INa Ringer's solution (low sodium INa Ringer's solution) was reduced in order to decrease the size of INa and thereby improve the space clamp (some neurons generate large INa responsive to the holding potential in the presents of 110 mM sodium ion in Ringer's solution, sometimes these currents saturate the amplifier). The composition of low sodium INa Ringer's solution is as follows (in mM): 30 NaCl, 65 NMG-Cl, 30 TEACl (tetraethylammonium chloride), 0.1 $CaCl_2$, 5 $MgCl_2$, 10 HEPES, pH adjusted to 7.4 with HCl and TEAOH. The osmolality was adjusted to 300-310 mOsM/l using glucose and sucrose. In order to improve the condition for obtaining TTX-S INa,

full sodium INa Ringer's solution was used. The composition of full sodium INa Ringer's solution is as follows (in mM): 110 NaCl, 30 TEACl, 0.1 $CaCl_2$, 5 $MgCl_2$, 10 HEPES, pH adjusted to 7.4 with HCl and TEAOH. The osmolality was adjusted to 300-310 mOsM/l using glucose. TEA was used in both solutions to block potassium currents. After establishing the whole-cell configuration, neurons were superfused with either low sodium or full sodium INa Ringer's solution, and stimulated with a series voltage steps (see Figure 8 for details) to record the total INa. The TTX-S INa was obtained by digital subtraction of the current traces before and after applying 500 nM TTX, a potent neurotoxin that blocks the TTX-S component of the total INa.

4). Normal pipette solution

The normal pipette solution was used in all experiments except for recording of the INa. The normal pipette solution had the following composition (in mM): 140 KCl, 5 $MgCl_2$, 4 ATP, 0.3 GTP, 2.5 $CaCl_2$, 5 EGTA (calculated free Ca^{2+} concentration of ~100 nM) and 10 HEPES, adjusted pH at 7.3 with KOH. In the experiments using the Ras blocking antibody, 30 μg/ml antibody was included in pipette solution.

5). Pipette solution for INa recording

For recording INa, the recording pipettes contained (mM): 80 aspartic acid, 80 CsOH, 55 CsCl, 10 NaCl, 5 $MgCl_2$, 4 ATP, 0.3 GTP, 1 $CaCl_2$, 10 EGTA, 10 glucose, and 10 HEPES, at pH 7.3 (adjusted with CsOH). For obtaining TTX-S

components, the recording pipettes were filled with solution with following components: 110 CsF, 25 CsCl, 10 NaCl, 5 $MgCl_2$, 4 ATP, 0.3 GTP, 1 $CaCl_2$, 10 EGTA, 10 glucose, and 10 HEPES, at pH 7.3 (adjusted with CsOH).

3. Recording procedures

All patch-clamp recordings were performed on small diameter (15-25 μm) sensory neurons that were maintained in culture for 4-12 hours after isolation. Prior to experiments, all solutions were brought to room temperature. Sensory neurons grown on plastic coverslip were removed from the culture dish in a laminar-flow hood and placed in the recording chamber filled with normal Ringer's solution. The plastic coverslip was secured to the recording chamber with a small drop of vaseline.

The recording chamber was brought to the Faraday cage and grounded with an agar bridge to the ground input of the amplifier headstage. The inflow and outflow polyethylene tubes were connected to the output of the perfusion system and the vacuum aspirator, respectively. The recording chamber was washed clean by superfusing normal Ringer's solution for several minutes. The small diameter neurons with minimum processes were selected for electrophysiology recordings. The liquid junction potential for all solutions was less than 8 mV; data were not corrected for this offset. At the end of the recordings, neurons were exposed to 100 nM capsaicin. Neurons sensitive to capsaicin (depolarized by capsaicin) are believed to be nociceptive sensory neurons (Holzer, 1991). The results using the patch-clamp technique reported in

this thesis were obtained from small diameter, capsaicin-sensitive neurons. All experiments were performed at room temperature (~23 °C).

A detailed description of patch-clamp recording process can be found in many sources, such as the Axon Guide (Axon instruments, Foster City, CA, USA) and other highly cited papers (Hamill et al., 1981; Neher and Sakmann, 1976). Briefly, under visual control, the recording pipette was lowered to touch the membrane of selected sensory neurons. After gentle suction, the cell membrane formed a tight seal with the pipette tip (giga seal, the resistance reaches more than 1 GΩ). During formation of the seal, a train of voltage pulses (5 mV) were applied to the stimulus input of the amplifier. By observing the shape of the resulting current pulses, the progress of the seal formation was monitored. After forming the seal (at least 1 GΩ), brief suction was applied to the pipette in order to rupture the attached cell membrane yielding the whole-cell configuration. The establishment of the whole-cell configuration was identified by the sudden widening of the current transients due to the inclusion of the capacitance of cell. After establishing the whole-cell configuration, the pipette has direct access to the intracellular compartment of cell, thereby delivering currents or voltage stimuli to neurons. In patch-clamp experiments, there is a potential drop across the pipette and other resistors in series with the pipette (series resistance). In order to keep the fidelity of the command potential, series resistance compensation was performed. Typically, 60-80% compensation of the series resistance could be achieved. Another factor that influenced the time resolution of changing the voltage across the cell membrane was the capacitance of the cell. When the

membrane potential was altered, there was a significant current transient in order to charge the capacitance. Since it is impossible to record any meaningful data during this transient, this transient was compensated as well in most voltage clamp recordings. By carefully manipulating the capacitance compensation provided by the patch-clamp amplifier, most transient currents were removed from the recording traces. By performing the compensation, the values of the membrane capacitance and series resistance were read directly from the amplifier. The value of cell capacitance was used to estimate the size of the recording neurons, whereas the value of the series resistance was used to estimate the accessibility of a recording pipette to internal milieu of the cell. In all voltage clamp recordings, series resistance and capacitance were monitored and compensated through entire time of the recording.

4. Electrophysiological protocols

1). Current clamp protocol

Current clamp protocols were designed to examine the neuronal excitability and other factors that regulated the firing properties of sensory neurons. The following parameters were measured from neurons.

A) AP variables.

The parameters of the AP that were measured from DRG neurons are shown in Figure 4 (Modified from Djouhri et al., 2001). These measurements indicate the properties of different ion channels in sensory neurons. For example,

the rise time of an AP (APRT) indicated the activation properties of sodium channels, whereas AP duration at 50% recovery (APD_{50}) and the falling time of an AP (APFT) represented the properties of some potassium channel subtypes, such as delayed rectifier potassium channels and calcium-dependent potassium channels. The alterations of channel properties could be inferred by examining these parameters measured from sensory neurons of different groups.

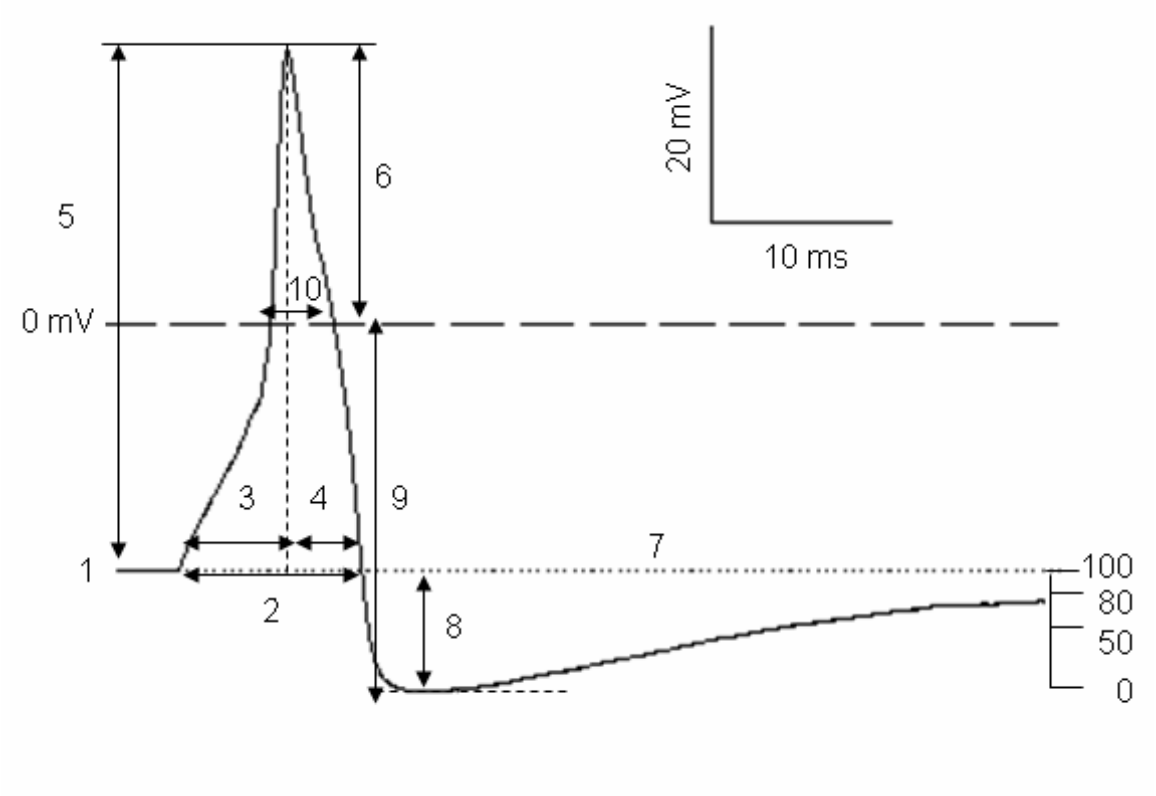

Figure 4. The measurements of AP parameters in the electrophysiology experiment (modified from Djouhri et al., 2001). The variables measured on an AP invoked by a single stimulation of the sensory neuron from DRG (dorsal root Ganglion). 1, Membrane potential; 2, APDB (AP at base); 3, APRT (AP rising time); 4, APFT (AP falling time); 5, AP height; 6, AP overshoot; 7, AHP duration to 80% recovery; 8, AHP depth measured from E_m, 9, AHP depth measured from 0 mV; 10, APD_{50}.

B) AP numbers, firing threshold and firing latency.

Figure 5A shows a representative neuron held at its resting membrane potential and APs evoked by injecting a 1 s ramp of depolarizing current that had a final amplitude of 1000 pA. AP number was the number of APs elicited by a standard amount of current. Since the amplitude of the current ramp was fixed at a specific value, the more APs elicited by the ramp, the higher the excitability of the neuron. The lower panel of Figure 5 is the *dV/dt* transformation of the APs shown in the upper panel. The baseline d*V*/d*t* was calculated as the average of all the values between the onset of the current ramp and just prior to the initiation of the AP. As described in Figure 5B, the firing threshold is the membrane voltage corresponding to the point at which d*V*/d*t* exceeded the baseline value by 20-fold. The lower the firing threshold, which means that the sensory neuron fires at a more negative membrane potential, the higher the excitability of sensory neurons. The firing latency is taken as the time between the onset of the current ramp and the time at which the firing threshold is attained (Wang et al., 2005). The shorter the firing latency (the neuron had less charging time to reach the firing threshold), the higher the excitability.

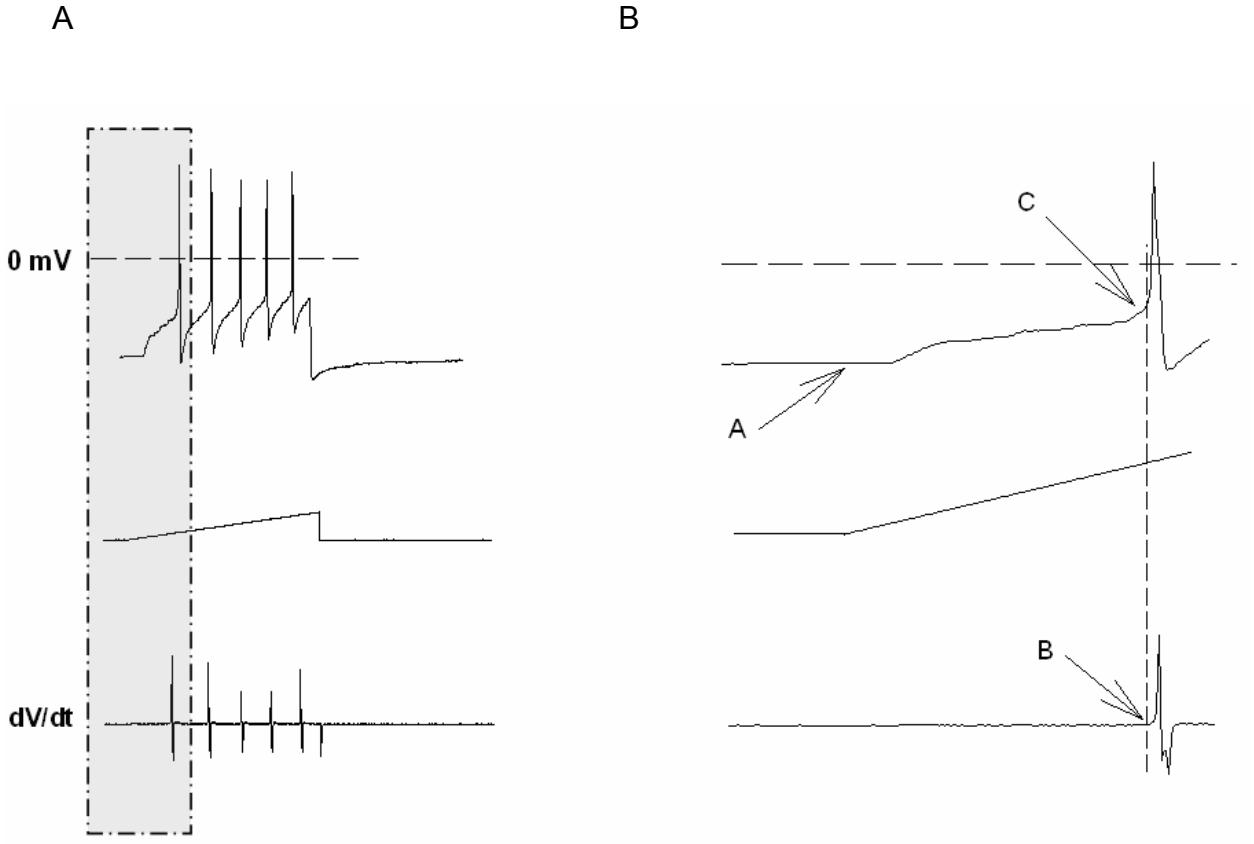

Figure 5. The method used to determine AP numbers, firing threshold and firing latency of APs recorded from isolated sensory neurons in culture. A: the neuron was held at its resting membrane potential and APs were evoked by injecting a 1 s ramp of depolarizing current that had a final amplitude of 1000 pA. Panel B is the enlarged version of the grey area of panel A. Point A: the starting point of the injected ramp current. Point B: the point whose value was 20 times above the base line value of the dV/dt trace. Point C: the firing threshold. The lower panel of A, B is the *dV/dt* transformation of the APs shown in the upper panel. See text for details.

C) Rheobase, input resistance and resting membrane potential (REM).

Rheobase is the minimum amount of current required to evoke an AP. As shown in the upper panel of Figure 6, sensory neurons were held at their resting membrane potential and injected with current steps that were 200 ms in duration; the initial step began at -30 pA and increased by 10 pA increments until an AP was elicited. The rheobase of this representative sensory neuron was 30 pA. The middle panel of Figure 6 shows the stimulation protocol used to generate the AP shown in the upper panel. The lower panel of Figure 6 demonstrates the method to determine the resistance of the cell membrane. A current-voltage plot was generated using the voltage values of points A, B, C, and D in the upper panel corresponding to the values of their stimulus currents. These results were fit with a linear regression line using SigmaPlot 9 software (Jandel Scientific, San Rafael, CA, USA). The slope of this regression line indicated the input resistance of the neuron. Resting membrane potential (REM) was determined by averaging all the data points of the recording trace whose stimulating current was 0 pA.

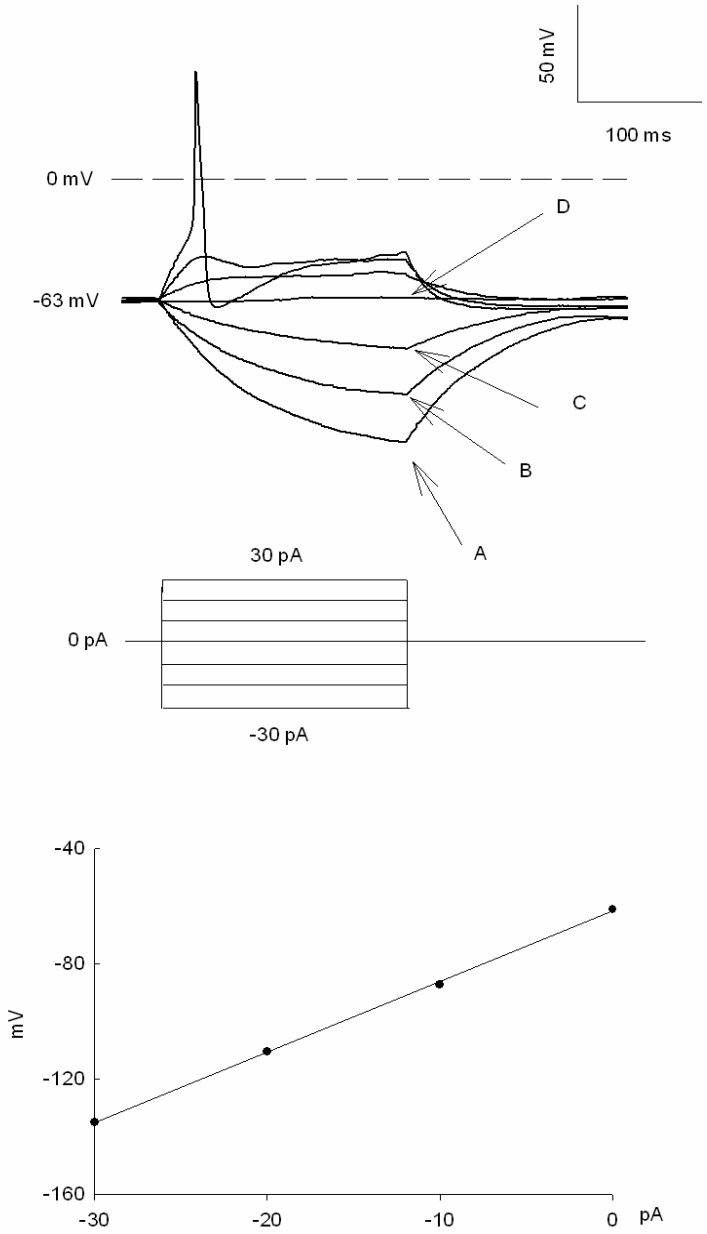

Figure 6. The method for determine rheobase, input resistance and resting membrane potential of sensory neurons. Upper panel: the change of membrane potential of a sensory neuron in responsive to the stimulating currents. Middle panel: stimulation protocol for this particular neuron. Lower panel: the current-voltage plot to determine the input resistance of the representative sensory neuron. Points A, B, C, D (upper panel): the four points whose values were plotted in the I-V trace of lower panel. See text for details.

2). Voltage clamp protocol

A) Voltage clamp protocol for recording potassium currents (IK)

A series of voltage clamp protocols for activation and inactivation of potassium currents (IK) were designed using pClamp 9 software (Axon Instruments, Foster City, CA, USA). As shown in Figure 7A, the membrane voltage was held at -60 mV; activation of the currents was determined by voltage steps of 300 ms, which were applied at 5 s intervals in +10 mV increments from -80 mV to +60 mV. Steady-state inactivation of IK was measured by applying a 15 s conditioning prepulse (-100 to +20 mV in 20 mV increments) after which the voltage was stepped to +60 mV for 200 ms; a 20 s interval separated each prepulse sweep (Figure 7B). The protocols described in Figure 7C and 7D were designed to isolate the fast inactivating potassium currents known as IA type. In Figure 7C, by utilizing the 4 s conditional prepulse to -100 mV, inactivation of the IA type of IK was removed based on previous characterization of IA performed in our laboratory (see results section for details). Activation of the currents was determined by the subsequent voltage steps of 300 ms, which were applied at 15 s intervals in +20 mV increments to +40mV. In Figure 7D, the 4 s conditional prepulse (-40 mV) inactivated IA type of potassium channels. The fast inactivating potassium currents (IA type) were obtained by digital subtraction of the current traces recorded using the protocols shown in Figure 7C and Figure 7D. The protocol in Figure 7E was designed to characterize the kinetics of potassium tail currents. In all IK recordings, after obtaining IK of sensory

neurons in normal Ringer's solution, the superfusate was changed to the NMG Ringer's solution and cells were superfused for the appropriate times. At the end of each recording, the neurons were exposed to 100 nM capsaicin. These neurons sensitive to capsaicin (depolarized by capsaicin) are believed to be nociceptive sensory neurons (Holzer 1991).

B) Voltage clamp protocol for sodium currents (INa)

As show in Figure 8, a series of voltage clamp protocols for activation and inactivation of INa were designed using pClamp 9 software (Axon Instruments, Foster City, CA, USA). For the recordings using aspartic acid and CsOH (to generate Cs-aspartate) based pipette solution, the membrane voltage was held at -60 mV after establishing the whole-cell configuration. Activation of INa was determined by voltage steps of 30 ms, which were applied at 10 s intervals in +5 mV increments from -80 to +40 mV. A 500 ms prepulse at -90 mV was used before the activation protocol to reprime the sodium channels. After obtaining the control INa in low sodium INa Ringer's solution, the superfusate was changed to the low sodium INa Ringer's solution containing 500 nM TTX and cells were superfused for the appropriate times. TTX-sensitive (TTX-S) INa was obtained by digital subtraction of the current traces recorded before and after TTX treatment. Steady-state inactivation of INa was achieved by applying a 200 ms conditioning prepulse (-100 to +10 mV in 10 mV increments) after which the voltage was stepped to +0 mV for 30 ms; a 5 s interval separated each prepulse sweep.

In order to maximize the condition for obtaining TTX-S INa, CsF based pipette solution was used. The membrane voltage was held at -100 mV after establishing the whole-cell configuration. Activation of INa was determined by voltage steps of 30 ms, which were applied at 10 s intervals in +5 mV increments from -80 to +40 mV. A 5 s interval separated each prepulse sweep. After obtaining the control INa in full sodium INa Ringer's solution, the superfusate was changed to the full sodium INa Ringer's solution containing 500 nM TTX and cells were superfused for the appropriate times. TTX-S INa was obtained by digital subtraction of the current traces recorded before and after TTX treatment.

5. Analysis and statistical procedures of electrophysiological recordings

All values represent the mean ± standard error of the mean (SEM). The voltage dependence for activation of IK was characterized by fitting the value of the peak currents responsive to their holding voltages with the Boltzmann relation $G/G\text{max} = 1/[1+\exp(V_{0.5}-V_m)/k]$, where G is the conductance that was determined from the equation $G = I/(V_m-V_E)$. I is the measured membrane current, V_m is the voltage step, and E is the equilibrium potential (calculated to be -84 mV for IK). G_{max} is the maximum conductance, $V_{0.5}$ is the voltage for half-maximal activation, V_m is the holding voltage, and *k* is a factor describing the steepness of the relation. The Boltzmann parameters (G_{max}, $V_{0.5}$, k) were determined for each individual neuron from which the mean ± S.E.M. was calculated. The peak IK responsive to their holding potentials was determined isochronally at a chosen time at which most of the currents were close to their peak value.

To fit the peak IK obtained after 15 s conditional prepulses from -100 mV to + 20 mV as described in Figure 7B, the Boltzmann relation $G/G_{max} = c+\{(1-c)/[1+\exp(V_{0.5}-V_m)/k]\}$ was used. C is the fraction of non-inactivating current (defined as the peak current obtained at +60 mV for the +20 mV prepulse) and the other parameters are as defined above. Fits were performed using the curve fitting protocols in SigmaPlot 9.0 (Jandel Scientific, San Rafael, CA, USA).

The voltage dependence for activation of INa was characterized by fitting the value of the peak currents responsive to their holding voltage with the Boltzmann relation as described above. The peak INa was determined by choosing the data point that has the biggest value compared to other points responsive to the same holding potential. The equilibrium potential for INa was determined individually for each neuron. For example, for a neuron generated -212 and 129 pA peak current responsive to 25 mV and 30 mV holding potential, a scatter plot describing the I-V relationship was created using SigmaPlot 9.0 soft ware. A linear regression line that is the best fit the data was generated. The reversal potential (equilibrium potential) was determined using the value of the point on the regression line (in mV) whose corresponding current was 0 pA. In this particular example, the reversal potential was 28 mV.

To fit the peak INa obtained after 200 ms conditional prepulses from -100 mV to + 10 mV as described in Figure 8B, the Boltzmann relation $G/G_{max} = c+\{(1-c)/[1+\exp(V_{0.5}-V_m)/k]\}$ was used. c is the fraction of non-inactivating current (defined as the peak current obtained at 0 mV for the +10 mV prepulse) and the

other parameters are as defined above. Fits were performed using the curve fitting protocols in SigmaPlot 9.0 (Jandel Scientific, San Rafael, CA, USA).

Statistical differences between the control recordings and those obtained under various treatment conditions were determined by using either a Student's t-test, analysis of variance (ANOVA), or a repeated measure ANOVA (RM ANOVA). When a significant difference was obtained with an ANOVA, *post hoc* analyses were performed using a Dunnett's analysis, as appropriate and is specified in the text. Values of $P < 0.05$ were judged to be statistically significant.

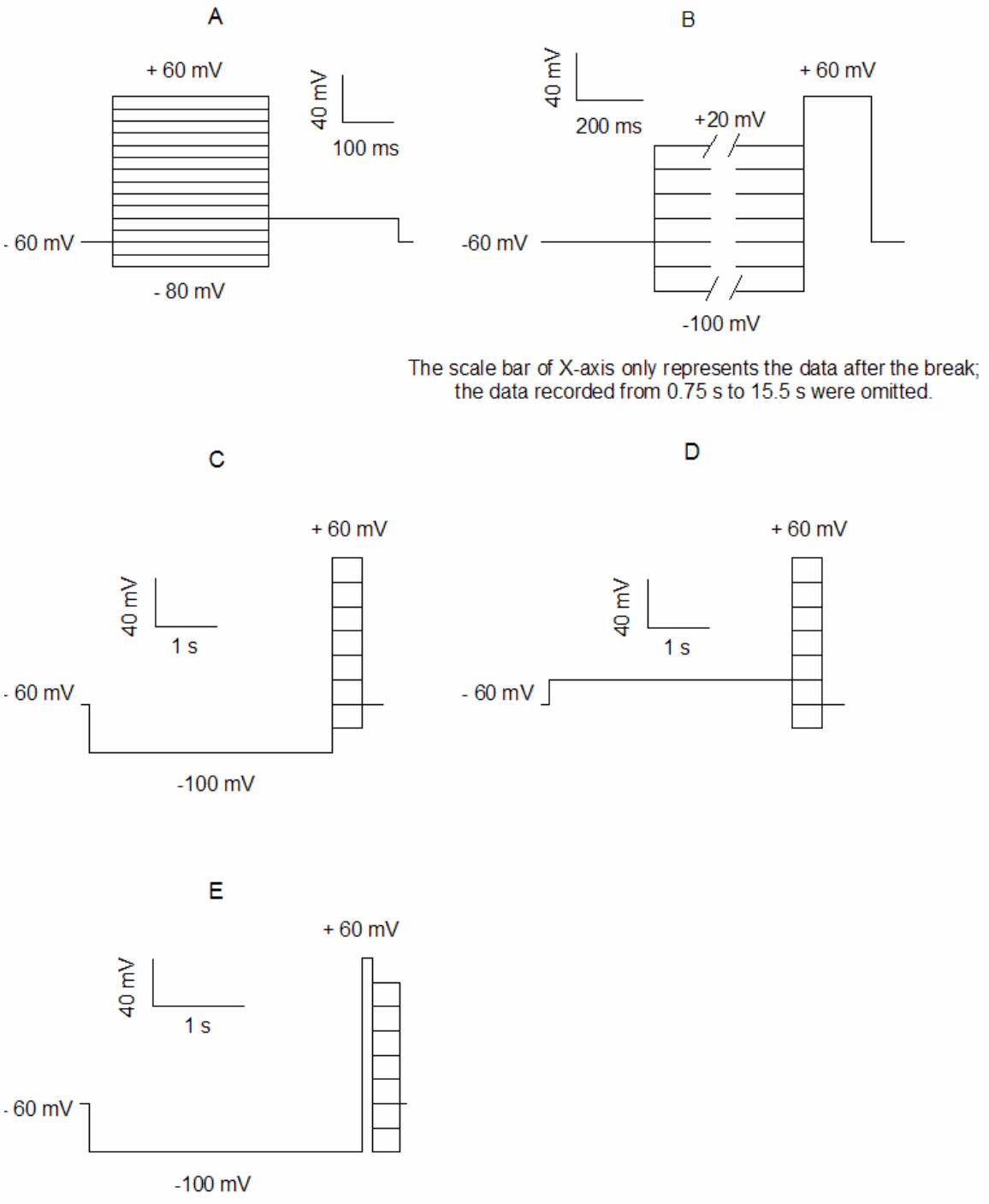

Figure 7. Protocols for the activation or inactivation of IK.

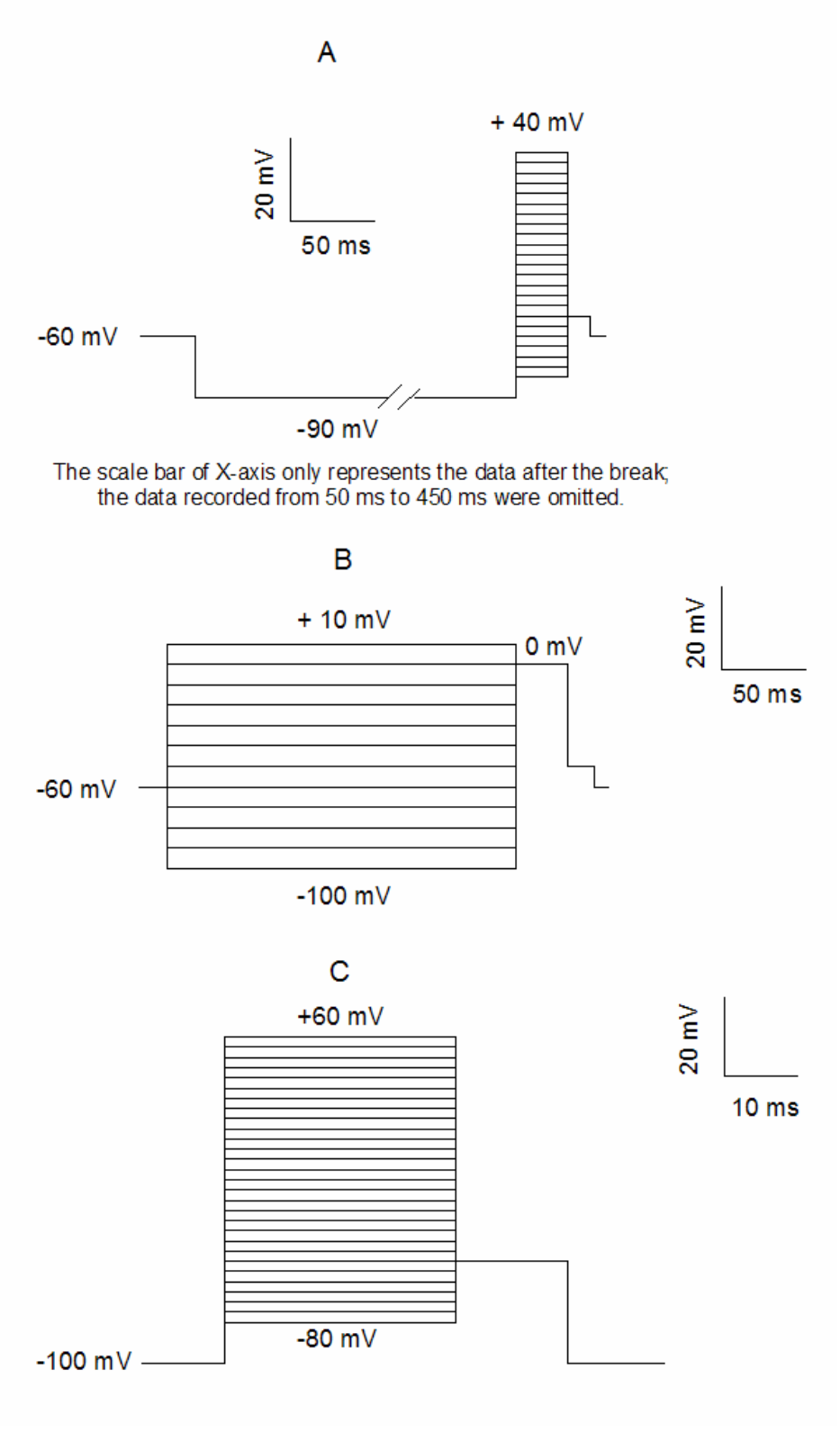

Figure 8. Protocols for the activation or inactivation of INa.

III. RESULTS

A. Sensory neurons from *Nf1+/-* mice have higher excitability than neurons from *Nf1+/+* mice.

Neurofibromatosis type 1 (NF1) is a common genetic disease that is characterized by multiple tumor formation. In addition, some people with NF1 also experience much more intense painful sensations to stimuli, such as minor injuries, that elicit only slight discomfort in normal people (Creange et al., 1999; Wolkenstein et al., 2001). Although the mechanism by which the NF1 mutation causes these symptoms has not been elucidated, it is likely that these abnormal painful states involve the sensitization (an exaggerated response to stimuli that generates more APs, or releases more neuronal transmitters) of small diameter nociceptive sensory neurons, cells that are known mediate the transmission of pain and itch.

Using isolated sensory neurons from a mouse model of neurofibromatosis (*Nf1+/-*), Hingtgen et al., (2006) found that the capsaicin or high potassium evoked release of SP and CGRP was increased in sensory neurons from *Nf1+/-* mice compared to wild-types. The increase in the release of these two peptides indicates a significant enhancement of the sensitivity of *Nf1+/-* neurons to noxious stimuli. Therefore, it is logical to infer the excitability of *Nf1+/-* neurons is enhanced. In this section, we explored the idea whether *Nf1+/-* neurons had augmented excitability compared to wild-types by using the whole-cell patch-clamp technique.

Several measures of excitability were used in this study. First is the number of APs elicited by a given amount of current. The neuron was held at its resting membrane potential and APs were evoked by injecting a 1 s ramp of depolarizing current that had a final amplitude of 1000 pA. The AP numbers evoked by the depolarizing ramp current were counted. Since the amplitude of the current ramp was fixed at a specific value (1000 pA), the more APs elicited by the ramp, the higher the excitability of the neuron. Figure 9 shows recordings from representative neurons in response to the current ramp from *Nf1*+/+ (A) and *Nf1*+/- (B) mice. As can be easily appreciated, identical ramps of current elicited 5 APs from the *Nf1*+/+ neuron, but 14 APs from the *Nf1*+/- neuron. Figure 10A summarizes the responses of 8 neurons in the *Nf1*+/+ group and 11 neurons in the *Nf1*+/- group. For identical stimuli, sensory neurons from *Nf1*+/- mice generated significantly more APs compared with *Nf1*+/+ neurons (6.0 ± 1.6 versus 14.8 ± 2.2 APs for *Nf1*+/+ and *Nf1*+/- neurons, respectively, $P < 0.05$ using a t-test). At the end of each recording, the neurons were exposed to 100 nM capsaicin. Figure 9C shows a typical neuronal response to capsaicin (100 nM). These neurons sensitive to capsaicin (depolarized by capsaicin) are believed to be nociceptive sensory neurons. The data reported in this work were obtained from capsaicin-sensitive neurons only.

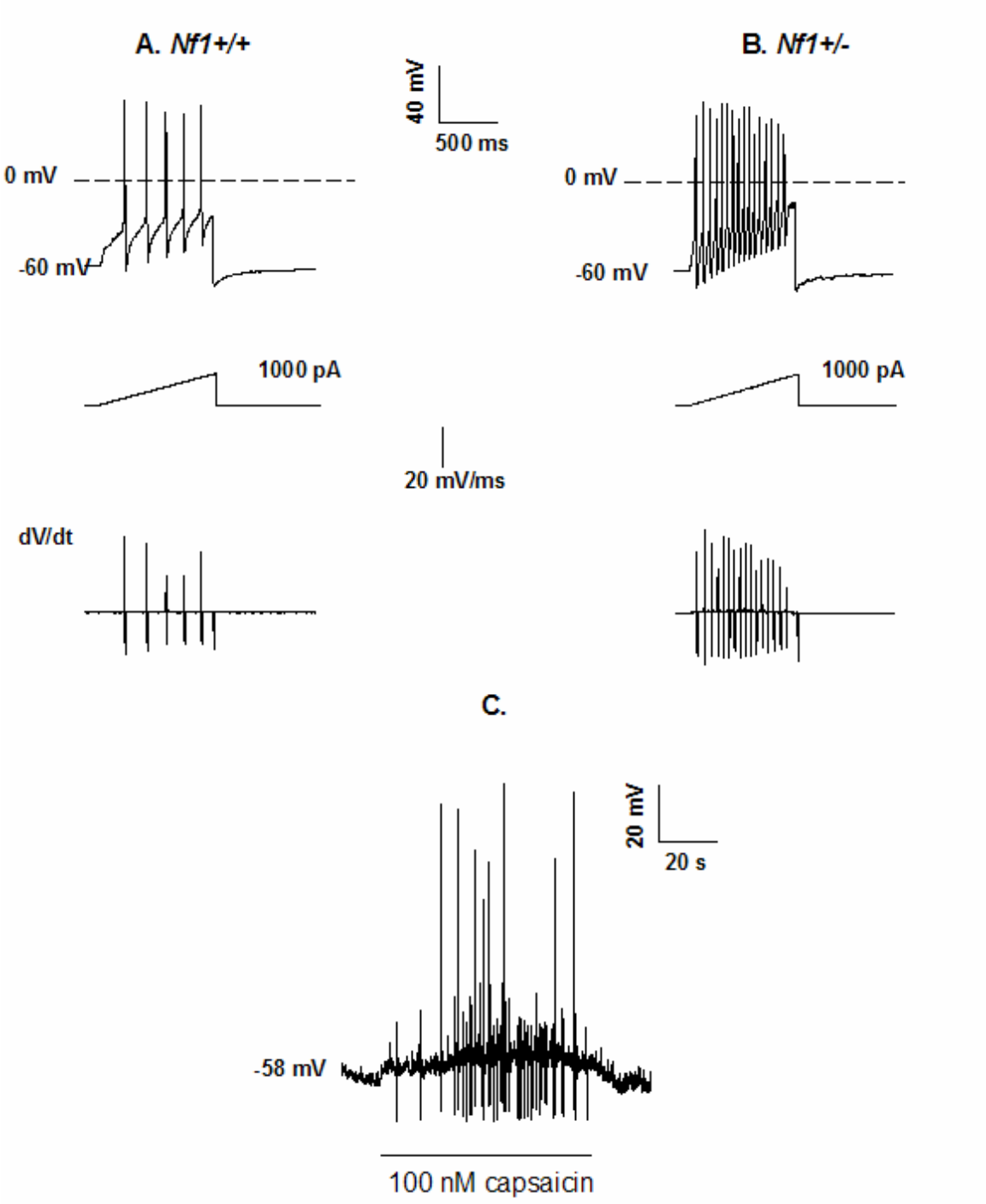

Figure 9. (Legend see next page).

Figure 9. *Nf1+/-* sensory neurons generate more APs in response to a given stimulus than *Nf1+/+* neurons. Voltage recordings from representative sensory neurons isolated from either a *Nf1+/+* (A) or a *Nf1+/-* mouse (B) illustrate the number of APs evoked by the ramp of current. The neurons were held at their resting membrane potential and APs were evoked by injecting a 1s ramp of depolarizing current that had a final amplitude of 1000 pA. The d*V*/d*t* trace represents the differentiation of the membrane voltage. The baseline d*V*/d*t* is calculated as the average of all the values between the injection of the ramp current and just prior to the initiation of the AP. The firing threshold is the membrane voltage corresponding to the point at which d*V*/d*t* exceeds the baseline value by 20-fold. The firing latency is calculated as the time between the onset of the current ramp and the time at which the firing threshold is attained. C. a typical neuronal response to capsaicin.

Two additional parameters indicative of the level of neuronal excitability are the firing threshold and firing latency. These measurements were determined in the same neurons for which the number of APs evoked by the current ramp was assessed in the preceding text. The firing threshold is the membrane voltage at which the AP is generated and was determined as described in the Methods. A lower firing threshold means that the sensory neuron fires at a more negative membrane potential, therefore, the neuron has higher excitability. As summarized in Figure 10B, neurons isolated from *Nf1+/-* mice had a significantly lower firing threshold compared with that of *Nf1+/+* neurons (-31.7 ± 1.6 vs. -25.7 ± 1.3 mV for 11 *Nf1+/-* and 8 *Nf1+/+* neurons, respectively, t-test). A lower firing threshold suggests that the *Nf1+/-* neurons are capable of generating APs at more hyperpolarized membrane potentials. Similar to the firing threshold, the firing latency, or the time from the onset of the current injection to the initiation of the first AP, was significantly shorter in the *Nf1+/-* sensory neurons (Figure 10C; 230 ± 55 versus 85 ± 14 ms, for 8 *Nf1+/+* and 11 *Nf1+/-* neurons, respectively, t-test). The shorter the firing latency, the higher the excitability of sensory neurons as this would suggest that the neuron had less charging time to reach the firing threshold. However, there was no difference in the average values for the resting membrane potentials between these genotypes (see Figure 10D, -62.7 ± 1.8 versus -60 ± 2.0 mV for 8 *Nf1+/+* and 11 *Nf1+/-* neurons, respectively). These results demonstrate that the firing threshold was reduced in neurons isolated from the *Nf1+/-* mice.

Consistent with this observation was the finding that the rheobase (the minimum amount of current required to evoke an AP) also was reduced in *Nf1*+/- neurons. Representative recordings to determine the rheobase from a *Nf1*+/+ and *Nf1*+/- neuron are shown in Figures 11A and B, respectively. As summarized in Figure 11C, *Nf1*+/- neurons had a significantly lower rheobase value compared with *Nf1*+/+ neurons (56 ± 9 versus 154 ± 36 pA for 11 *Nf1*+/- and 8 *Nf1*+/+ neurons, respectively, using a t-test). However, the input resistance was not significantly different between the two genotypes (712 ± 191 MΩ for *Nf1*+/+ neurons and 795 ± 79 MΩ for *Nf1*+/- neurons, Figure 11D). In addition, the AP variables, such as APD_{50} and the amplitude of AHP measured from REM, were not significantly different (APD_{50} was 5.3 ± 0.2 ms, n=8 and 3.86 ± 0.4, n=11 for *Nf1*+/+ and *Nf1*+/- neurons, respectively. The amplitude of AHP was 10.7 ± 1.1 mV, n=8 and 13.7 ± 1.76 mV, n=11 for *Nf1*+/+ and *Nf1*+/- neurons, respectively. Data for other AP variables were not shown). Taken together, these data clearly demonstrate that capsaicin-sensitive sensory neurons isolated from mice that are heterozygous for the *Nf1* mutation exhibit enhanced excitability compared with capsaicin-sensitive sensory neurons from *Nf1*+/+ mice.

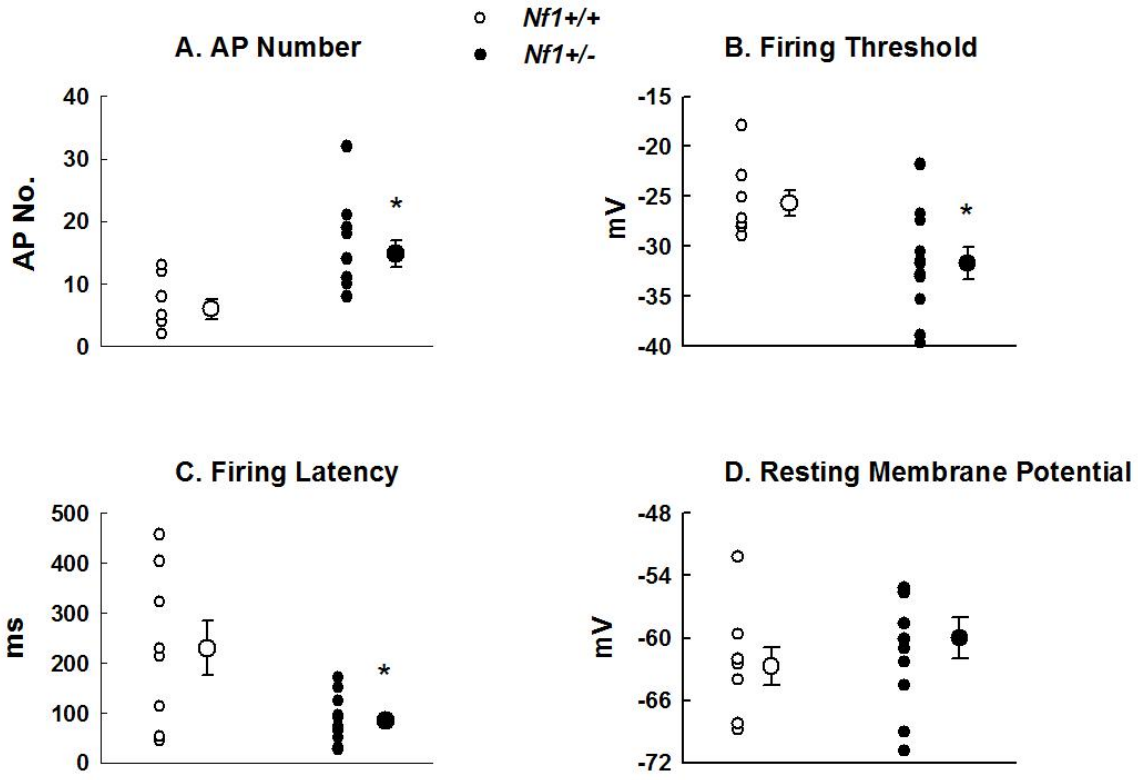

Figure 10. *Nf1+/-* sensory neurons exhibit increased excitability compared with *Nf1+/+* neurons. To the right of each series of individual values is the mean ± SEM for each genotype (The error for the firing latency of *Nf1+/-* neurons in C is smaller than the symbol). The values in each panel are from the same 8 *Nf1+/+* and 11 *Nf1+/-* neurons. The asterisks represent a statistically significant difference between genotypes using a t-test ($P < 0.05$).

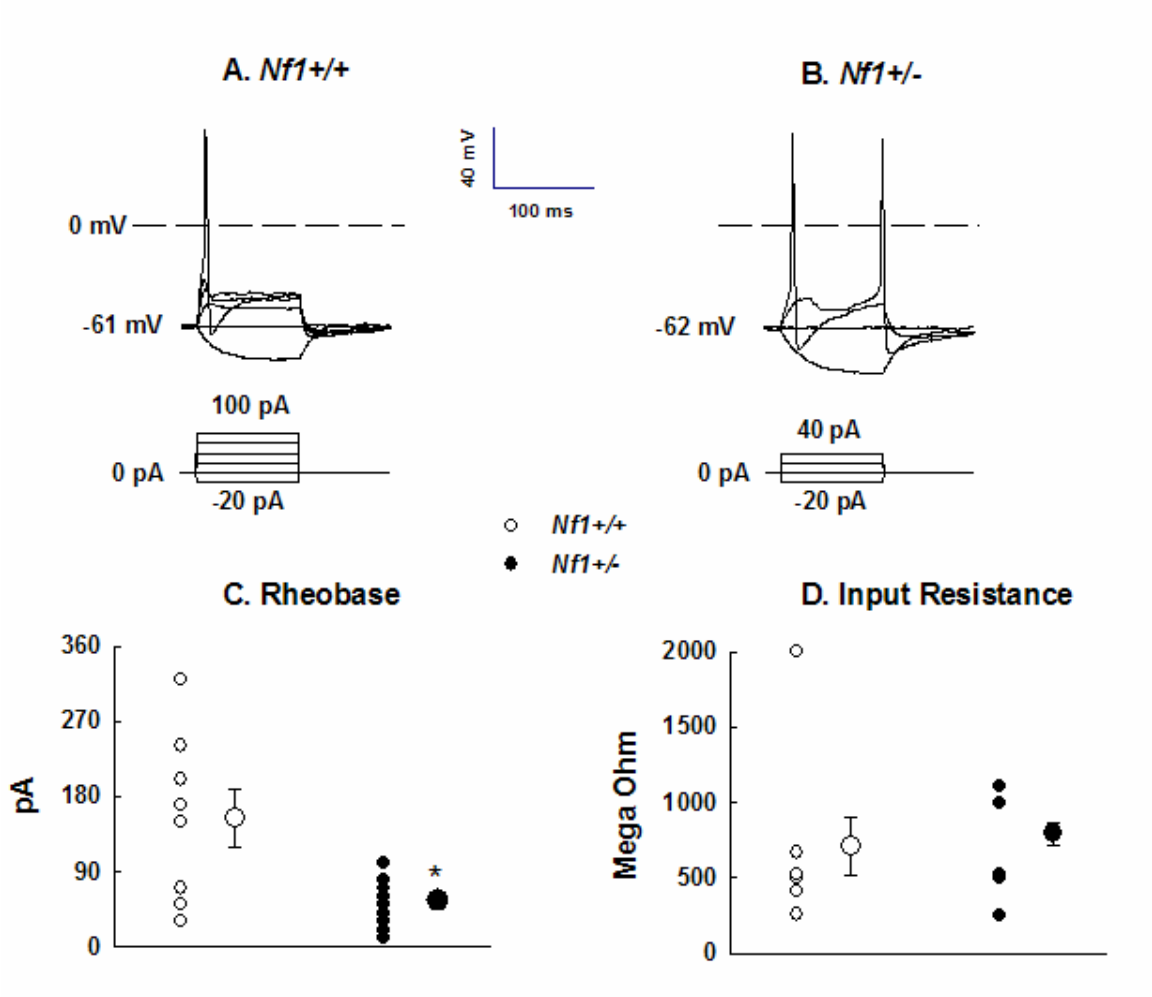

Figure 11. Sensory neurons from *Nf1+/-* mice show a lower rheobase compared with *Nf1+/+* neurons. Sensory neurons were held at their resting membrane potential and injected with current steps 200 ms in duration that began with a -20 pA step and increased by 20 pA increments until an AP was elicited. The rheobase is taken as the minimum current required to elicit an AP. Panels C and D summarize the rheobase and input resistance values, respectively, for 8 *Nf1+/+* and 11 *Nf1+/-* neurons. The mean ± SE is given to the right of each group. The asterisks represent a statistically significant difference between genotypes using a t-test ($P < 0.05$).

B. Treatment with NGF enhances the excitability of *Nf1*+/+ sensory neurons and mimics the effects of the *Nf1* mutation

NGF is a growth factor known to increase the excitability of small diameter, capsaicin-sensitive sensory neurons (Zhang et al., 2002) and is known to activate the Ras transduction cascade (Blochl et al., 2004; Huang and Reichardt 2003; Kaplan and Stephens 1994; Susen et al., 1999). Few investigations examined whether NGF augmented neuronal firing by activating Ras signaling pathway. Since *Nf1*+/- neurons supposedly have augmented Ras-GTP, whether NGF sensitizes *Nf1*+/- neurons in the same manner as in *Nf1*+/+ neurons could indicate the importance of Ras in NGF-induced sensitization. Therefore, the actions of NGF on excitability in *Nf1*+/+ and *Nf1*+/- sensory neurons were examined. The sensory neurons were maintained in culture media containing either no added NGF (to examine the excitability of cells without exogenous stimulation of Ras activity) or different concentrations of NGF (1, 30, and 100 ng/ml), to examine the excitability of cells with exogenous stimulation of Ras at different concentrations of NGF. The resting membrane potential, AP number, firing threshold, firing latency and rheobase were measured under conditions with different concentrations of NGF in culture media.

1. The presence of NGF in the culture media enhances the excitability of *Nf1*+/+ sensory neurons.

As shown in Figure 12A, incubation with NGF for 5-12 hours caused a significant increase in the number of APs elicited by a standard ramp of depolarizing current in capsaicin-sensitive sensory neurons isolated from *Nf1*+/+ mice. The number of evoked APs was significantly higher after treatment with NGF at 30 and 100 ng/ml (there were no significant difference between the values obtained from neurons with 1 ng/ml NGF and without NGF). For example, the number of evoked APs increased from 5.9 ± 1.5 (n=8) in the absence of NGF to 14.8 ± 2.8 (n=6) after exposure to 100 ng/ml NGF for *Nf1*+/+ neurons. NGF also decreased the firing latency and rheobase of *Nf1*+/+ sensory neurons (Figure 12C and D). Firing latency was significantly shortened from 229.7 ± 55.0 ms (n=8, no added NGF in media) to 58.2 ± 2.8 ms (n=10, 30 ng/ml NGF in media) or 63.8 ± 14.1ms (n=6, 100 ng/ml NGF in media). Similar to the firing latency, the rheobase of *Nf1*+/+ neurons was decreased by NGF. The rheobase of *Nf1*+/+ neurons in media containing no added NGF was 153.8 ± 35.5 pA (n=8) and was significantly higher compared to *Nf1*+/+ neurons treated with 30 ng/ml NGF (37.0 ± 4.2 pA, n=10) or 100 ng/ml NGF (35 ± 5.6 pA, n=6). The change in firing threshold measured in *Nf1*+/+ neurons treated with the higher concentrations of NGF (30 ng/ml and 100 ng/ml) was not statistically different from neurons not treated with NGF (Figure 12B). These data demonstrated that NGF dramatically altered the excitability of capsaicin-sensitive sensory neurons isolated from *Nf1*+/+ mice. Interestingly, NGF did not depolarize the resting

membrane potential of *Nf1*+/+ neurons from adult mice. The resting membrane potential of *Nf1*+/+ neurons was -63.0 ± 2.0 mV (n=8) in media containing no added NGF, which was not significantly different from the value obtained from neurons treated with NGF at various concentrations (-58.7 ± 1.6 mV, n=15; -56.5 ± 2.7 mV, n=10; -56.4 ± 2.8 mV, n=6 for the neurons treated by 1, 30, 100 ng/ml, respectively).

2. The presence of NGF in the culture media has little effect on the excitability of *Nf1*+/- sensory neurons.

To determine whether NGF alters the excitability of *Nf1*+/- neurons, the cells were maintained in culture media with NGF at various concentrations. Surprisingly, the presence of NGF in the culture media did not alter the excitability of *Nf1*+/- neurons. As shown in Figure 12A, NGF did not enhance the number of APs elicited by a standard ramp of depolarizing current (1000 pA) in capsaicin-sensitive sensory neurons isolated from *Nf1*+/- mice. The number of evoked APs from sensory neurons maintained in the absence of NGF was 14.8 ± 2.2 APs (n=11), which was not significantly different from the value obtained in neurons with 1 ng/ml, 30 ng/ml or 100 ng/ml NGF in culture media (17.8 ± 2.8, 15.5 ± 3.6, 11.8 ± 2.7 APs, respectively, n=5-12). A similar lack of effect of NGF on firing latency and rheobase was observed in *Nf1*+/- sensory neurons. The firing latency of *Nf1*+/- neurons without added NGF was 85 ± 14.2 ms, which was not significantly different from the value measured from *Nf1*+/+ neurons maintained in media containing 1ng/ml, 30 ng/ml, and 100 ng/ml NGF (43.7 ± 4.0

ms, 58.2 ± 2.8 ms and 77.4 ± 10 ms, respectively, n=5-12). NGF did not alter the input resistance of sensory neurons isolated from either genotype. The input resistance of *Nf1*+/+ neurons was 712.4 ± 190.8 MΩ, 794.6 ± 73.4 MΩ, 455.3 ± 52.0 MΩ and 807.3 ± 255.4 MΩ for neurons treated with 1 ng/ml, 30 ng/ml or 100 ng/ml NGF in the culture media, respectively. The input resistance for *Nf1*+/- sensory neurons was 876.3 ± 191 MΩ, 835.2 ± 172.2 MΩ, 645.2 ± 100 MΩ and 687 ± 165 MΩ for neurons treated with 1 ng/ml, 30 ng/ml or 100 ng/ml NGF in culture media, respectively.

In summary, treatment with NGF enhanced the excitability of *Nf1*+/+ neurons, but had no effect on the excitability of *Nf1*+/- sensory neurons. As a consequence, the difference in excitability observed between the genotypes in the absence of NGF was abolished after high doses of NGF (30 ng/ml and 100 ng/ml).

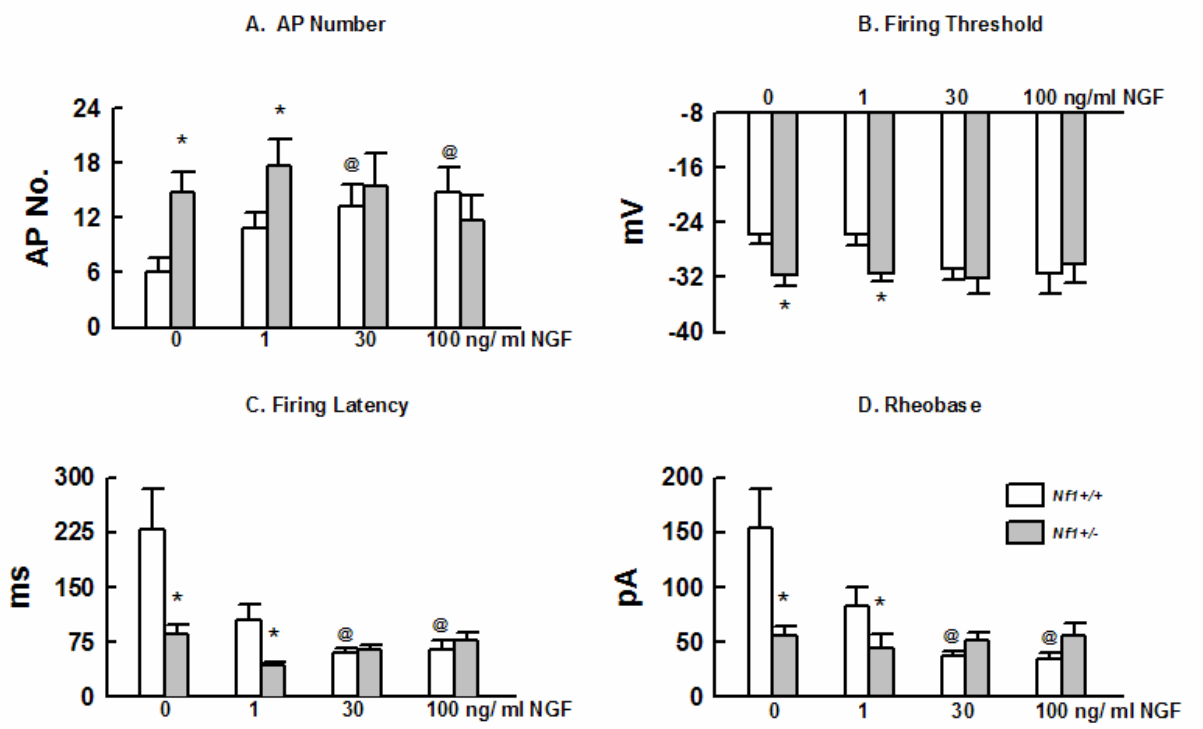

Figure 12. NGF enhances the excitability of *Nf1*+/+ neurons, but has little effect on *Nf1*+/- neurons. Sensory neurons isolated from adult mice were maintained in growth media for 5-12 hours in the absence or presence of NGF prior to recordings. The columns represent the means ± SEM (5-12 neurons per group). A depolarizing current ramp (1000 pA) was used to elicit APs. *, statistically significant difference between genotypes at a given concentration of NGF using a t-test ($P < 0.05$). @, statistically significant difference between NGF treatments within a given genotype using a one way ANOVA followed by using a Dunnet's post hoc analysis ($P < 0.05$).

C. Y13-259, a neutralizing antibody for Ras, abolishes the NGF-induced sensitization of *Nf1*+/+ sensory neurons, but does not reduce the enhanced excitability of *Nf1*+/- neurons.

Since *Nf1*+/- neurons have only one functional copy of the *Nf1* gene, the protein product of this gene, neurofibromin, should be lower in *Nf1*+/- neurons. Neurofibromin helps to switch the active form of Ras (Ras-GTP) to its inactive form (Ras-GDP) by serving as a GTPase activating protein (GAPs). The decrease of neurofibromin levels frequently results in both basal and cytokine-stimulated Ras activity in many cell types, including sensory neurons (Guha et al., 1996; Ingram et al., 2001; Klesse and Parada, 1998; Largaespada et al., 1996; Sherman et al., 2000). To determine whether the enhanced excitability of *Nf1*+/- neurons was dependent on the Ras signaling pathway, a specific Ras-blocking antibody, Y13-259 (Oncogene Science, Uniondale, NY), was used to neutralize intracellular Ras activity. Y13-259 neutralizes Ras by directly binding to amino acid residues of the Ras protein and stimulates the intrinsic GTPase activity of Ras; this converts the active Ras back to its inactive form (Sigal et al., 1986). This antibody (30 μg/ml) was added to the solution filling the pipette and internally perfused into the neurons. Although the capacity of this antibody to neutralize Ras activity is well established, only a few studies have used internal perfusion. For example, Hida et al., (1998) showed that the inhibition of inwardly rectifying potassium currents (IKir) by ceramide, an important lipid second messenger, was abolished by inclusion of 0.2 μg/ml Y13-259 in the recording pipettes. In addition, Fitzgerald and Dolphin (1997) reported that neutralization of

endogenous Ras by microinjection of Y13-259 solution (0.1 mg/ml, 20 femto liter reduced the peak calcium current recorded from DRG neurons isolated from neonatal rats. As a rough calculation, if one injected 20 femto liter of a 0.1 mg/ml antibody solution into a spherical neuron that was 25 μm in diameter, then the intracellular concentration was approximately 0.25 μg/ml. Because 30 μg/ml Y13-259 is more than 100 times the value appearing in the literature, I would expect this concentration to be sufficient to block intracellular Ras activity.

Another factor that must be considered in the experiments delivering the antibody inside a cell by internal perfusion is the necessary length of time for the antibody to enter the cell. Pusch and Neher (1988) extensively studied the diffusional time course of small molecules up to 15 kD entering cells via diffusion from the recording pipette. Based on the formulas provided in their paper, the time constant (τ, describing how fast a diffusing system reaches equilibrium) could be calculated by using the following equations:

$$\tau = (78.44 \pm 6.6) * R_A/D \quad (1)$$

$$\tau = (0.6 \pm 0.17)*R_A*M^{1/3} \quad (2)$$

$$\tau/\tau_0 = (C_M/C_o)^{1.5} \quad (3)$$

where R_A is the access resistance in MΩ, D is the diffusion coefficient in $10^{-11}m^2s^{-1}$, molecular weight (M) is in Daltons, τ_o is the time constant for cells having a mean capacitance of 5.91 pF (C_o), C_M is the cell capacitance. For mouse DRG neurons with 12.8 ± 1.1 pF capacitance (the series resistance was 5.3 ± 0.9 MΩ

in my patch-clamp experiments, n=23), τ was calculated to be between 5 and 9 min. Thus, 15 min should be sufficient for a considerable amount of antibody to enter the cells after establishing the whole-cell configuration.

Therefore, in order to examine whether this antibody decreased the neuronal excitability of *Nf1+/-* neurons by neutralizing intracellular Ras activity, the antibody was delivered inside sensory neurons via diffusion from the recording pipette after establishing the whole-cell configuration. As shown in Figure 13, the design of the experimental group was as follows: after establishing the whole-cell configuration, the control recording was obtained after 1-2 min to determine the basal excitability of either mouse genotype using the protocols described in the Materials and Methods section. At 5, 10 and 15 min after establishing the whole-cell configuration, the current clamp protocols were used to examine the effect of internal perfusion of the Ras-blocking antibody on the excitability of sensory neurons. Immediately after the 15 min recording, the neuron was exposed to NGF (100 ng/ml) via bath perfusion. My data presented above demonstrated that NGF increased neuronal excitability of *Nf1+/+* neurons. If NGF sensitizes neurons via Ras activation, the effect of NGF should be abolished by this antibody. In addition, the efficacy and the length of time necessary for the antibody to diffuse into cells could be established if the antibody successfully abolished the NGF-induced sensitization (based on the assumption that most neurons could be sensitized by NGF). The purified non-specific rat IgG was used as negative control. To eliminate the possibility that a high concentration of antibody in the pipette may alter the ability of neurons to be

sensitized, the obvious control experiment is to examine whether NGF can enhance the excitability of neurons in the presence of 30 μg/ml non-specific rat IgG in the pipette. In addition, if activation of the Ras cascade contributed to the enhanced excitability of sensory neurons from *Nf1*+/- mice, I would expect the neurons treated with Y13-259 to have lower excitability compared to untreated neurons from the same *Nf1*+/- harvest, and be similar to the excitability of those neurons isolated from *Nf1*+/+ mice. However, if the Y13-259 fails to decrease the excitability of *Nf1*+/- neurons, it is possible the downstream effectors that are critical in modulating neuronal excitability are activated by Ras, and this activation lasts longer than my recording period. The experimental design is summarized in Figure 13.

1. Internal perfusion with the non-specific IgG does not affect the sensitization of *Nf1*+/+ neurons by NGF

It is well established that NGF enhances the excitability of isolated sensory neurons in culture (Wang et al., 2005; Zhang et al., 2002). The studies described below examined whether the presence of non-specific IgG (30 ng/ml) in the pipette altered this NGF-induced sensitization.

As shown in Figure 14E, NGF (100 ng/ml) caused a significant increase in the number of APs elicited by a standard ramp of depolarizing current in a representative *Nf1*+/+ sensory neuron in the presence of IgG in the pipette. As summarized in Figure 14F, in six *Nf1*+/+ sensory neurons, after exposure to NGF (100 ng/ml), the number of evoked APs increased to 5.0 ± 1.0 compared with 3.2

± 0.7 in the absence of NGF. In the first 15 min period of recording (before treatment with NGF), the evoked APs remained constant (the evoked APs were 3.0 ± 0.5, 3.0 ± 0.9, 2.8 ± 0.9 for 5 min, 10 min, 15 min, respectively, n=6). This finding suggests that the control antibody does not alter the basal neuronal excitability of *Nf1*+/+ neurons in this 15 min recording.

Consistent with the increased production of APs, NGF also significantly decreased the rheobase in the *Nf1*+/+ neurons in the presence of IgG in pipette. The rheobase of *Nf1*+/+ neurons was decreased from 110.0 ± 19.8 to 33.3 ± 7.1 pA after applying 100 ng/ml NGF (the rheobase of *Nf1*+/+ neurons was 108 ± 19.7, 98 ± 14.2, 91 ± 16.8 pA for 5 min, 10 min, 15 min, respectively, n=6). NGF did not depolarize *Nf1*+/+ sensory neurons. The REM of *Nf1*+/+ neurons was constant over the 20 min testing period, even after applying NGF (The REM was -56 ± 2, -57 ± 2, -56 ± 1, -55 ± 2, -53 ± 1.5 mV for control, 5 min, 10 min, 15 min, and after 5 min exposure to NGF, respectively, n=6). Firing threshold is another parameter that was not altered by NGF. The firing threshold of *Nf1*+/+ neurons was -28 ± 2 mV after applying NGF, and was not significantly different from the firing thresholds measured under the IgG control conditions, the firing threshold was -27 ± 2, -26 ± 3, -25 ± 3, -25 ± 2 mV for control, 5 min, 10 min and 15 min, respectively, n=6. Similar to REM and firing threshold, the membrane resistance of *Nf1*+/+ neurons was not altered by NGF. The membrane resistance of *Nf1*+/+ neurons remained constant over the 20 min recording period (the membrane resistance was 789 ± 171, 605 ± 99, 657 ± 116, 534 ± 112 MΩ and 539 ± 112 MΩ at 1 min, 5 min, 10 min, 15 min and 20 min, n=6). In summary, these data

demonstrated that NGF enhanced the excitability of *Nf1+/+* sensory neurons from adult mice on a rapid time scale by enhancing the frequency of neuronal firing. The firing threshold, REM and membrane resistance were not altered by NGF. The presence of 30 µg/ml non-specific antibody did not eliminate this NGF-induced sensitization. Therefore, a high concentration of IgG in the pipette did not alter the ability of neurons to be sensitized.

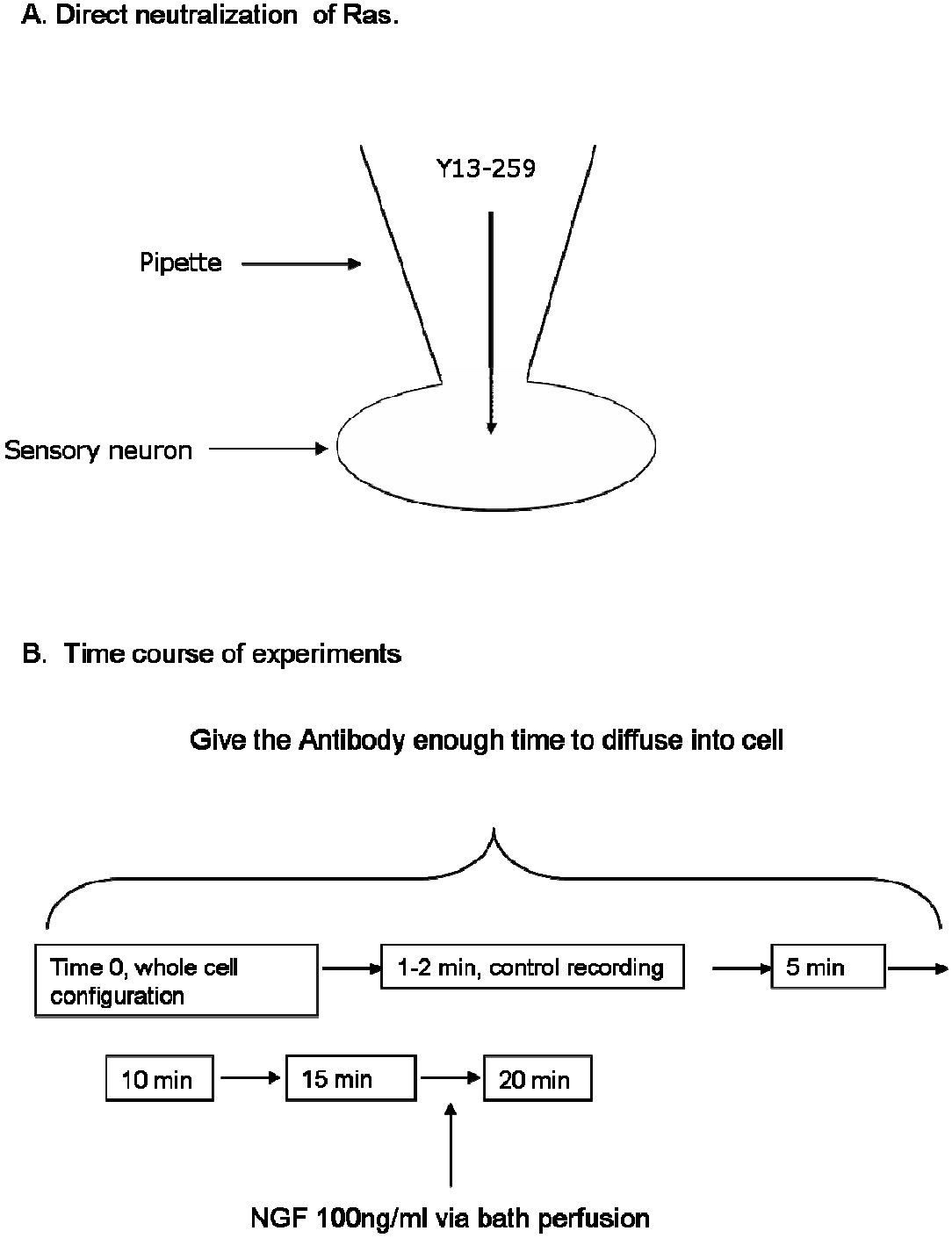

Figure 13. The experimental design of using Ras-blocking antibodies. A: The schematic draft of experiments using antibody in pipette solution. B: the time course of experiments.

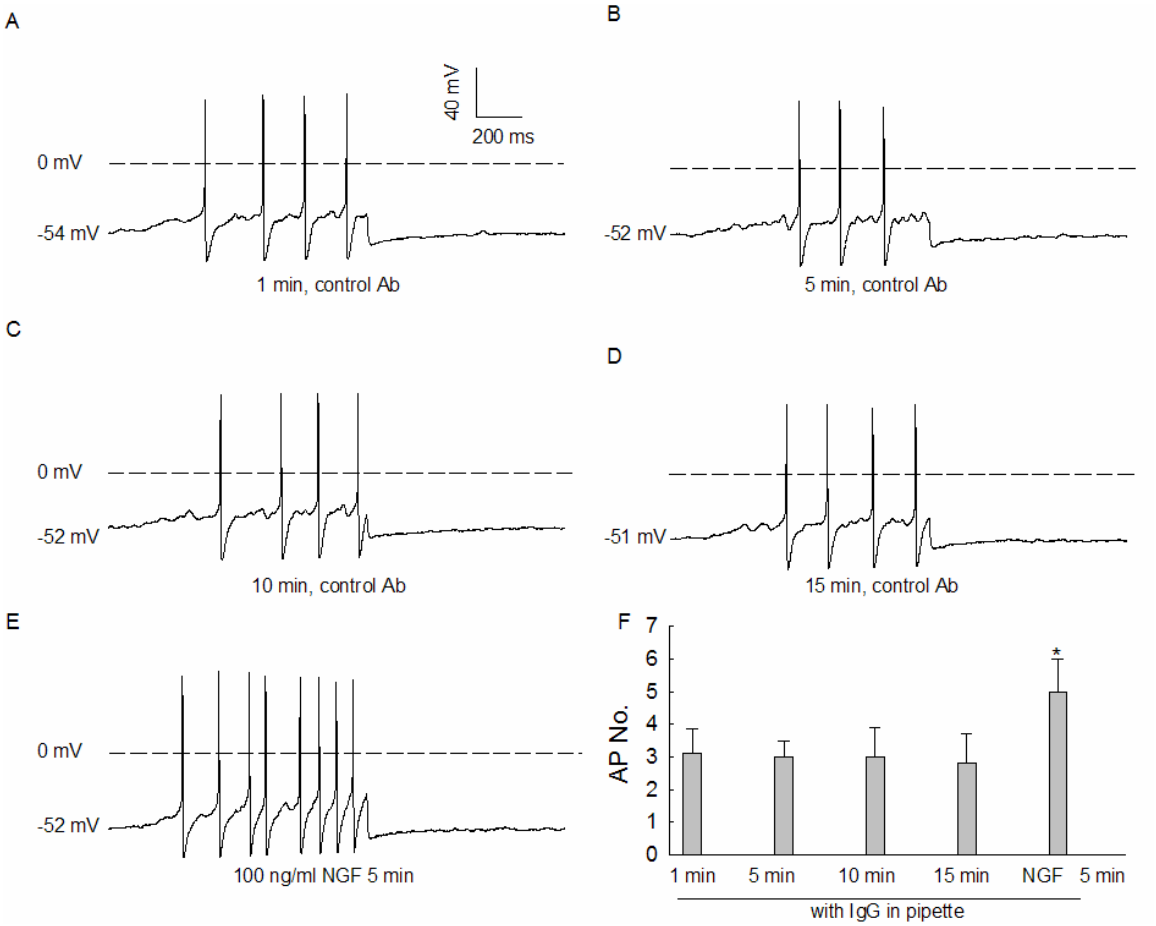

Figure 14. NGF enhances the excitability of *Nf1*+/+ sensory neurons in the presence of 30 µg/ml IgG in the pipette. A: Voltage recordings from a representative *Nf1*+/+ sensory neuron illustrate the number of APs evoked by a ramp of current after 1 min of establishing the whole-cell configuration. The neuron was held at its resting membrane potential and APs were evoked by injecting a 1 s ramp of depolarizing current that had a final amplitude of 100 pA. B, C, and D: Voltage recordings from the same neuron after 5 min, 10 min, and 15 min of establishing the whole-cell configuration. IgG did not change the number of evoked APs. E: In the presence of 30 µg/ml non-specific IgG antibody in pipette, the representative neuron generated more APs in response to the same stimulation protocol in A-D after exposure to NGF (100 ng/ml). F: The summary of data obtained from 6 *Nf1*+/+ DRG neurons. The asterisk represents a statistically significant difference in *Nf1*+/+ sensory neurons before and after NGF treatments using a one way ANOVA followed by a Dunnet's post hoc analysis ($P < 0.05$).

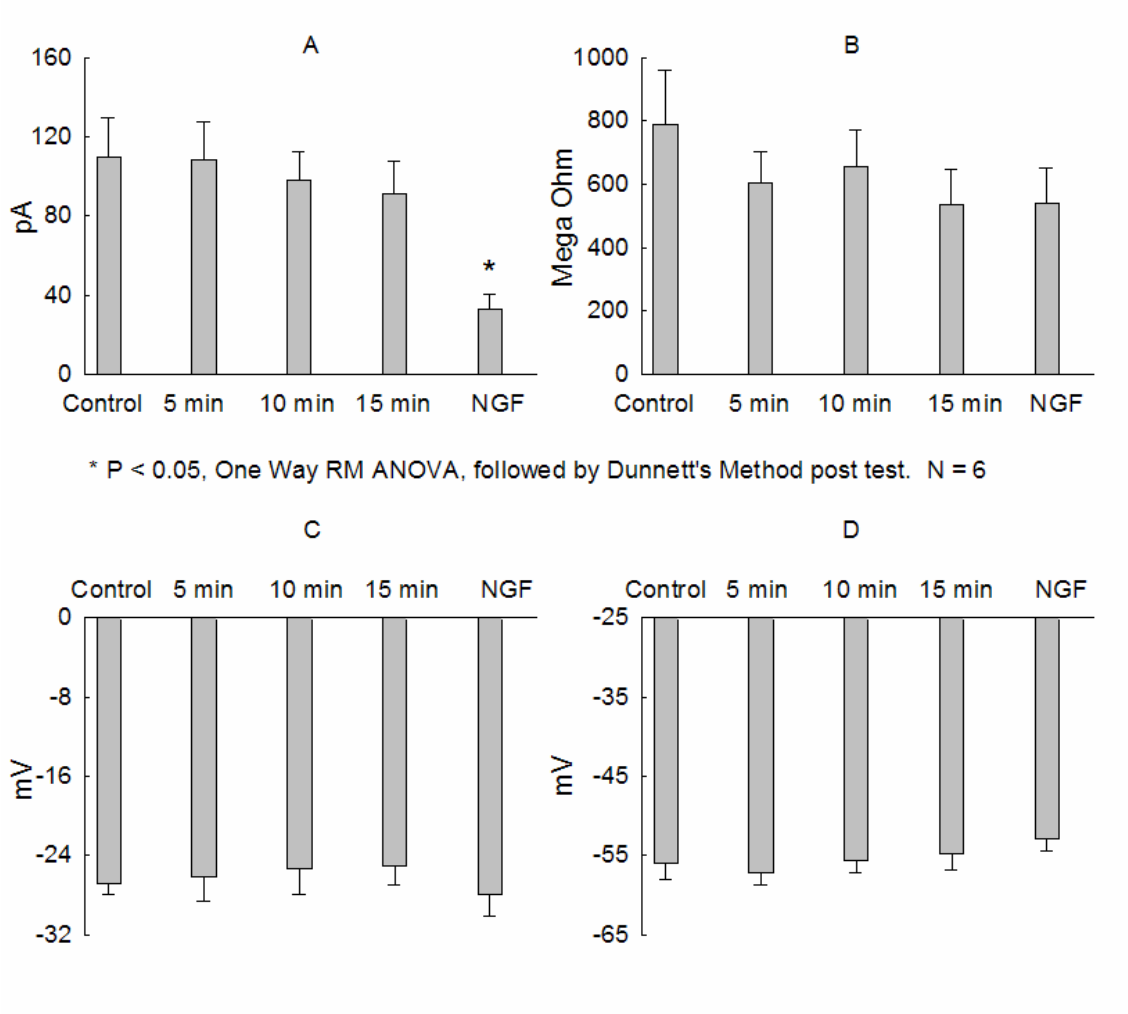

Figure 15. NGF sensitizes *Nf1*+/+ sensory neurons in the presence of 30 µg/ml non-specific IgG in the pipette. Panels A, B, C and D summarize the rheobase, membrane resistance, firing threshold and REM for 6 *Nf1*+/+ neurons, respectively. To monitor the changes in those parameters over the time as well as by NGF, the protocols to determine those parameters were repeated at 1 min, 5 min, 10 min, 15 min and 20 min (NGF 5 min) after established the whole-cell configuration. A: The rheobase did not significantly change at the first 15 min recording period. Exposure to NGF 5 min significantly decreased rheobase of *Nf1*+/+ sensory neurons. B, C and D: NGF did not significantly alter input resistance, firing threshold and REM of *Nf1*+/+ sensory neurons in the presence of 30 µg/ml control antibody in pipette. The data in this Figure were collected from same 6 *Nf1*+/+ sensory neurons. The asterisk represents a statistically significant difference in *Nf1*+/+ sensory neurons before and after NGF treatments using a 1-way ANOVA followed by a Dunnet's post hoc analysis ($P < 0.05$).

2. Internal perfusion with the Ras neutralizing antibody, Y13-259, blocks the sensitization induced by NGF.

My results showed that the capacity of NGF to augment the excitability of small diameter, capsaicin-sensitive neurons was not affected in the presence of 30 μg/ml non-specific IgG in pipette. These experiments indicated that this NGF-induced sensitization was not altered by a high concentration of IgG in the pipette and thereby provided a valid control for Y13-259. The studies described below established whether the NGF-induced sensitization could be abolished by the Ras-blocking antibody, Y13-259. Since considerable amount of antibody should diffuse into neurons during the 15 min recording period after establishing the whole-cell configuration, the neurons were exposed to NGF after the recording at 15 min to examine whether NGF-induced sensitization was affected by internal perfusion with Y13-259. With Y13-259 in the recording pipette, the number of evoked APs did not increase after NGF treatment. Figures 16A-E show the results obtained from a representative neuron at 1 min, 5 min, 10 min, 15 min and 20 min (NGF 5 min) after establishing the whole-cell configuration. Treatment with NGF did not increase the number of evoked APs in the presence of Y13-259 in pipette. As summarized in Figure 16F, after exposure to 100 ng/ml NGF for 5 min, the number of evoked APs from *Nf1*+/+ neurons was 1.6 ± 1.5, which was not significantly different from the value obtained in the control recording (3.6 ± 1.5, n=5). Y13-259 alone does not seem to modulate the neuronal excitability because the numbers of evoked APs remained constant as this antibody diffused into the cells (the APs were 4.4 ± 1.5, 3.8 ± 1.1, 2.8 ± 1.1 at

5 min, 10 min, 15 min respectively, after establishing the whole-cell configuration). These values did not significantly change in the 20 min recording period. Similar to number of APs, the effect of NGF on other parameters revealing neuronal excitability, such as rheobase, was abolished by internal perfusion with Y13-259. Neither NGF nor Y13-259 altered the firing threshold, membrane resistance and REM of *Nf1*+/+ cells. As shown in Figure 17, at 1 min, 5 min, 15 min and after exposure to NGF for 5 min, the rheobase of *Nf1*+/+ neurons was 154 ± 67, 146 ± 65, 148 ± 63, 170 ± 68 and 194 ± 77 pA, the input resistance was 735 ± 309, 822 ± 301, 858 ± 319, 733 ± 263 and 671 ± 262 MΩ, the firing threshold was -24 ± 5, -28 ± 3, -28 ± 2, -28 ± 3 and -25 ± 5 mV and the resting membrane potential was -54 ± 5, -51 ± 5, -52 ± 5, -52 ± 4 and -57 ± 3 mV (n=5). The values of all these parameters were not significantly different during the 20 min recording period. Therefore, the NGF-induced sensitization was abolished by the Ras-blocking antibody, Y13-259.

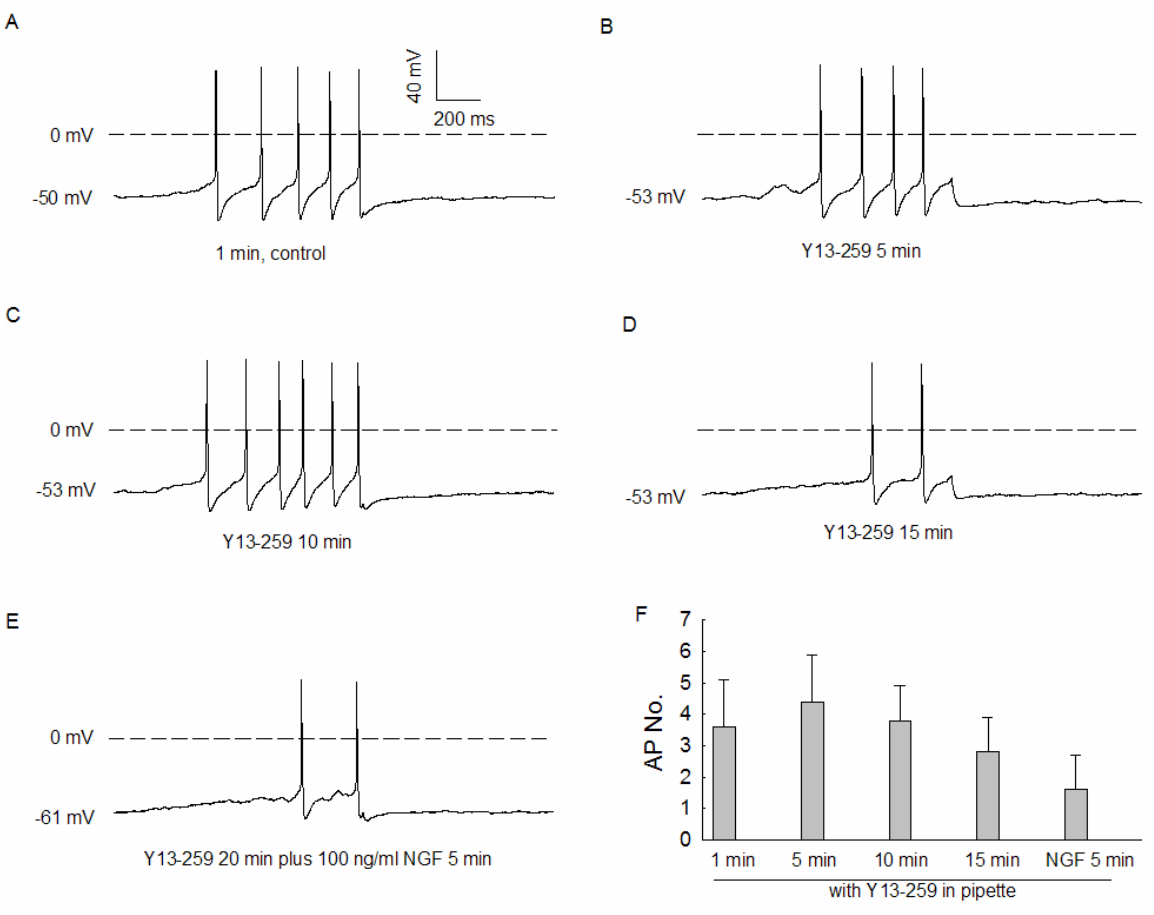

Figure 16. NGF fails to enhance of the numbers of evoked APs as the Ras-blocking antibody is internally perfused into *Nf1*+/+ sensory neurons. A: Voltage recordings from a representative *Nf1*+/+ sensory neuron illustrate the number of APs evoked by a ramp current after 1 min of establishing the whole-cell configuration. The neuron was held at its resting membrane potential and APs were evoked by injecting a 1s ramp of depolarizing current that had a final amplitude of 30 pA. B, C, and D: By using the same stimulation protocol as in A, the evoked APs from the same neuron after 5 min, 10 min, and 15 min of establishing the whole-cell configuration. E: in the presence of Y13-259, the number of APs evoked from this representative neuron was not increased by 100 ng/ml NGF. F: The summary of data obtained from 5 *Nf1*+/+ DRG neurons. The evoked APs after neurons were exposed to NGF for 5 min were not significantly different from control values.

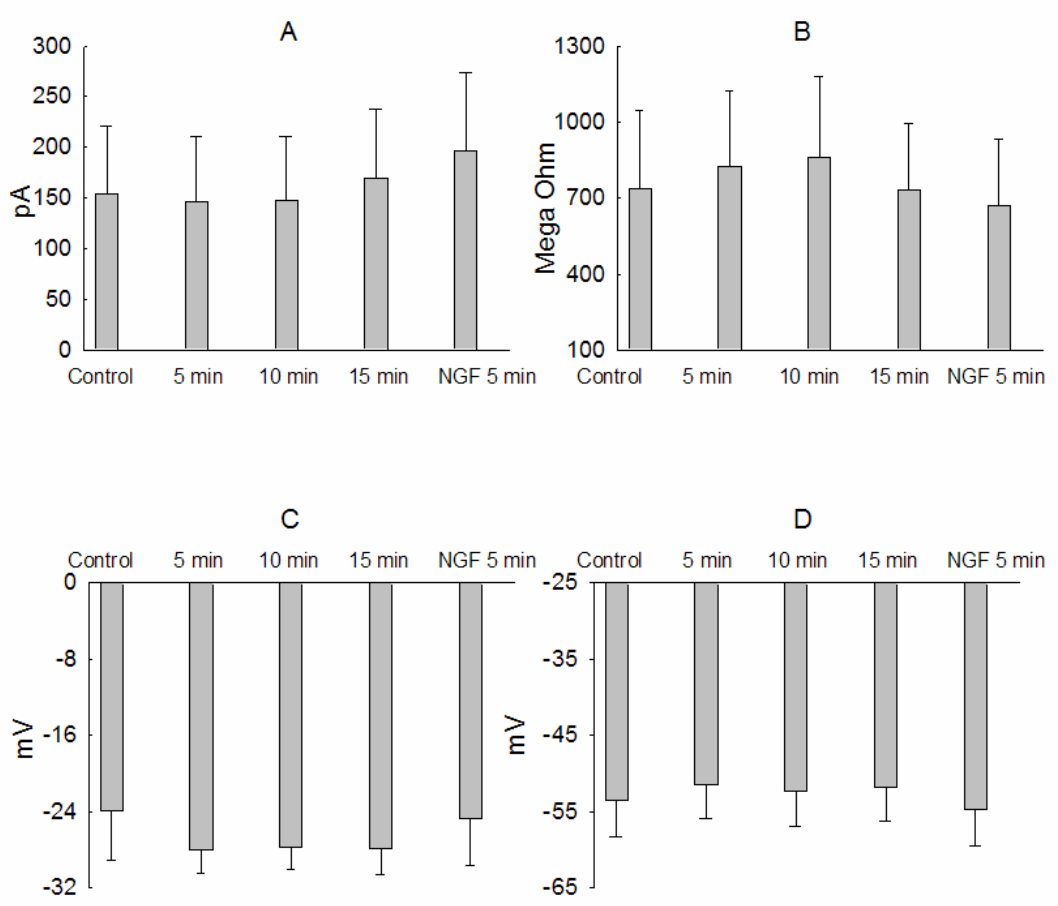

Figure 17. NGF does not sensitize *Nf1*+/+ sensory neurons in the presence of 30 µg/ml Ras-blocking antibody in pipette. Panels A, B, C and D summarize the rheobase, membrane resistance, firing threshold and resting membrane potential for 5 *Nf1*+/+ neurons, respectively. To monitor the changes of those parameters by the Ras-blocking antibody as well as by NGF, the protocols to determine those parameters were repeated at 1 min, 5 min, 10 min, 15 min and 20 min (NGF 5 min) after established the whole-cell configuration. A: The rheobase did not significantly altered at the first 15 min holding period as the Ras-blocking antibody entering cells. Exposure to NGF 5 min did not change the rheobase of *Nf1*+/+ sensory neurons. B, C and D: Neither the Ras-blocking antibodies nor NGF did not significantly alter input resistance, firing threshold and REM of *Nf1*+/+ sensory neurons.

3. Internal perfusion with the Ras-blocking antibody, Y13-259 does not alter the basal excitability of *Nf1*+/+ neurons.

The studies described below determined whether the Ras-blocking antibody, Y13-259 alone could alter neuronal excitability in *Nf1*+/+ sensory neurons and thereby provide valid control experiments for the studies using NGF as a stimulus for the Ras cascade. Figures 18A-E describe the APs evoked from a representative neuron in the presence of Y13-259 in pipette. In the 20 min recording period, Y13-259 did not significantly alter the number of APs elicited by a standard ramp of depolarizing current in a capsaicin-sensitive sensory neuron isolated from *Nf1*+/+ mouse. The number of evoked APs remained constant as Y13-259 diffused into the cells. As summarized in Figure 18F, in 5 *Nf1*+/+ sensory neurons, this Ras-blocking antibody did not alter the neuronal excitability of *Nf1*+/+ neurons because the number of evoked APs remained constant in the 20 min recording period as the Ras-blocking antibody perfused into the cells (the evoked APs were 2.8 ± 1, 3.6 ± 0.9, 3.6 ± 0.9, 4.4 ± 1.2 and 4 ± 1, at 1 min, 5 min, 10 min, 15 min, 20 min, respectively, n=5).

Like AP numbers, the values of the other parameters used to examine neuronal excitability like rheobase, membrane resistance, firing threshold and REM were not altered by Y13-259. As summarized in Figure 19, in the 20 min recording period, the rheobase of *Nf1*+/+ neurons was 136 ± 32, 124 ± 36, 126 ± 37, 120 ± 36 and 114 ± 40 pA, the input resistance was 828 ± 177, 844 ± 274, 797 ± 228, 742 ± 172 and 566 ± 88 MΩ, the firing threshold was -15 ± 3, -18 ± 3,

-19 ± 3, -20 ± 2 and -20 ± 3 mV and the resting membrane potential was -55 ± 3, -57 ± 3, -56 ± 3, -56 ± 2 and -57 ± 3 mV. The values of all these parameters were not significantly different from their control values. Therefore, the Ras-blocking antibody alone did not modulate neuronal excitability of *Nf1*+/+ neurons in the 20 min holding period.

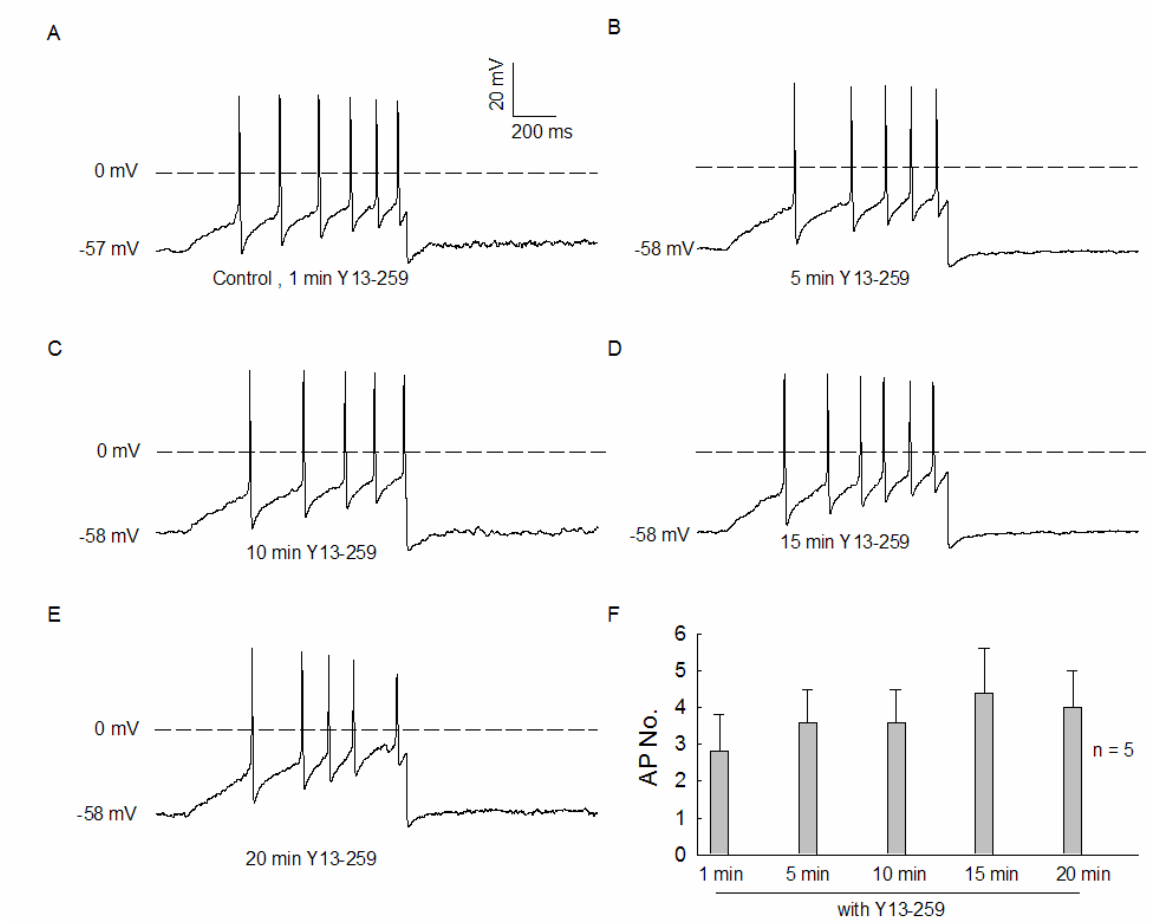

Figure 18. Internal perfusion of Y13-259 alone does not alter the numbers of APs evoked from *Nf1*+/+ sensory neurons. A: Voltage recordings from a representative *Nf1*+/+ sensory neuron illustrate the number of APs evoked by a ramp current after 1 min of establishing the whole-cell configuration. The neuron was held at its resting membrane potential and APs were evoked by injecting a 1s ramp of depolarizing current that had a final amplitude of 500 pA. B, C, D and E: By using the same stimulation protocol as in A, the evoked APs from the same neuron at 5 min, 10 min, 15 min and 20 min after established the whole-cell configuration. The evoked APs did not change significantly as the Ras-blocking antibody was internally perfused into cells in the 20 min recording period. F: The summary of data obtained from 5 *Nf1*+/+ DRG neurons. The APs evoked from 5 *Nf1*+/+ neurons were not significantly different during the 20 min recording period.

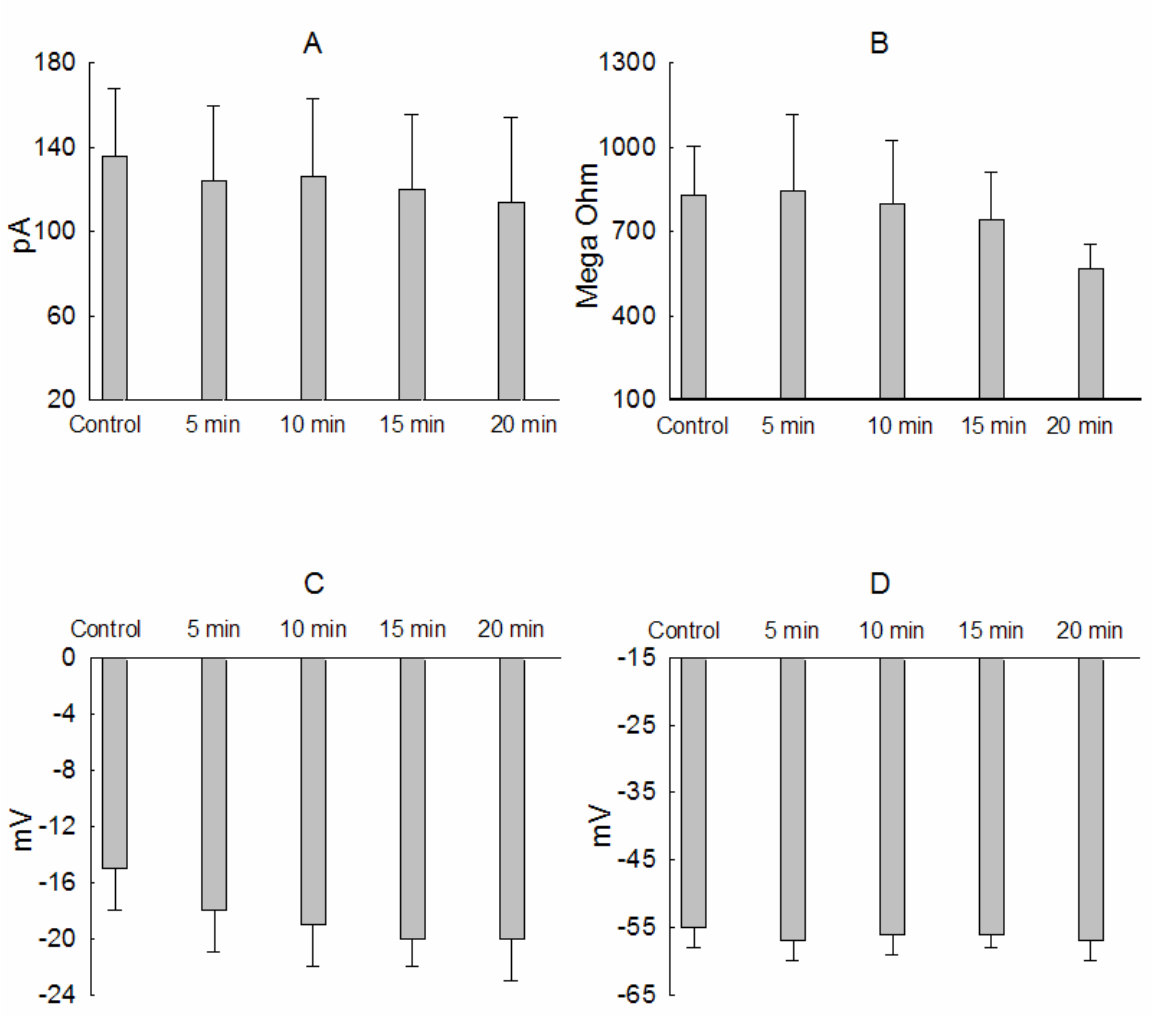

Figure 19. Y13-259 alone did not alter excitability of *Nf1*+/+ sensory neurons. Panels A, B, C and D summarize the rheobase, membrane resistance, firing threshold and REM, respectively, for 5 *Nf1*+/+ neurons. To monitor the changes in those parameters by the Ras-blocking antibody, the protocols to determine those parameters were repeated at 1 min, 5 min, 10 min, 15 min and 20 min (NGF 5 min) after established the whole-cell configuration. A: The rheobase did not significantly change at the 20 min recording period as the Ras-blocking antibody was internally perfused into sensory neurons. B, C and D: The input resistance, firing threshold and REM of *Nf1*+/+ sensory neurons did not significantly changed by Y13-259.

4. Internal perfusion with the Ras blocking antibody, Y13-259, fails to alter the basal excitability of *Nf1*+/- neurons.

As established above, the Ras-blocking antibody, Y13-259 abolished the neuronal sensitization induced by NGF in *Nf1*+/+ neurons. This suggests that the activation of Ras is a critical step in NGF-induced sensitization. Because *Nf1*+/- neurons had enhanced excitably that was supposedly due to higher levels of Ras-GTP, the experiments described below focused on whether internal perfusion with the Ras-blocking antibody could alter the excitability of *Nf1*+/- neurons. Surprisingly, Y13-259 did not suppress the number of APs elicited by a standard ramp of depolarizing current in *Nf1*+/- sensory neurons (see Figure 20A-F). The number of evoked APs remained elevated and constant as Y13-259 was internally perfused into the cells over the 20 min recording period. As summarized in Figure 20F, in 5 *Nf1*+/- sensory neurons, this Ras-blocking antibody did not alter the number of evoked APs by a standard ramp of current. The final level of the ramp was adjusted to evoke 5-7 APs in the control. The amplitude then remained constant throughout the recording period for each individual neuron (small ramp, compared to the large ramp used in the experiments described below, the value of this ramp level is relatively small). The number of evoked APs at 1 min, 5 min, 10 min, 15 min, 20 min after establishing the whole-cell configuration was 5 ± 1.3, 5.2 ± 1.4, 6 ± 1, 6.4 ± 1.2 and 5.4 ± 1.2 (n=5), which do not change as the Ras-blocking antibody was perfused internally into sensory neurons. To exclude the possibility that the value of the ramp was too small to detect subtle changes in neuronal excitability,

another ramp (large ramp) designed to evoke 10-15 APs under control conditions was used to increase the experimental resolution. Consistent with the data described above using the small ramp, Y13-259 did not alter the number of APs elicited by the large ramp whose amplitude was adjusted to evoke 10-15 APs under control conditions. As shown in Figure 21, the number of evoked APs did not change as the Ras-blocking antibody was internally perfused into sensory neurons. Consistent with the evoked APs, the values of the other parameters assessing neuronal excitability were not altered by Y13-259. As shown in Figure 22, as Y13-259 was internally perfused into cells, the rheobase at 1 min, 5 min, 10 min, 15 min, 20 min after establishing the whole-cell configuration was 78 ± 21, 64 ± 24, 50 ± 15, 46 ± 13 and 48 ± 15 pA, the input resistance was 570 ± 179, 882 ± 250, 896 ± 247, 676 ± 168 and 680 ± 185 MΩ, the firing threshold was -29 ± 5, -28 ± 4, -29 ± 3, -29 ± 2 and -29 ± 3 mV and the resting membrane potential was -54 ± 4, -51 ± 2, -52 ± 2, -51 ± 1 and -50 ± 3 mV. The values of all these parameters collected at 5 min, 15 min and 20 min after establishing the whole-cell configuration were not significantly different from their control values. Therefore, my data suggests that direct neutralization of Ras activity in *Nf1+/-* neurons did not suppress the enhanced neuronal excitability.

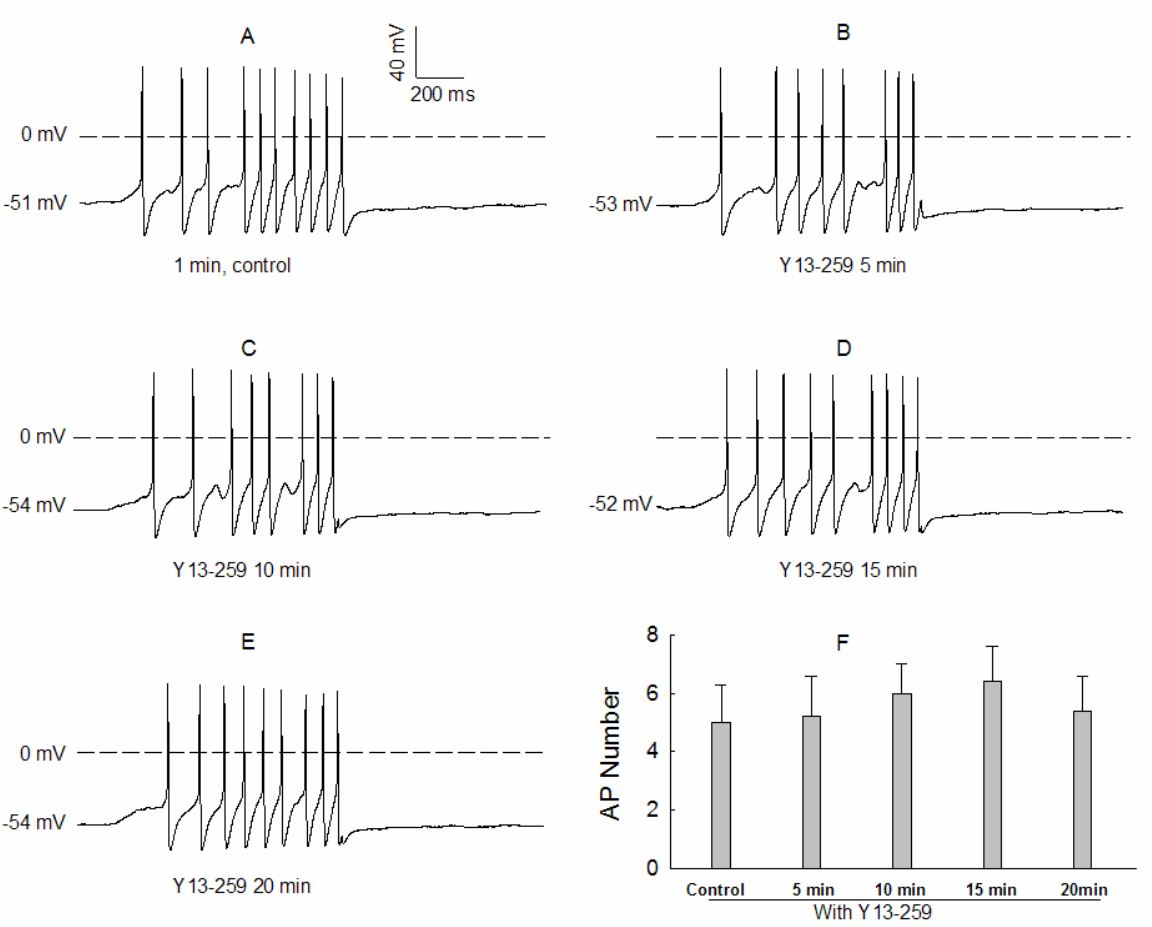

Figure 20. Internal perfusion of Y13-259 does not alter the numbers of APs evoked from *Nf1+/-* sensory neurons by using small ramps. The final level of the ramp was adjusted to evoke 5-7 APs in the control, the amplitude then remained constant throughout the recording period for each individual neuron. A: Voltage recordings from a representative *Nf1+/-* sensory neuron illustrate the number of APs evoked by a ramp current after 1 min of establishing the whole-cell configuration. The neuron was held at its resting membrane potential and APs were evoked by injecting a 1s ramp of depolarizing current that had a final amplitude of 100 pA. The final value of the ramp was adjusted to evoke 5-7 APs in the control condition. B, C, D and E: By using the same stimulation protocol as in A, the evoked APs from the same neuron at 5 min, 10 min, 15 min and 20 min after established the whole-cell configuration. The evoked APs did not change significantly as the Ras-blocking antibody was internally perfused into cells in the 20 min recording period. F: The summary of data obtained from 5 *Nf1+/+* DRG neurons. The APs evoked from 5 *Nf1+/-* neurons were not significantly different during the 20 min recording period.

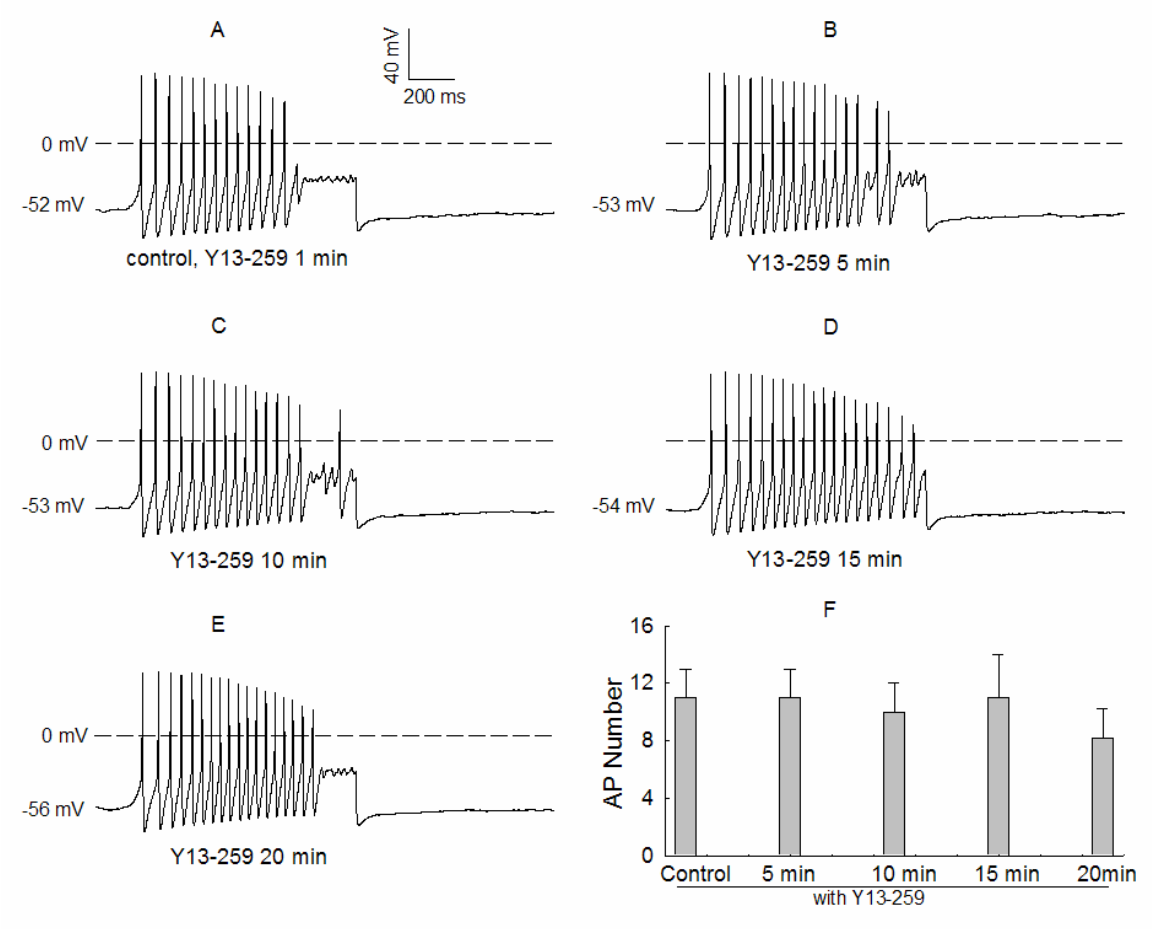

Figure 21. Y13-259 does not alter the evoked APs of *Nf1+/-* sensory neurons by using large ramps (The final value of the ramp was adjusted to evoke 10-15 APs in the control condition). A: Voltage recordings from a representative *Nf1+/-* sensory neuron illustrate the number of APs evoked by a ramp current after 1 min of establishing the whole-cell configuration. The neuron was held at its resting membrane potential and APs were evoked by injecting a 1s ramp of depolarizing current that had a final amplitude of 500 pA. The final value of the ramp was adjusted to evoke 5-7 APs in the control condition. B, C, D and E: By using the same stimulation protocol as in A, the evoked APs from the same neuron at 5 min, 10 min, 15 min and 20 min after established the whole-cell configuration. The evoked APs did not change significantly as the Ras-blocking antibody was internally perfused into cells in the 20 min recording period. F: The summary of data obtained from 5 *Nf1+/+* DRG neurons. The APs evoked from 5 *Nf1+/-* neurons were not significantly different during the 20 min recording period.

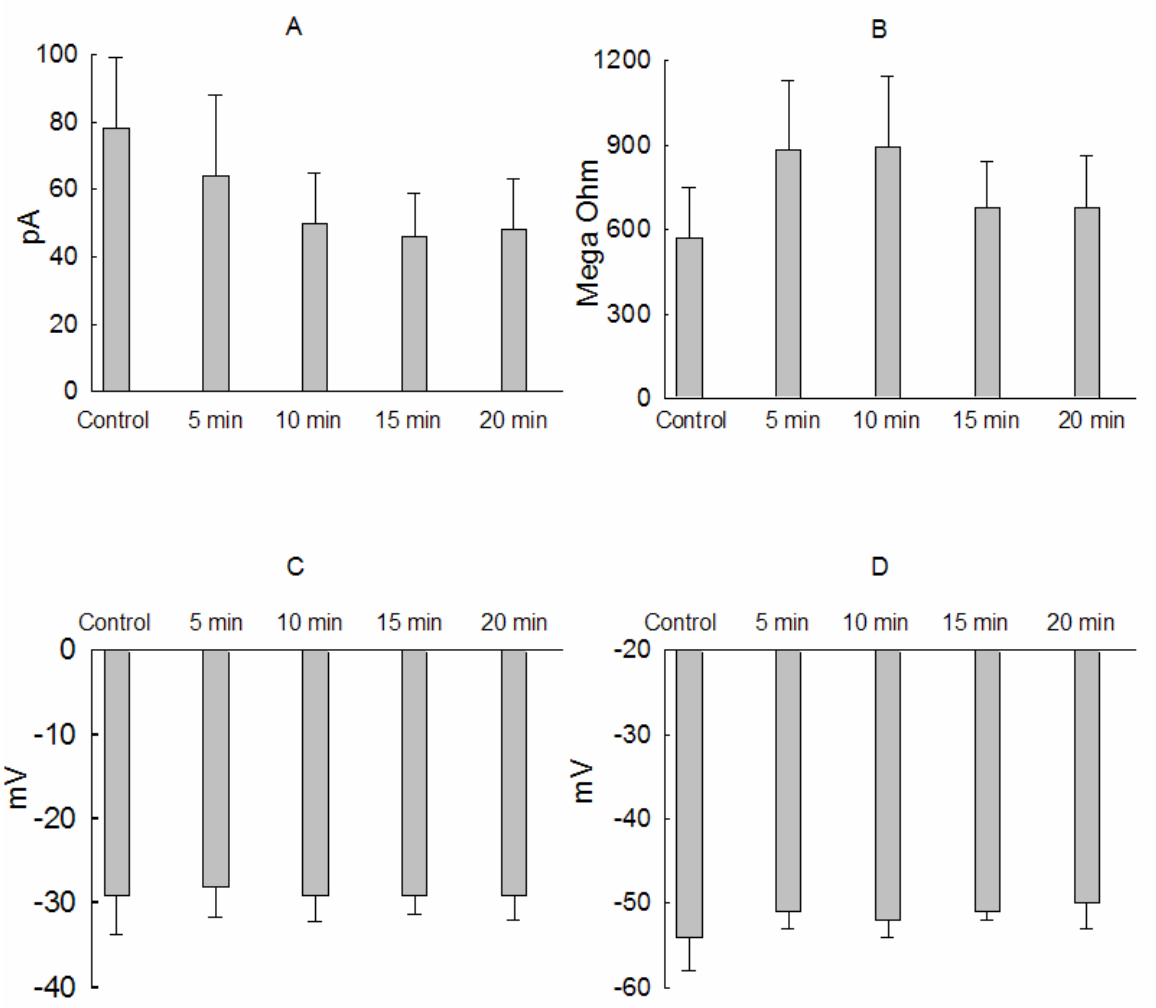

Figure 22. Y13-259 does not alter the excitability of *Nf1*+/- sensory neurons. Panels A, B, C and D summarize the rheobase, membrane resistance, firing threshold and REM for 5 *Nf1*+/- neurons. To monitor the changes in those parameters by the Ras-blocking antibody, the protocols to determine those parameters were repeated at 1 min, 5 min, 10 min, 15 min and 20 min after established the whole-cell configuration. A: The rheobase did not significantly change during the 20 min recording period as the Ras-blocking antibody was internally perfused into sensory neurons. B, C and D: The input resistance, firing threshold and REM of *Nf1*+/- sensory neurons did not significantly changed by Y13-259.

5. NGF does not sensitize neurons isolated from *Nf1+/-* mice in recordings with IgG in pipette.

Since NGF sensitized wild-type sensory neurons on a rapid time scale and the duration of this sensitization remains unclear, the studies described below determined whether NGF could sensitize *Nf1+/-* neurons acutely. Interestingly, *Nf1+/-* neurons did not show sensitization after treatment by NGF (100 ng/ml) via bath perfusion. Although there was a slight increase in the number of evoked APs by the current ramp in 2 out of 6 neurons, 4 neurons remained unresponsive to NGF. As shown in Figure 23A-D, the numbers of APs evoked by a 50 pA current ramp from a representative neuron were unchanged in the first 15 min recording period in the presence of 30 μg/ml non-specific IgG in the pipette. Immediately after the recording obtained at 15 min, the neurons were superfused by normal Ringer's solution containing 100 ng/ml NGF (Figure 23E). Under these conditions, NGF did not increase the number of APs evoked from the representative sensory neuron. Figure 23F summarizes the data obtained from 6 *Nf1+/-* sensory neurons. Treatment with NGF did not enhance the numbers of APs in response to a standard ramp of current (4 ± 1 in control versus 6 ± 2 after NGF treatment). The values of other parameters indicating neuronal excitability were not altered by NGF as the IgG was internally perfused into cells. As shown in Figure 24, the rheobase of *Nf1+/-* neurons at 1 min, 5 min, 10 min, 15 min, 20 min (NGF 5 min) after establishing the whole-cell configuration was 75 ± 12, 63 ± 15, 65 ± 14, 65 ± 22 and 67 ± 14 pA, the input resistance was 928 ± 198, 980 ± 230, 909 ± 232, 844 ± 210 and 690 ± 194 MΩ, the firing threshold was -29 ± 2, -

29 ± 2, -27 ± 2, -27 ± 3 and -30 ± 1 mV and the resting membrane potential was -54 ± 1, -53 ± 1, -55 ± 1, -53 ± 2 and -56 ± 1 mV. The values of all these parameters did not change after establishing the whole-cell configuration. Therefore, NGF did not sensitize *Nf1+/-* neurons in the presence of IgG in pipette.

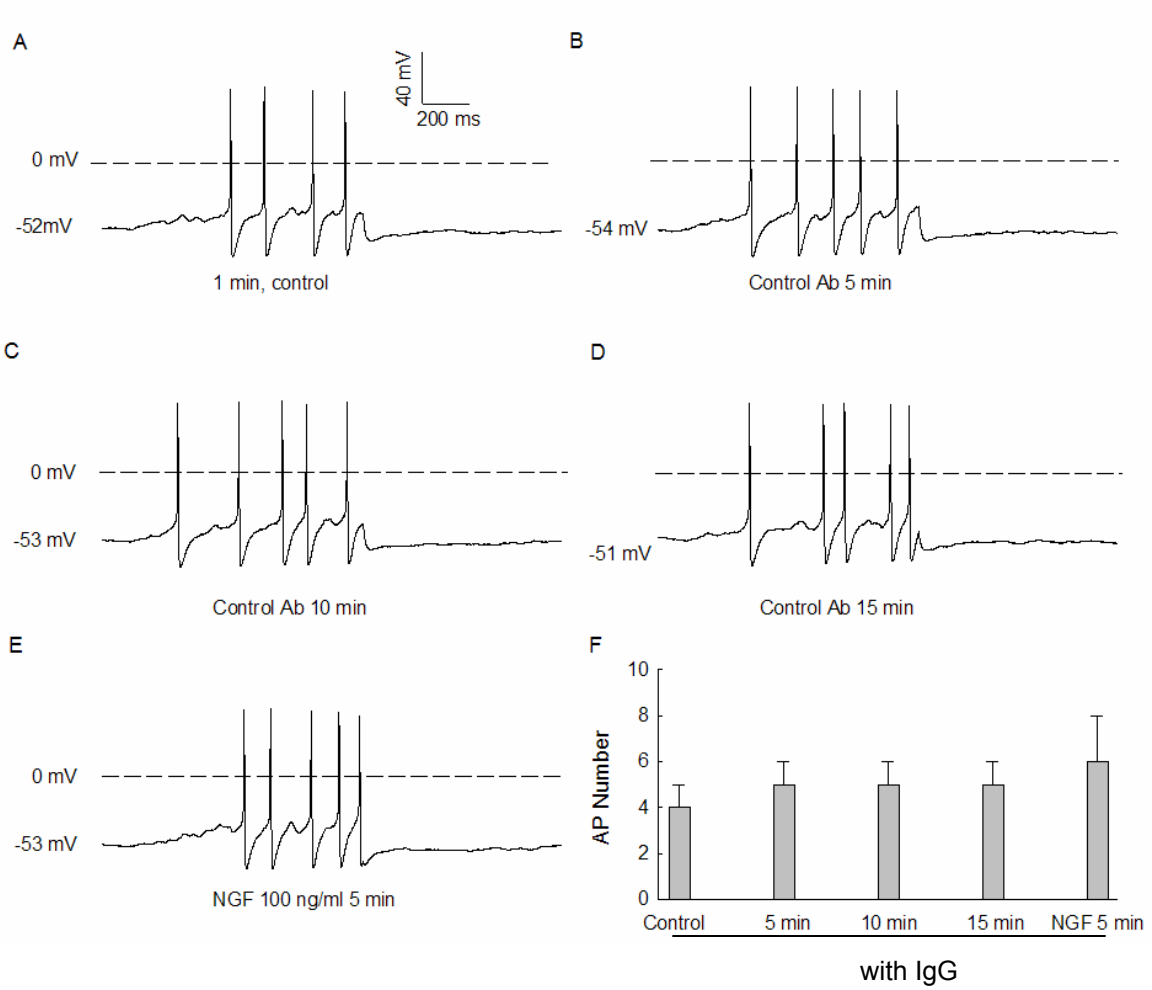

Figure 23. NGF does not enhance the excitability of *Nf1+/-* sensory neurons in the presence of IgG in pipette. A: Voltage recordings from a representative *Nf1+/-* sensory neuron illustrate the number of APs evoked by a ramp current after 1 min of established the whole-cell configuration. The neuron was held at its resting membrane potential and APs were evoked by injecting a 1s ramp of depolarizing current that had a final amplitude of 50 pA. The final value of the ramp was adjusted to evoke 5-7 APs in the control condition. Panel B, C, D and E: By using the same stimulation protocol as in A, the evoked APs from the same neuron at 5 min, 10 min, 15 min and 20 min (NGF 5 min) after established the whole-cell configuration. As shown in E, sensory neuron generated similar number of APs when treated by 100 ng/ml NGF. F: the summary of data obtained from 6 *Nf1+/-*DRG neurons. NGF did not enhance the evoked APs from *Nf1+/-* sensory neurons.

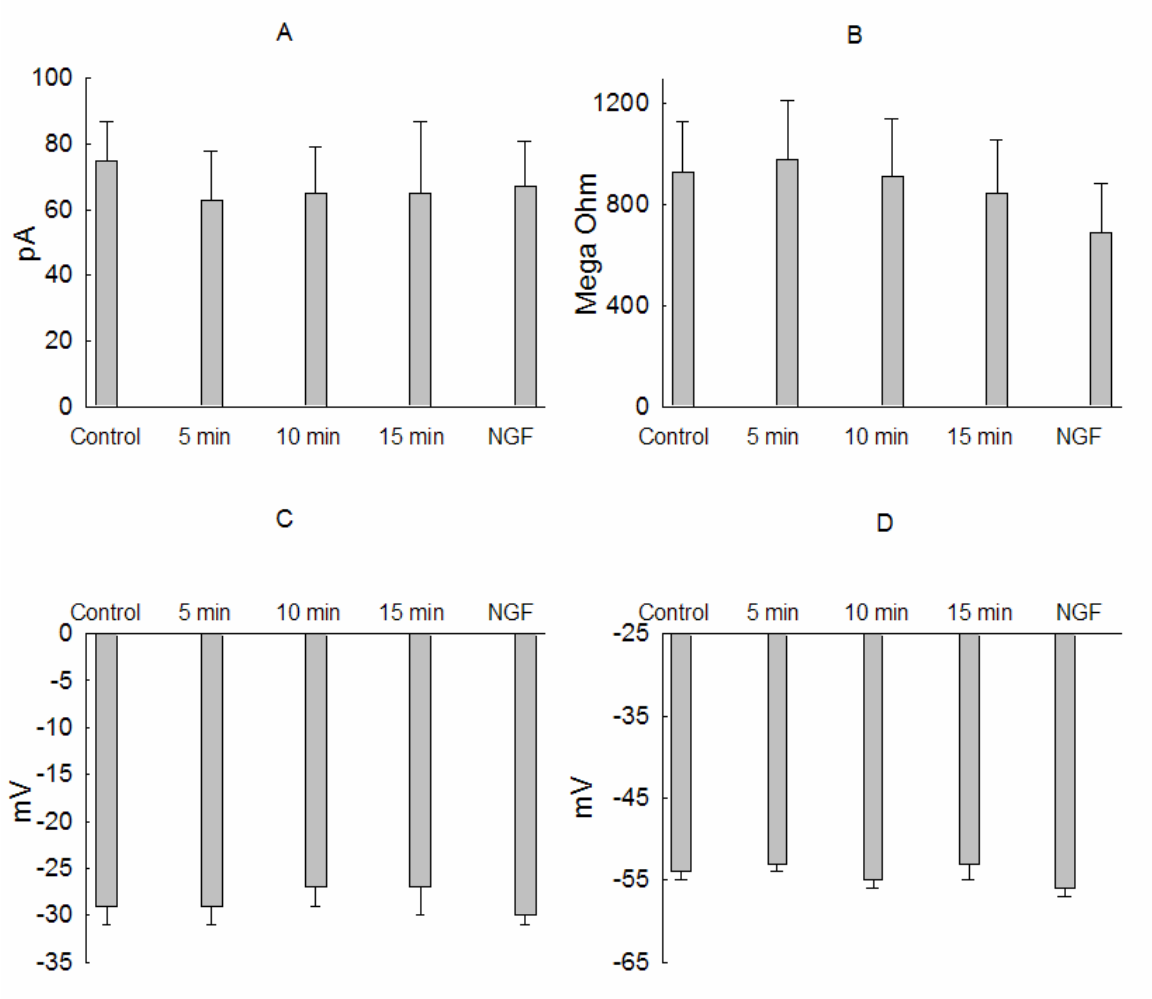

Figure 24. NGF does not sensitize *Nf1+/-* sensory neurons in the presence of IgG in pipette. Panels A, B, C and D summarize the rheobase, membrane resistance, firing threshold and REM for 6 *Nf1+/-* neurons. To monitor the changes of these parameters indicating neuronal excitability by NGF as well as over the time, the protocols to examine those parameters were repeated at 1 min, 5 min, 10 min, 15 min and 20 min (NGF 5 min) after established the whole-cell configuration. A: The rheobase did not change significantly during the 20 min recording period, even after exposure to NGF for 5 min. B, C and D: The input resistance, firing threshold and REM of *Nf1+/-* sensory neurons did not significantly changed by NGF.

6. The Ras blocking antibody, Y13-259, does not alter the inability of NGF to sensitize *Nf1+/-* neurons

Based on the assumption that the augmented Ras-GTP level in *Nf1+/-* neurons caused the insensitivity of these cells to NGF, I asked whether the neutralization of Ras can restore the sensitivity of *Nf1+/-* cells to NGF treatment. Therefore, *Nf1+/-* neurons were exposed to NGF as Y13-259 was internally perfused into the sensory neurons. In the presence of the Ras-blocking antibody, none of the 6 *Nf1+/-* cells studied was sensitized by NGF. As shown in Figure 25, in the presence of Ras-blocking antibody (30 μg/ml) in pipette, the number of APs evoked by a ramp of current (final amplitude of 1000 pA) remained constant over the 20 min recording period. Immediately after the recording obtained at 15 min, the neurons were exposed to 100 ng/ml NGF. Figure 25 F summarizes the data obtained from 6 *Nf1+/-* sensory neurons wherein none of the 6 *Nf1+/-* cells was sensitized by NGF. The numbers of APs evoked by the ramp of current did not change during the 20 min holding period (the evoked APs were 4.8 ± 0.9, 6 ± 1, 7 ± 2, 6 ± 2, 4 ± 2 at control, 5 min, 10 min, 15 min and after NGF treatment, respectively). Other parameters indicating neuronal excitability were not altered by NGF as Y13-259 was internally perfused into cells. At control, 5 min, 10 min, 15min and 20 min (NGF treatment for 5 min), the rheobase of *Nf1+/-* neurons was 68 ± 16, 68 ± 22, 67 ± 22, 75 ± 24 and 110 ± 35 pA, the input resistance was 955 ± 225, 1066 ± 202, 1026 ± 207, 1062 ± 200 and 957 ± 189 MΩ, the firing threshold was -26 ± 2, -26 ± 2, -26 ± 2, -24 ± 3 and -24 ± 5 mV, and the resting membrane potential was -55 ± 2, -56 ± 2, -56 ± 4, -57 ± 4 and -58 ± 4 mV (n=6,

Figure 26). The values of these parameters measured at 5 min, 10 min, 15 min and 20 min (NGF 5 min) were not significantly different from their control values obtained at 1 min after establishing the whole-cell configuration. Therefore, none of the 6 *Nf1+/-* neurons enhanced its excitability in the presence of the Ras-blocking antibody in pipette at the 20 min recording period.

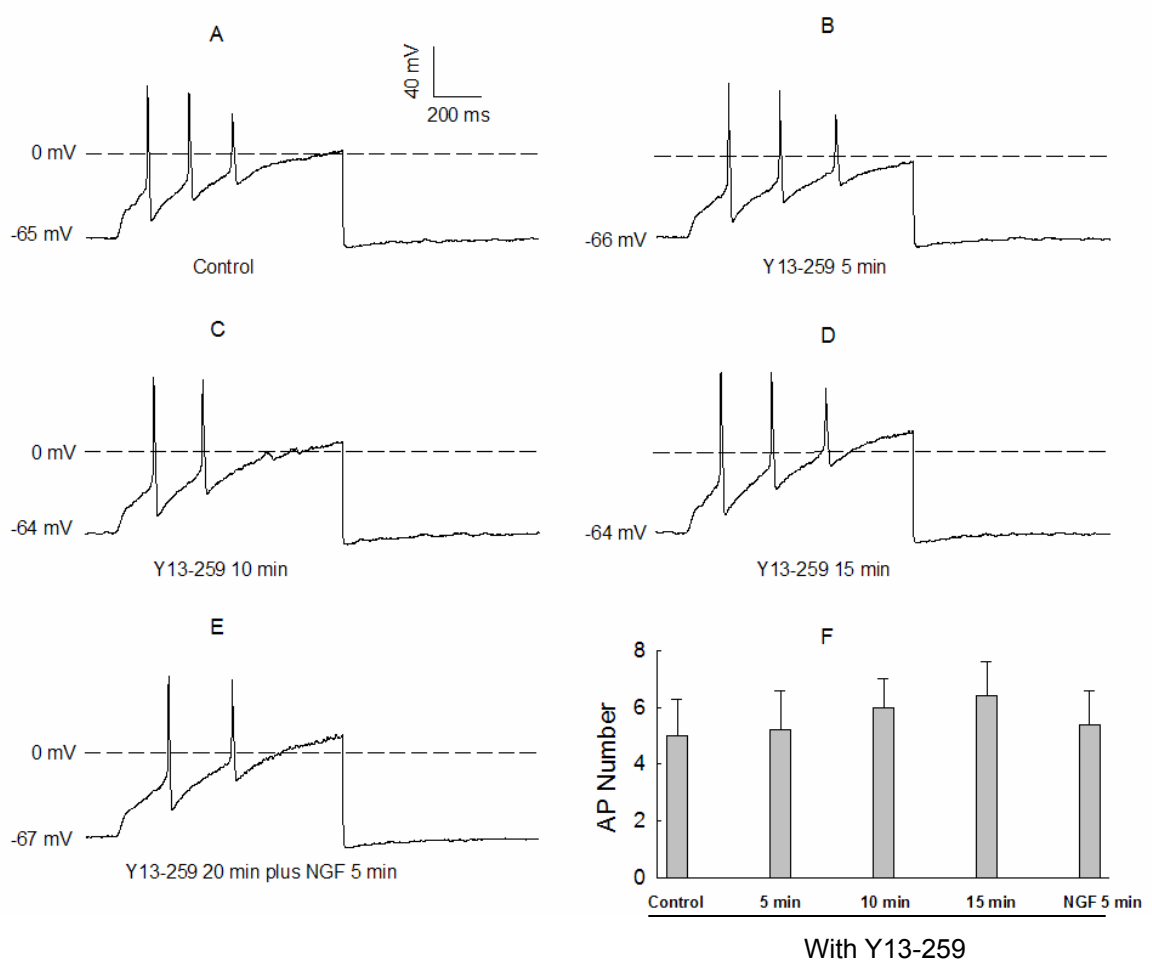

Figure 25. NGF does not enhance the excitability of *Nf1+/-* sensory neurons in the presence of 30 µg/ml Y13-259 in pipette solution. A: Voltage recordings from a representative *Nf1+/-* sensory neuron illustrate the number of APs evoked by a ramp current after 1 min of established the whole-cell configuration. The neuron was held at its resting membrane potential and APs were evoked by injecting a 1s ramp of depolarizing current that had a final amplitude of 1000 pA. The final value of the ramp was adjusted to evoke 5-7 APs in the control condition. Panel B, C, D and E: By using the same stimulation protocol as in A, the evoked APs from the same neuron at 5 min, 10 min, 15 min and 20 min (NGF 5 min) after established the whole-cell configuration. As shown in E, sensory neuron generated similar number of APs when treated by 100 ng/ml NGF. F: the summary of data obtained from 6 cells. NGF did not enhance the evoked APs from *Nf1+/-* sensory neurons.

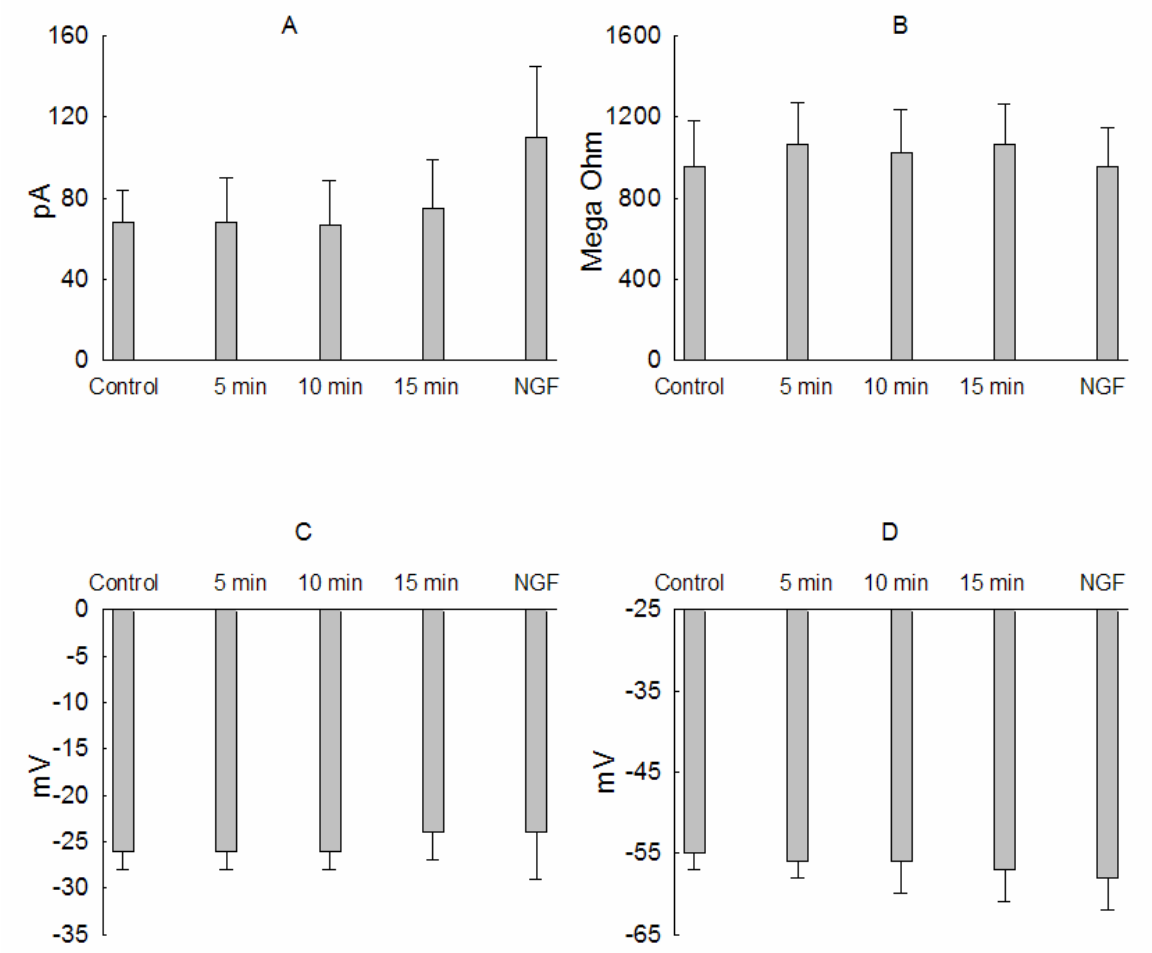

Figure 26. NGF does not sensitize neuronal excitability of *Nf1+/-* sensory neurons with 30 µg/ml Ras-blocking antibody in pipette. Panels A, B, C and D summarize the rheobase, membrane resistance, firing threshold and REM for 6 *Nf1+/-* neurons. To monitor the changes of these parameters indicating neuronal excitability by NGF as well as by the Ras-blocking antibody, the protocols to examine those parameters were repeated after 1 min, 5 min, 10 min, 15 min and 20 min (NGF) of established the whole-cell configuration. A: NGF did not significantly change the rheobase as the Ras-blocking antibody was internally perfused into pipette. Panels B, C and D: The input resistance, firing threshold and REM of *Nf1+/-* sensory neurons did not significantly change by NGF in the presence of the Ras-blocking antibody.

D. IK does not contribute to the augmented excitability observed of *Nf1+/-* neurons.

It is well established that potassium channels regulate neuronal excitability. The outflow of potassium ions from the inside to the outside of the cell draws the membrane potential closer to the equilibrium potential of potassium (calculated to be -84 mV in sensory neurons) and decreases neuronal excitability. When the potassium channels are blocked or inhibited by certain chemicals, sensory neurons enhance their excitability (Birinyi-Strachan et al., 2005; Nicol et al., 1997; Zhang et al., 2002). Under pathological conditions, such as inflammation (Gold and Flake, 2005; Katz and Gold, 2006) and neuropathic pain (Cherkas et al., 2004; Liu et al., 2001), IK was reduced. Because we have established that capsaicin-sensitive, small diameter sensory neurons from *Nf1+/-* mice exhibit greater excitability than *Nf1+/+* neurons, an important question that arises is whether this augmentation of neuronal excitability results from the suppression of IK in *Nf1+/-* sensory neurons. Therefore, isolated IK that is critical in controlling neuronal firing were examined by using the whole-cell patch-clamp technique.

1. The total potassium currents (IK) and the delayed-rectifier potassium currents (IKd) of *Nf1*+/+ and *Nf1*+/- mice are not different.

The suppression of IK enhances the excitability of sensory neurons (Evans et al., 1999; Nicol et al., 1997; Zhang et al., 2002). Therefore, a series of experiments were performed to determine whether IK was decreased in the *Nf1*+/- neurons compared to wild-types. As illustrated in Figure 27, IK was elicited from *Nf1*+/+ neurons and *Nf1*+/- neurons by voltage steps from -80 mV to +60 mV in 10 mV increments. Figure 27A shows a representative trace of IK recorded from a *Nf1*+/+ sensory neuron. The trace of IK from *Nf1*+/- neurons looked exactly the same as the wild-types. The peak currents of IK (measured close to the point indicated by the arrow in Figure 27A) reflect the current amplitude of both the fast-inactivating IA types and the slow inactivating delayed-rectifier types of IK (IKd), therefore, the peak IK (total IK) was measured in *Nf1*+/+ and *Nf1*+/- sensory neurons. The current-voltage relation (Figure 27B) demonstrates that the total IK from either genotype was not significantly different as determined by using a t-test (the average peak value of IK in *Nf1*+/+ and *Nf1*+/- neurons was 7638.6 ± 1538.6 and 6724.7 ± 1105.9 pA for the step to +60 mV, n=7-11). To minimize the variance of currents recorded from different sizes of cells, currents were normalized to the cell surface area and expressed as current density (pA/pF). The membrane capacitance was read directly from the patch-clamp amplifier after performing the compensation for capacitance and series resistance. The current density-voltage relation of *Nf1*+/+ and *Nf1*+/- neurons is illustrated in Figure 27C. It is unlikely that the activation of IK was

altered in *Nf1*+/- neurons, because the two curves representing the current density-voltage relation of *Nf1*+/+ and *Nf1*+/- neurons are almost identical (the average peak current density of IK in *Nf1*+/+ and *Nf1*+/- neurons was 569.2 ± 96.3 pA/pF and 559.9 ± 103.4 pA/pF, respectively, for the step to +60 mV, n=7-11). A similar result was observed for the conductance-voltage relation. As summarized in the Figure 27D, the G/Gmax relation plotted as a function of voltage for *Nf1*+/- neurons was not different compared to *Nf1*+/- neurons. The values of G/Gmax were fitted by the Boltzmann relation. The Boltzmann parameters, such as half-activation voltage ($V_{0.5}$) and k (slope factor), for the activation of IK in neurons of the two genotypes were not different (Table 1). In summary, the total outward IK in *Nf1*+/- neurons is not different from *Nf1*+/+ neurons.

Similar to IK, IKd in neurons of the two genotypes was not significantly different. IKd was measured at the point indicated by the arrow and represents the steady-state IK (see Figure 28A). In Figure 28B, the average value for the peak IKd of *Nf1*+/+ neurons was 6704.9 ± 1189.9 pA (for the step to +60 mV, n=11), and was not different from the peak IKd recorded from *Nf1*+/- neurons (6243.8 ± 921.3 pA, n=7). In Figures 28C and D, the current density-voltage relation and the conductance-voltage relation of *Nf1*+/+ and *Nf1*+/- neurons were not significantly different (the peak current density of IKd was 497.8 ± 83.2 pA/pF and 511.8 ± 71.8 pA/pF for *Nf1*+/+ and *Nf1*+/- neurons, respectively. N=7-11). The Boltzmann parameters, like $V_{0.5}$ and k, for the activation of IKd in neurons of two genotypes were not significantly different (See Table 1).

Taken together, the activation of both total IK and IKd in neurons of the two genotypes was not significantly different. It is unlikely that the activation of total IK and IKd contribute to the enhanced excitability of *Nf1+/-* neurons.

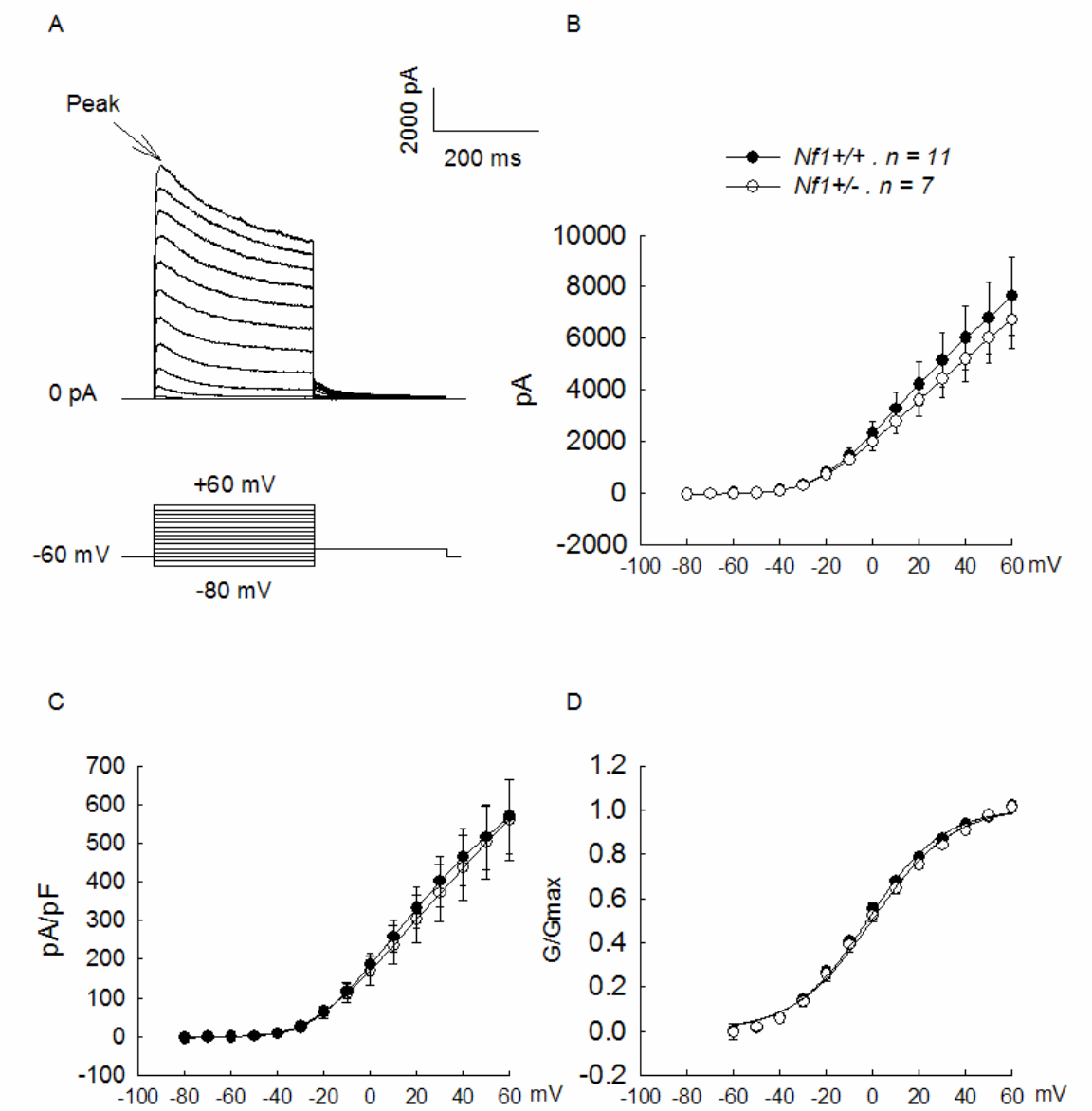

Figure 27. Total IK in *Nf1*+/+ and *Nf1*+/- sensory neurons are not different. Panel A shows the representative trace of IK recorded from a *Nf1*+/+ sensory neuron. The arrow in A approximately points the location where the peak IK was measured. The lower part of panel A shows the protocol to evoke IK. The membrane voltage was held at -60 mV; activation of the currents was determined by voltage steps of 300 ms, which were applied at 5 s intervals in +10 mV increments from -80 mV to +60 mV. Panel B summarizes the current-voltage relation of IK in both genotypes. Panel C illustrates the current density-voltage relations of IK in both genotypes. The conductance-voltage relation is illustrated in panel D. The data points in D have been fitted by the Boltzmann relation and are shown as the continuous lines. The values in each panel are from the same 11 *Nf1*+/+ and 7 *Nf1*+/- neurons.

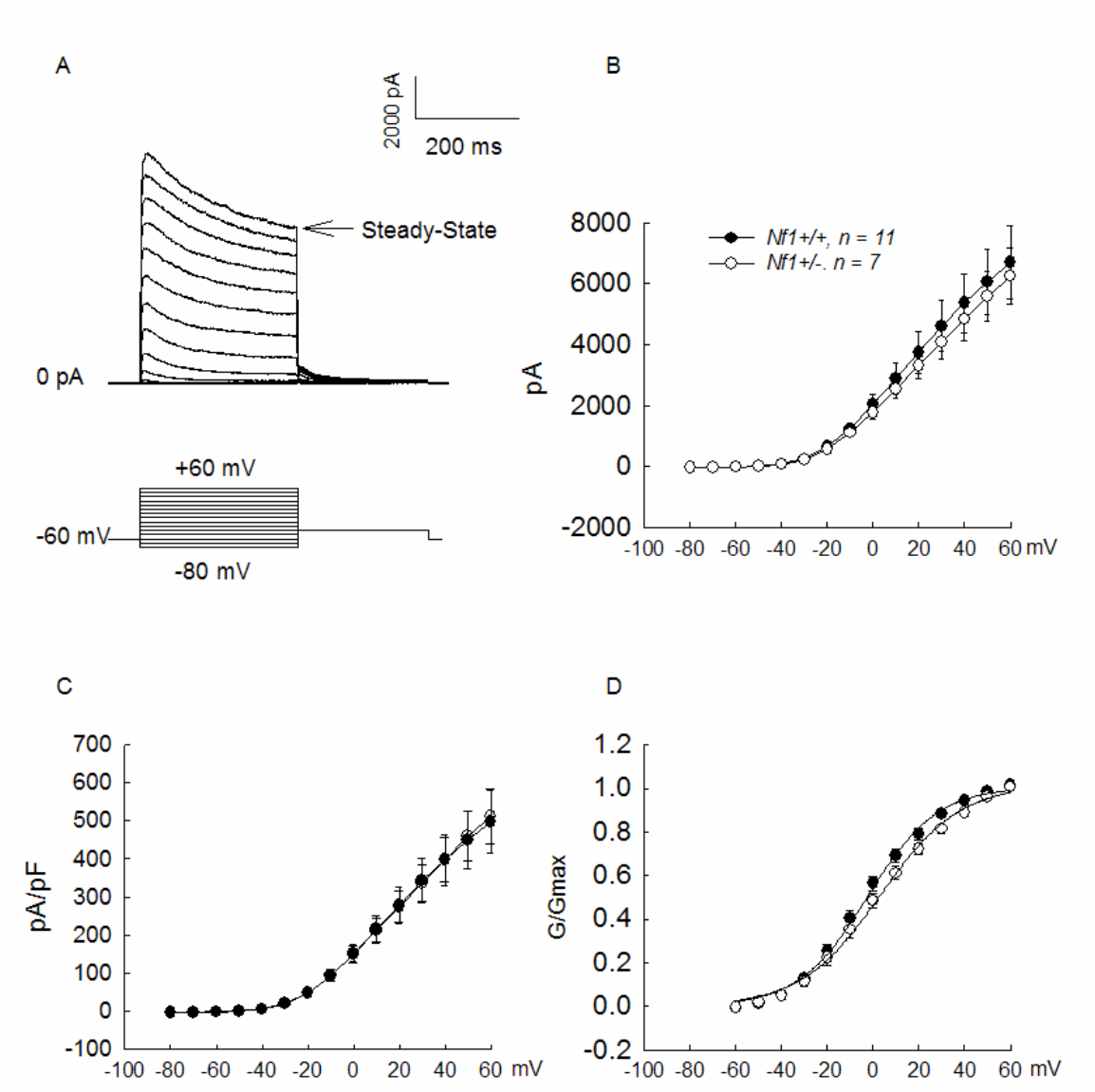

Figure 28. IKd in *Nf1*+/+ and *Nf1*+/- sensory neurons are not different. Panel A shows the representative trace of IK recorded from a *Nf1*+/+ sensory neuron. The arrow in A approximately points the location where the data were measured. The membrane voltage was held at -60 mV; activation of the currents was determined by voltage steps of 300 ms, which were applied at 5 s intervals in +10 mV increments from -80 mV to +60 mV. Panel B summarizes the current-voltage relation of IK in both genotypes. Panel C illustrates the current density-voltage relations of IK in both genotypes. The conductance-voltage relation is illustrated in panel D. The data points in D have been fitted by the Boltzmann relation and are shown as the continuous lines. The values in each panel are from the same 11 *Nf1*+/+ and 7*Nf1*+/- neurons.

Table 1. Boltzmann parameters for the activation of IK in *Nf1+/+* and *Nf1+/-* sensory neurons.

	$V_{0.5}$ (mV)	k (mV)
Nf1+/+ (n=11)		
IK	-2 ± 2	15 ± 1
IKd	-3 ± 2	14 ± 1
Nf1+/- (n=7)		
IK	-1 ± 2	16 ± 1
IKd	2 ± 2	16 ± 0

2. There is no difference in the steady state inactivation of IK between the *Nf1*+/+ and *Nf1*+/- neurons.

Inactivation is a process that blocks the conduction of potassium channels during a depolarization. Once the potassium channels have been inactivated, the membrane must be hyperpolarized to reprime the channels. The ratio of inactivated channels to total channels determines the amplitude of the total currents. To further characterize the IK recorded from *Nf1*+/+ and *Nf1*+/- sensory neurons, the steady-state inactivation was examined. Figure 29A illustrates the steady-state inactivation of IK obtained from a representative *Nf1*+/+ neuron. Figure 29B is the enlarged version of the circled area of A. The inactivation properties of IK in neurons isolated from the two genotypes were not significantly different. For example, after the conditioning prepulse to 20 mV, IK in *Nf1*+/+ cells was inactivated by 70 ± 5% (n=7), which was not different from *Nf1*+/- neurons (71 ± 7 %, n=5). As illustrated in Figure 29C, the I/Imax-voltage relation in *Nf1*+/+ neurons was not different from *Nf1*+/- neurons. The values of I/Imax as a function of the conditioning prepulse were fitted by the Boltzmann relation and the Boltzmann parameters for the inactivation of IK were provided in Figure 29C. Again, the $V_{0.5}$ and k were similar in the two groups of neurons. In summary, the inactivation of IK in *Nf1*+/- neurons was not different from *Nf1*+/+ neurons.

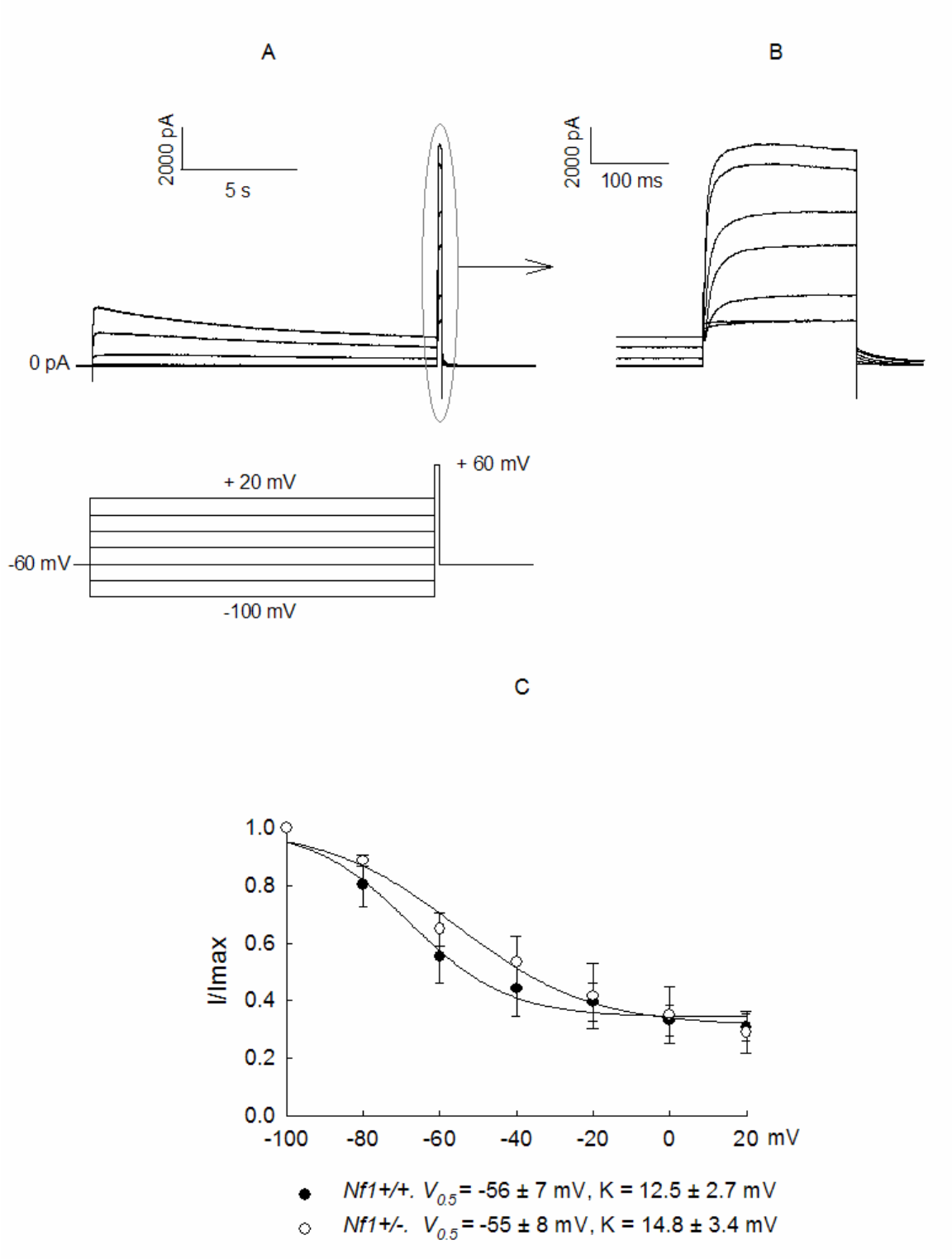

Figure 29. (Legend see next page).

Figure 29. Steady-state inactivation of IK in *Nf1*+/+ and *Nf1*+/- sensory neurons are not different. A. Upper panel shows the IK obtained by applying 15 s conditioning prepulses (-100 to +20 mV in 20 mV increments) after which the voltage was stepped to +60 mV for 200 ms; a 20 s interval separated each prepulse sweep. Lower panel shows the protocol to evoke the IK shown in upper panel. B. The enlarged version of the circled area of panel A that represents the steady-state IK obtained at + 60 mV following the conditional prepulses. C. Steady-state inactivation curves for IK. Membrane currents were normalized to the maximal current obtained after -100 mV prepulse. The data points in C have been fitted by the Boltzmann relation and are shown as the continuous lines. Boltzmann parameters for the inactivation of IK were provided in C. The values in C are from 7 *Nf1*+/+ and 5 *Nf1*+/- neurons.

3. The A-types (IA) of IK do not contribute to the augmented excitability observed of *Nf1*+/- neurons.

IA is another type of IK that modulates neuronal excitability by decreasing the frequency of neuronal firing (Connor and Stevens, 1971). After firing an AP, most channels conducting IA are inactivated. These channels can be reprimed during the repolarization of the membrane potential, especially during the phase of AHP. IA can be activated when a cell is depolarized again to approach the firing threshold; the transient outward IA could oppose the depolarization. The membrane potential can continue to approach the firing threshold as IA inactivates (Connor, 1978). Therefore, IA is a key factor to determine the interspike interval, the time between the successive APs. The suppression of IA results in a faster depolarization of the membrane potential and shortens the interspike intervals. Since *Nf1*+/- neurons fire APs at a much higher frequency when stimulated by a depolarizing ramp of current, experiments were performed to determine whether *Nf1*+/- neurons had smaller IA currents than that of *Nf1*+/+ neurons. As shown in Figure 30, IA was obtained by manipulating the holding potential. A hyperpolarized holding potential of -100 mV was used to remove the inactivation of IA, whereas, in a different protocol, a depolarized holding potential (-40 mV) was used to inactivate IA. After a 4 s prepulse at a holding potential of -100 mV, the total IK was recorded in response to voltage steps from -80 mV to +60 mV in +20 mV increments (Figure 30A). The sustained IK was obtained when the membrane potential was held at -40 mV for 4 s, followed by the same activating voltage steps above (Figure 30B). Isolated IA was then obtained by

digital subtraction of sustained IK from total IK. Since all isolated IA traces have a peak that decayed with time and then reached a stable plateau (Figure 30C), the isolated IA was speculated to be contaminated by a slowly inactivating, delayed-rectifier IK. Based on the assumption that the steady-state currents of isolated IA were the contamination of delayed-rectifier types of IK, the final amplitude of IA was calculated as the peak value of IA minus the steady-state value measured at the ending point of 500 ms voltage steps (Figure 30C).

To minimize the variance of the currents recorded from different sizes of the cells, currents were normalized for cell surface area and expressed as current density (pA/pF). In *Nf1*+/+ neurons, the average peak IA was 5092.5 ± 1680.4 pA and yielded a value of 369 ± 110.3 pA/pF (for the step to + 60 mV), the steady-state current was 2596.3 ± 1007.6 pA and yielded a value of 177.8 ± 67.8 pA/pF (n=5). These values were not significantly different from the values measured in *Nf1*+/- neurons (peak IA was 7388.2 ± 1018.9 pA, 587.7 ± 83.0 pA/pF; steady-state current was 3542.3 ± 681.0 pA, 280.7 ± 54.9 pA/pF, n=3). Although the amplitude of IA in *Nf1*+/+ and *Nf1*+/- neurons was not statistically different, *Nf1*+/- neurons exhibited a trend for having bigger IA currents. Because the augmentation of IA could suppress neuronal excitability and my interest is how those *Nf1*+/- neurons enhanced their excitability, further investigation was not performed. Figure 30F summarizes the conductance-voltage relation of IA in either genotype. The G/Gmax of IA as a function of voltage for *Nf1*+/- neurons was not different compared to *Nf1*+/- neurons. The values of G/Gmax were fitted by the Boltzmann relation. The Boltzmann

parameters, $V_{0.5}$ and k for the activation of IA in neurons of the two genotypes were not different (Figure 30F). To determine whether the kinetics of IA in *Nf1*+/- neurons was altered, the decay of the currents was fitted with an exponential function by using the pClamp 9 software. In *Nf1*+/+ neurons, the decay phase of the currents was well fitted with a double exponential, this indicates that two kinetically distinct components are present in the IA currents of *Nf1*+/+ neurons: one is a slow component with a time constant (τ) of 155.9 ± 36.8 ms at a step of +60 mV, the other is a fast component with a τ of 15 ± 4.2 ms at the same activating voltage step (n=5). The correlation coefficient of the fit was 0.992 ± 0.002 (n=5; the sum of squared errors was much smaller than those fitted by one or three exponentials). In the three *Nf1*+/- neurons having obvious IA components, the decay phase for two neurons was well fitted with a double exponential (the slow τ is 209.3 ms and 98.4 ms, the fast τ is 57.3 and 23.1 ms for two neurons at a voltage step of 60 mV, respectively). In contrast to these two cells, the decay phase for one *Nf1*+/- neuron was fitted with a single exponential (τ is 199.6 ms at a voltage step of 60 mV). Since there is no clear trend revealing a significant alteration of IA kinetics between genotypes, further investigation was not performed.

Based on the experimental results, the IA currents in *Nf1*+/- and *Nf1*+/+ neurons were not different in amplitude, kinetics and profiles of activation. It is unlikely that IA contributes the augmented neuronal excitability of *Nf1*+/- neurons.

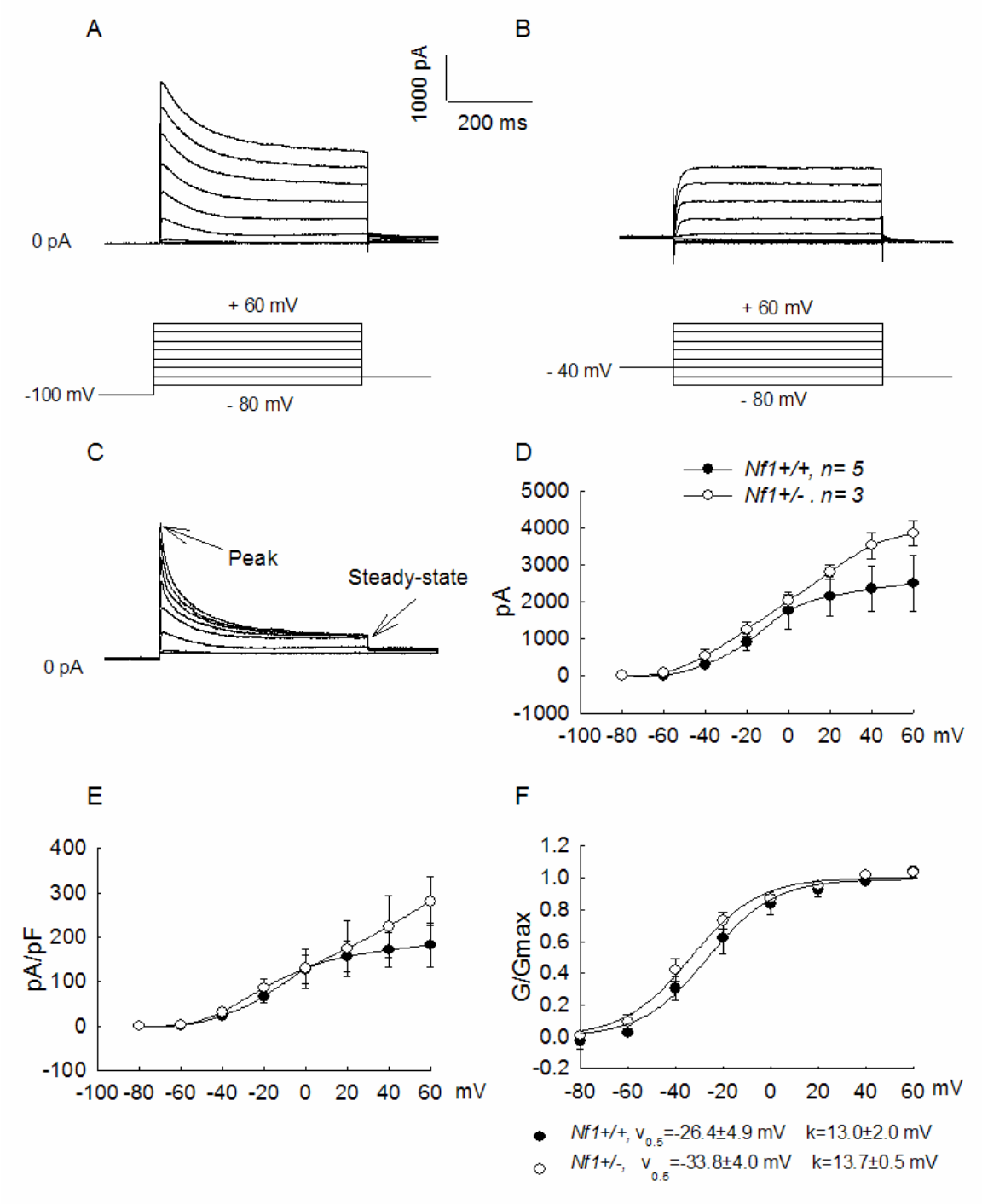

Figure 30. (Legend see next page).

Figure 30. The A-types of IK in *Nf1+/-* neurons are not suppressed in *Nf1+/-* neurons. Currents were measured at different holding potentials. A: For total IK, the membrane potential was held at -100 mV for 4 s and voltage steps were from -80 mV to +60 mV with 10 mV increments and 500 ms in duration. B: For sustained IK, the membrane potential was held at -40 mV for 4 s and the voltage steps were the same as above. C: The currents generated by the two protocols in A and B were subtracted to obtain the A-types of IK. The peak currents (PK) of IA were measured at the peak of the fast inactivating component and the steady-state (SS) currents were measured at the ending point of 500 ms voltage steps (the two arrows in C point to the approximate locations where the PK and SS value of IA were measured). The amplitude of IA was determined as the value of the peak subtracted by steady-state value. The value of IA and the IA density (pA/pF) versus holding potential (I-V) was plotted in D and E, respectively. The current density (pA/pF) was calculated by dividing the current amplitude by the capacitance of cell membrane. The conductance-voltage relation is illustrated in panel F. The data points in F have been fitted by the Boltzmann relation and are shown as the continuous lines. The values in D, E and F are from same 5 *Nf1*+/+ neurons and 3 *Nf1*+/- neurons.

4. The voltage-dependency of steady-state deactivation of tail currents is not different in *Nf1*+/+ and *Nf1*+/- neurons

My results have shown that the activation and inactivation of total IK and IA were not significantly altered in *Nf1*+/- neurons. In the following experiments, a different protocol was used to investigate the I-V relationships and the voltage-dependency of deactivation of the potassium tail currents. Under normal physiological conditions, channels are sitting at different states: open, closed, or inactivated. In order to study the gating properties of potassium channels, two voltage steps were used to synchronize the channels. The membrane potential was hyperpolarized to -100 mV for 3 s to reprime the potassium channels, then membrane potential was depolarized to +60 mV for 100 ms (almost all channels are opened by the depolarization). After the two steps, the membrane potential was repolarized to a series of potentials ranging from -100 mV to + 40 mV for 300 ms in 20 mV increments. The peak currents/current densities versus voltage (I-V) curves are plotted in Figures 31C and D. In *Nf1*+/+ neurons, the average peak value for the tail currents was 4504.0 ± 1636.4 pA (n=5; for the step to + 40 mV, 347.2 ± 120.0 pA/pF), which was not significantly different from the value in *Nf1*+/- neurons (n=4; peak tail currents were 6513.0 ± 1224.9 pA, 515.0 ± 57.7 pA/pF). To determine whether the kinetics of the tail current in *Nf1*+/- neurons was different from that in wild-types, the decay of the currents was fitted with an exponential function by using the pClamp 9 software. The potassium tail currents in *Nf1*+/+ and *Nf1*+/- neurons were well fitted by a single exponential, indicating that there is only one major current component in the tail. As shown in

Figure 31E, the deactivation kinetics (τ) of tail currents is voltage-dependent, being faster at more negative potentials and slower at more positive potentials. Surprisingly, the deactivation kinetics of *Nf1+/-* neurons were significantly slower compared to *Nf1+/+* neurons. This may indicate that one component of IK with slow kinetics becomes the dominant currents in *Nf1+/-* neurons.

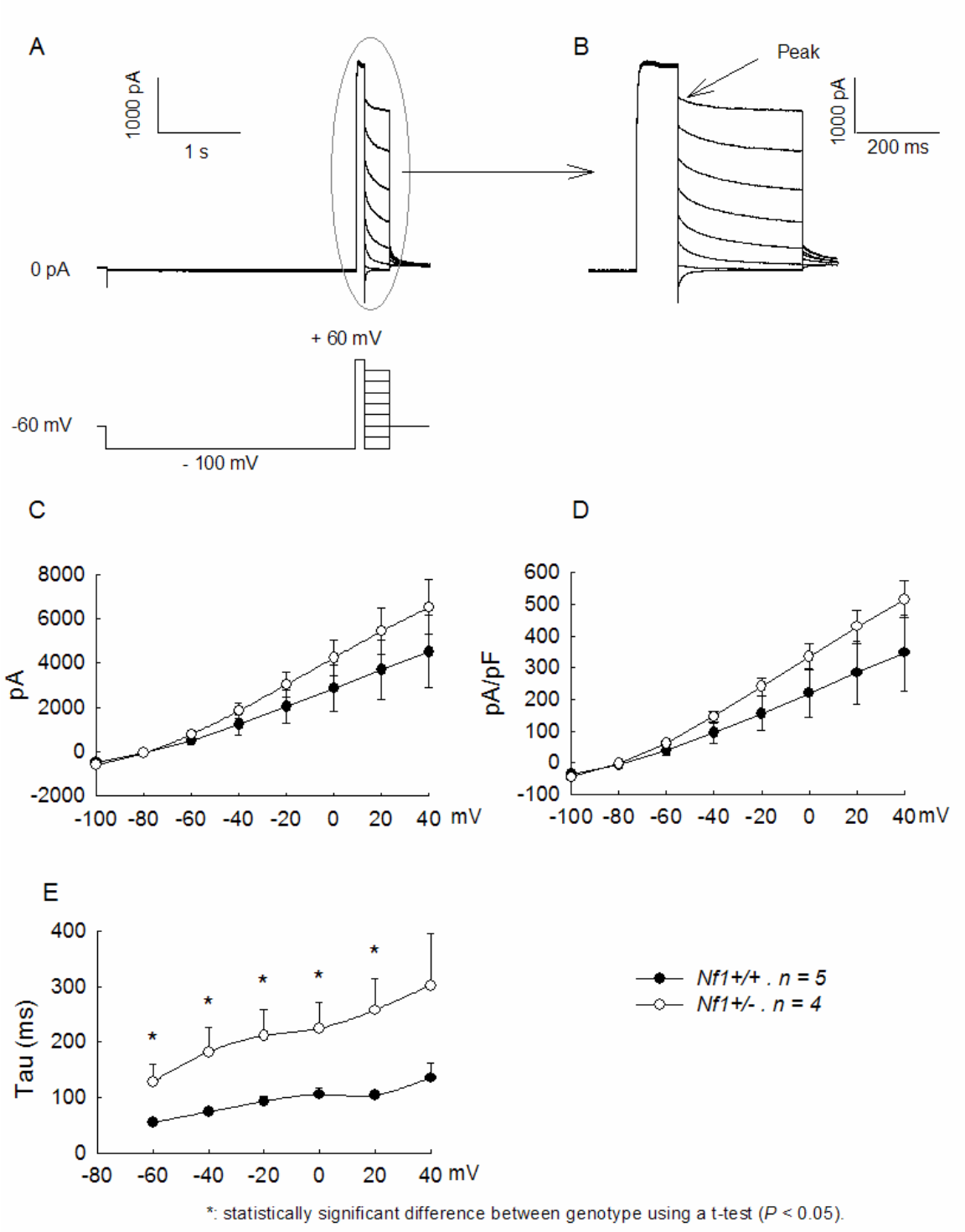

Figure 31. (Legend see next page).

Figure 31. The potassium tail currents in *Nf1*+/+ and *Nf1*+/- neurons are not significantly different. A. The membrane potential was depolarized to + 60 mV for 100 ms after a 3 s, -100 mV prepulse and then repolarized to a series of potentials ranging from -100 mV to + 40 mV for 300 ms in 20 mV increments. The upper panel shows a representative trace recorded from a *Nf1*+/+ sensory neuron. The lower panel shows the protocol to evoke the IK shown in upper panel. B: the enlarged version of the circled area in A. The amplitudes of the tail current were measured at the peak (the arrow in B approximately points the location from where data were collected). The value of tail currents and current densities versus holding potentials was plotted in C and D, respectively. The current density (pA/pF) was calculated by dividing the amplitude of tail currents by the capacitance of cell membrane. E: the relationship of the deactivation kinetics (τ) of tail currents versus different holding potentials. The asterisk represents a statistically significant difference in *Nf1*+/+ and *Nf1*+/- sensory neurons using a t-test ($P < 0.05$).

E. Augmented INa could underlie the enhanced excitability of *Nf1+/-* neurons

INa plays an essential role in controlling neuronal excitability. In sensory neurons and many other types of excitable cells, INa generates the rapid upstroke of the AP. Therefore, the properties of sodium channels, such as distribution, density, trafficking as well as the threshold of activation and repriming characteristics could all influence the firing patterns of sensory neurons. Based on the sensitivity to TTX, two general classes of voltage-gated INa have been identified in small-diameter, nociceptive-like sensory neurons: TTX-S INa and TTX-R INa (Elliott and Elliott, 1993; Roy and Narahashi, 1992). It is well documented that the alteration of INa is an important underlying mechanism for a variety painful disorders, such as inflammation (Black et al., 2004; Li et al., 2006; Tanaka et al., 1998), neuropathic pain (Dib-Hajj et al., 1999; Lai et al., 2002), a painful inherited neuropathy called erythermalgia (Cummins et al., 2004), experimental ulcers (Bielefeldt et al., 2002) and nerve injury (Black et al., 1999; Dib-Hajj et al., 1996; Rizzo et al., 1995; Sleeper et al., 2000). Since people with neurofibromatosis experience enhanced painful sensation and the sensory neurons isolated from *Nf1+/-* mice have augmented excitability, the experiments described below were designed to study the INa in both *Nf1+/+* and *Nf1+/-* sensory neurons to determine whether the enhanced firing of *Nf1+/-* neurons results from an alteration of INa.

1. The total INa is larger in *Nf1+/-* neurons with reduced extracellular sodium (30 mM) and a Cs-aspartate based pipette solution.

Activation of INa was determined by voltage steps 30 ms in duration, which were applied at 10 s intervals in +5 mV increments from -80 to +40 mV following a 500 ms prepulse to -90 mV (see Figure 32A). INa is usually studied using a fluoride-based pipette solution. However, Coste et al., (2004) showed that fluoride caused a significant leftward shift in the I-V curve for both the activation and inactivation of INa (fluoride may generate a strong "bias" for sodium channels towards the open state, thus producing the leftward shift in the I-V curve). Therefore, a Cs-aspartate based pipette solution was used in the studies described below. Low sodium extracellular solution (30 mM) was used in the experiments to decrease the amplitude of INa and thereby minimize the errors in controlling membrane voltage (voltage error = current amplitude * uncompensated series resistance). In Figure 32, the total INa recorded from *Nf1+/-* neurons were significantly larger compared to the INa measured from wild-type neurons. The average peak value of INa in *Nf1+/-* neurons was -1437 ± 237 pA for the step to +0 mV (n=10). This value was significantly larger compared to the INa measured in *Nf1+/+* neurons (-676.0 ± 81.9 pA, n=9, for the step to +0 mV, t-test). To minimize the variance of currents resulting from different sizes of the cells, currents were normalized to the cell surface area and expressed as current density (pA/pF). The capacitance of the cells was read directly from the patch-clamp amplifier after performing the capacitance and series resistance compensation. The reversal potential for INa was calculated to

be +28 mV. The current density-voltage relation of INa in *Nf1*+/+ and *Nf1*+/- neurons is illustrated in Figure 32D. Again, the peak current density of INa in *Nf1*+/- neurons was significant larger than that in *Nf1*+/+ neurons (-48.3 ± 6.6 pA/pF, n=9 versus -103.5 ± 20.7 pA/pF, n=10 for *Nf1*+/+ and *Nf1*+/- neurons, respectively, for the step to +0 mV). Figure 33C shows the conductance-voltage relation of *Nf1*+/+ and *Nf1*+/- sensory neurons. Activation of total INa in *Nf1*+/- neurons appeared to be unaltered because $V_{0.5}$ was -3.1 ± 1.8 mV (n=10), which was not different from the -2.7 ± 1.7 mV (n=9) determined in *Nf1*+/+ neurons. Therefore, it is clear that *Nf1*+/- neurons have augmented INa that could contribute to the enhanced excitability observed in *Nf1*+/- neurons.

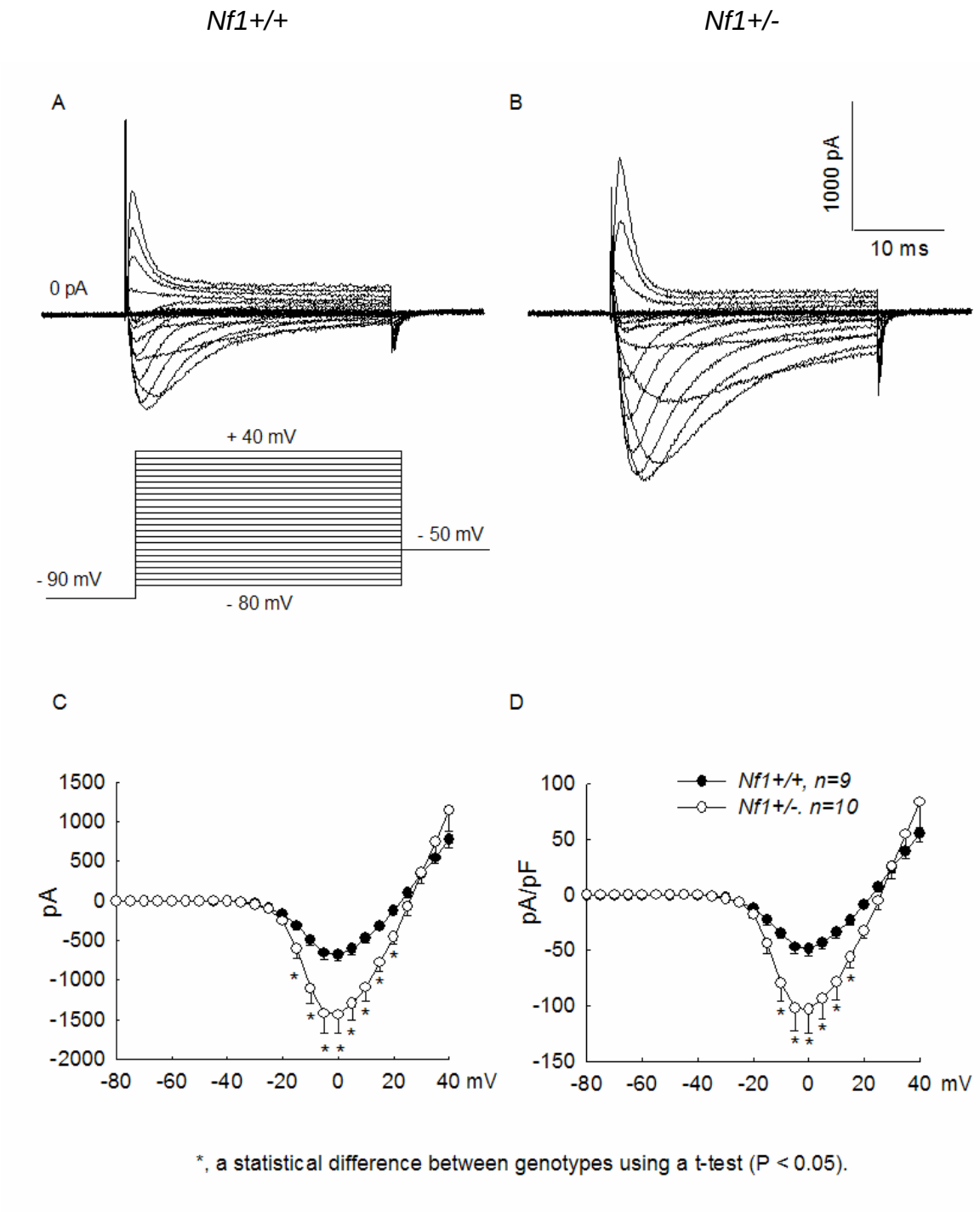

Figure 32. (Legend see next page).

Figure 32. The total INa is larger in *Nf1+/-* neurons with reduced extracellular sodium (30 mM) and a Cs-aspartate based pipette solution. The recordings of total INa from representative sensory neurons isolated from either a *Nf1*+/+ (panel A) or a *Nf1*+/- mouse (panel B). The lower part of panel A shows the protocol to evoke INa. The membrane potential was held at -90 mV for 4 s and voltage steps were from -80 mV to +40 mV with +5 mV increments and 30 ms in duration. The traces in A and B show only the recordings from 500 ms to 550 ms. Panel C summarizes the current-voltage relation of INa in both genotypes. The values of the currents were determined at the peak of each recorded trace. Panel D illustrates the current density-voltage relations of INa in both genotypes. The values in each panel are from the same 9 *Nf1*+/+ and 11 *Nf1*+/- neurons. The asterisk represents a statistically significant difference between *Nf1*+/+ and *Nf1*+/- sensory neurons using a t-test ($P < 0.05$).

2. There is a significant depolarizing shift in the $V_{0.5}$ for steady-state inactivation of total INa in *Nf1*+/- neurons with reduced extracellular sodium (30 mM) and a Cs-aspartate based pipette solution.

Inactivation is a process that closes sodium channels and prevents channels from reopening until the membrane is repolarized to reprime the channels. The property of inactivation could influence the numbers of channels that are capable to open during a given stimulus. Given the importance of inactivation in regulating the availability of sodium channels, I asked whether the inactivation of INa was altered in the *Nf1*+/- sensory neurons. The level of inactivation of INa was established by using a 400 ms conditioning prepulse (-100 to +10 mV in 10 mV increments), after which the voltage was stepped to +0 mV for 30 ms, a 5 s interval separated each sweep (the lower panel of Figure 33A). The upper panel of figure 33A demonstrates the steady-state inactivation of total INa from a representative *Nf1*+/+ neuron. Figure 33B is the enlarged version of the circled area of A. Interestingly, as illustrated in Figure 33C (dashed lines), the I/Imax-voltage relation in *Nf1*+/- neurons was significantly shifted to the right compared to that obtained from *Nf1*+/+ neurons. The values of I/Imax were fitted by the Boltzmann relation and the Boltzmann parameters for the inactivation of INa in both genotypes are provided in Table 2. There was a significant depolarizing shift in $V_{0.5}$ of the inactivation of INa in *Nf1*+/- neurons (-18 ± 1 mV vs. -25 ± 1 mV for *Nf1*+/+ neurons, n=7, $p<0.05$, t-test). As a consequence, the total INa was inactivated by 74 ± 9% (n=7) in *Nf1*+/+ neurons after the conditioning prepulse to -20 mV (a value close to the $V_{0.5}$ for the

inactivation of INa in both genotypes), which is significantly higher compared to *Nf1*+/- neurons (39 ± 7%, n=7). Therefore, the inactivation of total INa in *Nf1*+/- neurons was altered, which can lead to more sodium channels capable to open in response to a given stimulus, thereby augment INa. In addition, the depolarizing shift in the inactivation of INa resulted in a bigger window current. The window current is represented by the area created by the overlap of the activation and inactivation functions of the sodium channel (the shadowed and pointed area in Figure 33C). The window current can result from the opening of the non-inactivated sodium channels (known as persistent INa). Therefore, it is possible that the *Nf1* mutation somehow increases the expression of more persistent INa, or shifts the inactivation of more sodium channels to a depolarized potential.

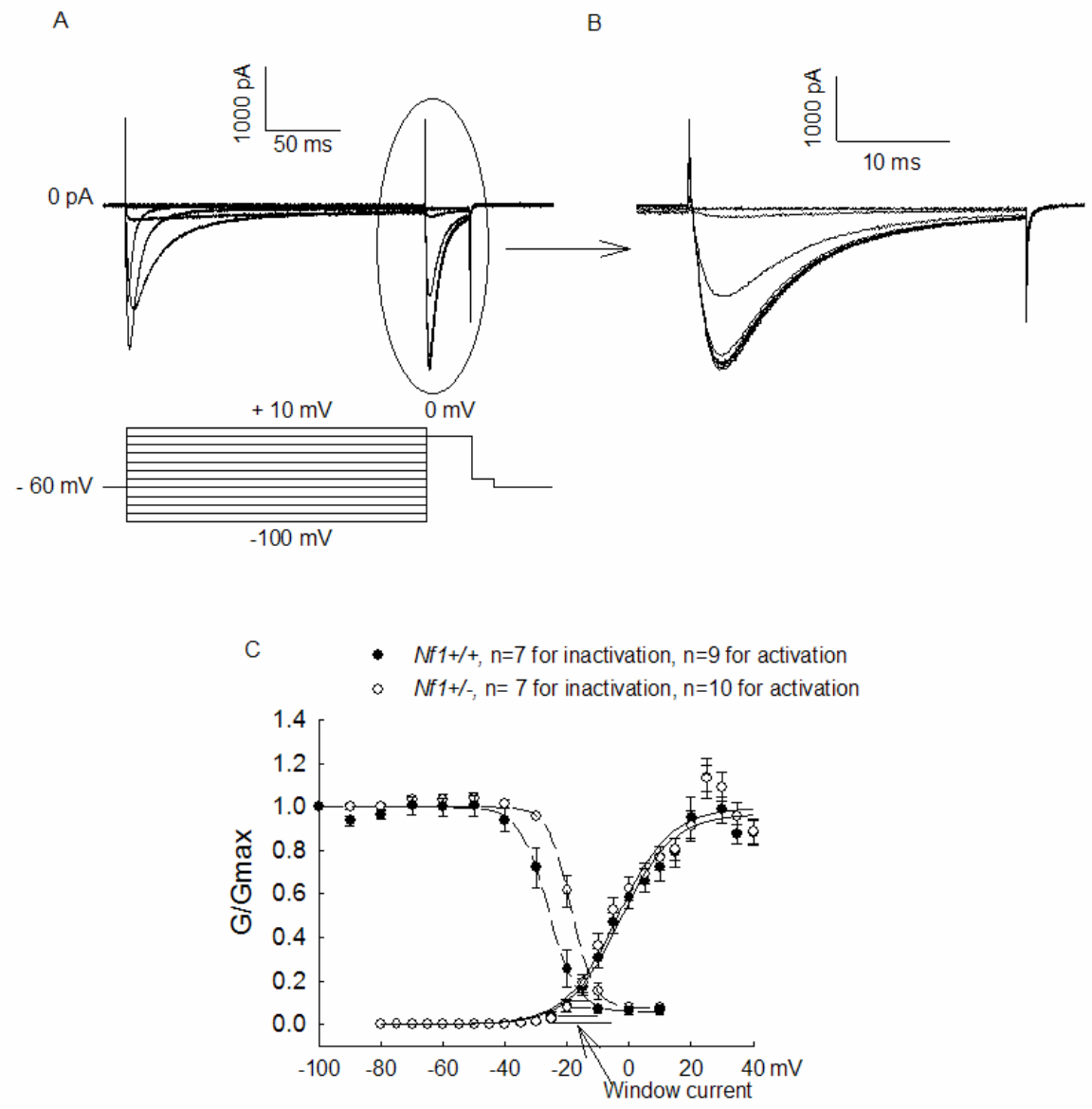

Figure 33. (Legend see next page).

Figure 33. There is a significant depolarizing shift in the $V_{0.5}$ for steady-state inactivation of total INa in *Nf1+/-* neurons with reduced extracellular sodium (30 mM) and a Cs-aspartate based pipette solution. A. Upper panel shows the representative traces of steady-state inactivation of INa obtained by applying 4 s conditional prepulses (-100 to +10 mV in 10 mV increments). After the conditional prepulse, the voltage was stepped to 0 mV for 30 ms, a 5 s interval separated each prepulse sweep. Lower panel shows the protocol to evoke the INa shown in upper panel. B. The enlarged version of the circled area of panel A that represents the INa obtained at + 0 mV following the conditional prepulses. C. The G/Gmax-voltage relationship (the activation of INa) and the I/Imax-voltage relationship (the inactivation of INa) of *Nf1+/+* and *Nf1+/-* sensory neurons. The activation of INa is shown as the continuous lines (n=9-10), whereas the inactivation of INa is represented as dashed lines (n=7). For the steady-state activation, the conductance was normalized with Gmax, which were determined by fitting conductance-voltage curves of data obtained from each neuron using the Boltzmann relation (G/Gmax). For the steady-state inactivation, membrane currents were normalized to the maximal current obtained after -100 mV prepulse (I/Imax). Boltzmann parameters for the activation and inactivation of INa in *Nf1+/+* and *Nf1+/-* sensory neurons were determined by fitting the conductance-voltage or current-voltage curves by Boltzmann equation. Means ± SEM values for $V_{0.5}$ and k (slope) are collected in Table 2.

Table 2. Boltzmann parameters for the activation and inactivation of total INa in *Nf1+/+* and *Nf1+/-* sensory neurons.

	$V_{0.5}$ (mV)	k (mV)
INa activation		
Nf1+/+ (n=10)	-2.7 ± 1.7	7.5 ± 1.0
Nf1+/- (n=10)	-3.1 ± 1.8	7.7 ± 0.9
INa inactivation		
Nf1+/+	-25.3 ± 1.9	4.3 ± 0.3
Nf1+/-	-17.9 ± 1.4 *	4.2 ± 0.2

*: represents a statistically significant difference between *Nf1+/+* and *Nf1+/-* sensory neurons using a t-test ($P < 0.05$).

3. The *Nf1+/-* neurons have augmented TTX-R INa with reduced extracellular sodium (30 mM) and a Cs-aspartate based pipette solution.

The augmentation of TTX-R INa has been proposed to be an important underlying mechanism in neuronal sensitization (England et al., 1996; Gold et al., 1996a; Gold et al., 2002; Jeftinija, 1994; Rush and Waxman, 2004; Tanaka et al., 1998; Waxman et al., 1994; Zhang et al., 2002). Based on the observation that *Nf1+/-* neurons had much higher excitability, I determined whether TTX-R INa in *Nf1+/-* neurons was augmented. The TTX-R INa was obtained by using the same voltage protocol to evoke total INa in the presence of 500 nM TTX in the bath solution. Figure 34A and B show representative traces for TTX-R INa in *Nf1+/+* neurons and *Nf1+/-* neurons. The peak currents of TTX-R INa in *Nf1+/-* neurons were significantly larger than that in *Nf1+/+* neurons. The current-voltage relation for the maximum average peak value of TTX-R INa in *Nf1+/-* neurons was -1073.7 ± 230.1 pA (n=6, for the step to 0 mV), which was significantly larger than that in *Nf1+/+* neurons (-404.1 ± 60.7 pA, n=5, for the step to 0 mV, t-test, Figure 34C). To minimize the variance of currents resulting from different sizes of the cells, currents were normalized for cell surface area and expressed as current density (pA/pF). The current density-voltage relation of TTX-R INa in *Nf1+/+* and *Nf1+/-* neurons is illustrated in Figure 34D. The peak current density of TTX-R INa in *Nf1+/-* neurons was significantly larger than that in *Nf1+/+* neurons (-22.5 ± 3.7 pA/pF, n=5 versus -65.8 ± 16.9 pA/pF, n=6 for *Nf1+/+* and *Nf1+/-* neurons, respectively, for the step to +5 mV). The voltage dependence for activation of TTX-R INa was determined by fitting the

conductance-voltage curve by Boltzmann relation (Figure 35C) and their corresponding Boltzmann fits are shown in Table 3. The activation of TTX-R INa seems to be unaltered because the $V_{0.5}$ in *Nf1*+/+ neurons was -5.7 ± 1.5 mV (n=6), which was not different from that in *Nf1*+/+ neurons (-6.8 ± 2.5 mV, n=5). Both the slope factor (k) and the reversal potential for TTX-R INa were not different between neurons of the two genotypes. Based on these results, the TTX-R INa in *Nf1*+/- neurons was significantly enlarged, which can contribute to the enhanced excitability in *Nf1*+/- neurons.

4. There is a significant depolarizing shift in the $V_{0.5}$ for steady-state inactivation of TTX-R INa in *Nf1*+/- neurons with reduced extracellular sodium (30 mM) and a Cs-aspartate based pipette solution.

In order to study the inactivation of TTX-R INa in *Nf1*+/- neurons, the same protocol as described in Figure 32A was used while the neurons were in the recording chamber with 500 nM TTX in the bath solution. Similar to total INa, the steady-state inactivation of TTX-R INa was shifted significantly to the right (Figure 35C). The voltage dependence for inactivation of TTX-R INa was determined by fitting the I/Imax-voltage curve by the Boltzmann relation (Figure 35C) and their corresponding Boltzmann fits are illustrated in Table 3. A significant depolarizing shift in $V_{0.5}$ of the inactivation of TTX-R INa in *Nf1*+/- neurons was observed (-20.8 ± 1.5 mV, n=5 for *Nf1*+/- neurons vs. -29.0 ± 2.4 mV for *Nf1*+/+ neurons, n=4, $p<0.05$, t-test). In *Nf1*+/- neurons, as a result of the leftward shift of I/Imax-voltage relationship, the TTX-R INa was inactivated by

55.0 ± 7.8% (n=5) after the conditioning prepulse to -20mV, which was significantly lower compared to that in the *Nf1*+/+ neurons (90 ± 2%, n=4). This change in the inactivation of TTX-R INa of *Nf1*+/- neurons indicated that more sodium channels were available for a given stimulus, resulting in bigger INa.

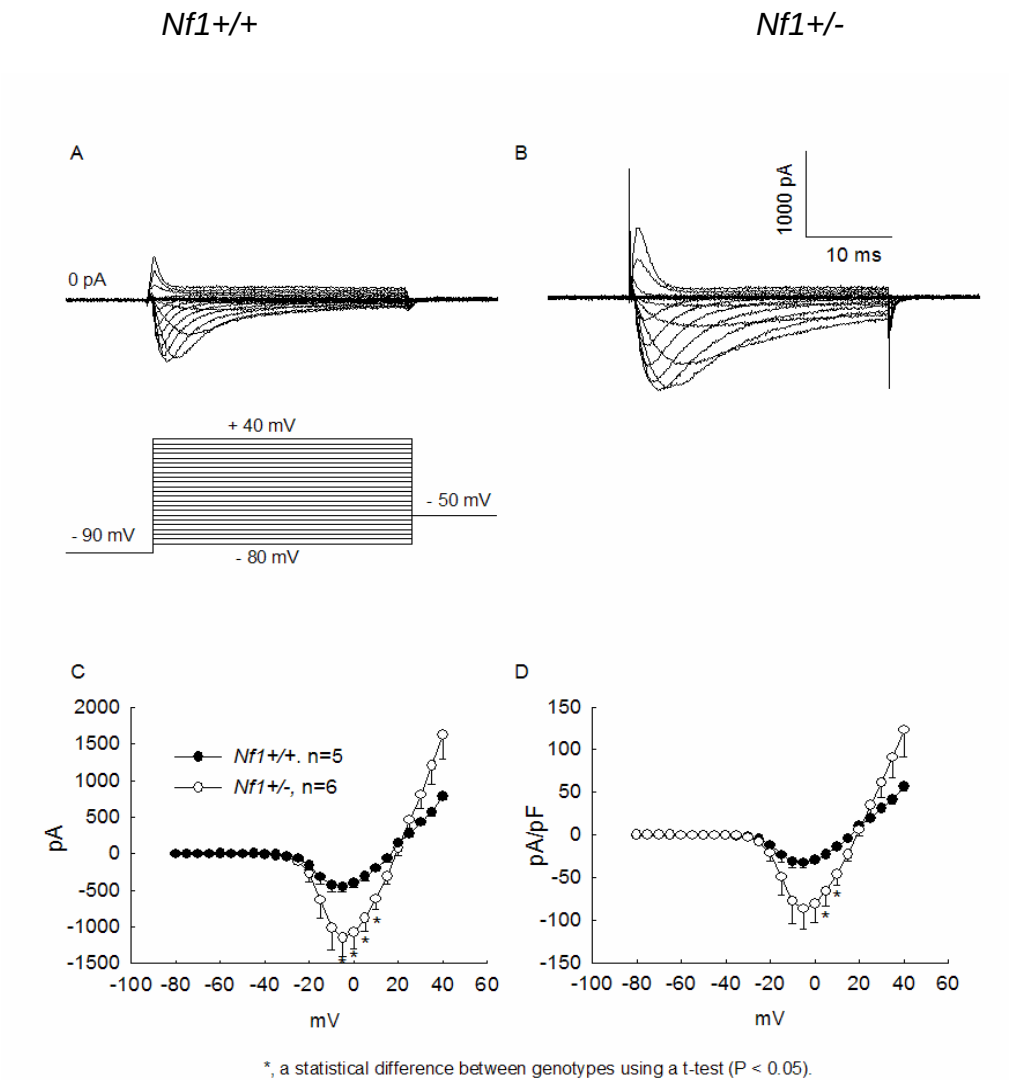

Figure 34. *Nf1+/-* neurons have augmented TTX-R INa with reduced extracellular sodium (30 mM) and a Cs-aspartate based pipette solution. The recordings of TTX-R INa from representative sensory neurons isolated from either a *Nf1+/+* (A) or a *Nf1+/-* mouse (B) at the presence of 500 nM TTX. The lower part of panel A shows the protocol to evoke INa. the membrane potential was held at -90 mV for 4 s and voltage steps were from -80 mV to +40 mV with + 5 mV increments and 30 ms in duration. The traces in A and B only show the recordings from 500 ms to 550 ms. Panel C summarizes the current-voltage relation of TTX-R INa in both genotypes. The values of the currents were collected at the peak of each recorded trace. Panel D illustrates the current density-voltage relations of TTX-R INa in both genotypes. The values in each panel are from the same 5 *Nf1+/+* and 9 *Nf1+/-* neurons. The asterisk represents a statistically significant difference between *Nf1+/+* and *Nf1+/-* sensory neurons using a t-test ($P < 0.05$).

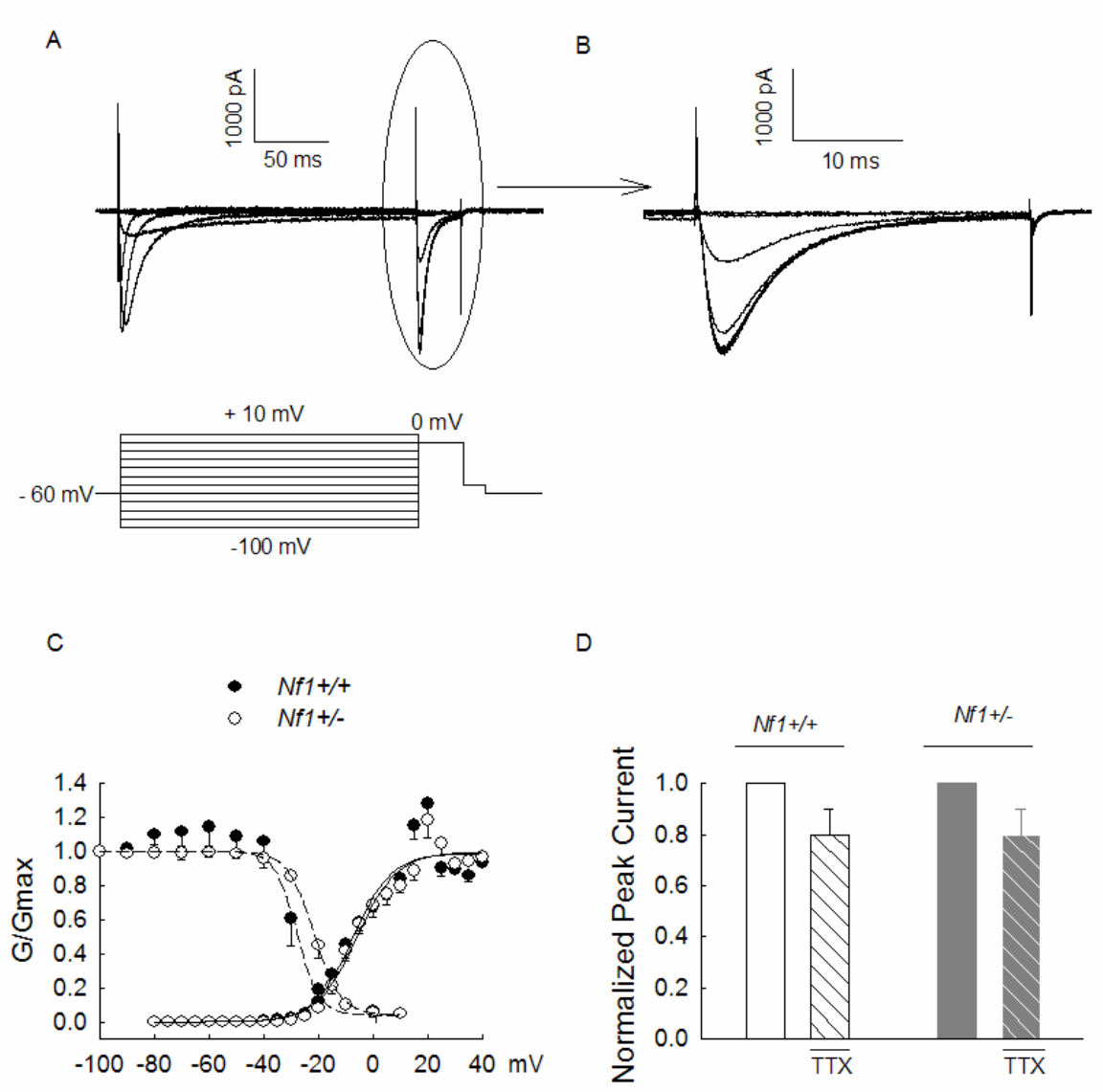

Figure 35. (Legend see next page).

Figure 35. There is a significant depolarizing shift in the $V_{0.5}$ for steady-state inactivation of TTX-R INa in *Nf1+/-* neurons with reduced extracellular sodium (30 mM) and a Cs-aspartate based pipette solution. A. Upper panel shows the representative traces of steady-state inactivation of TTX-R INa by applying the same protocol described in the legend of Figure 32. B. The enlarged version of the circled area of panel A that represents the TTX-R INa obtained at 0 mV following the conditional prepulses. C. The G/Gmax-voltage relationship (the activation of INa) and the I/Imax-voltage relationship (the inactivation of INa) of TTX-R INa in *Nf1+/+* and *Nf1+/-* sensory neurons. The activation of INa is shown as the continuous lines (n=5-6), whereas the inactivation of INa is represented as dashed lines (n=4-5). For the steady-state activation, the conductance was normalized to Gmax, which was determined by fitting the conductance-voltage curves of data obtained for each neuron using the Boltzmann relation (G/Gmax). For the steady-state inactivation, membrane currents were normalized to the maximal current obtained after -100 mV prepulse (I/Imax). The voltage dependence for activation and inactivation of TTX-R INa was determined by fitting the G/Gmax-voltage curve or I/Imax-voltage curve by Boltzmann relation and their corresponding Boltzmann fits are demonstrated in Table 3. D. shows the normalized average peak INa before and after TTX in *Nf1+/+* and *Nf1+/-* neurons. The peak currents were normalized to their respective control values (the peak values obtained before applying TTX). N=6-7.

Table 3. Boltzmann parameters for the activation and inactivation of INa in *Nf1+/+* and *Nf1+/-* sensory neurons.

	$V_{0.5}$ (mV)	k (mV)
TTX-R INa activation		
Nf1+/+ (n=5)	-6.8 ± 2.5	6.8 ± 0.6
Nf1+/- (n=6)	-5.7 ± 1.5	7.2 ± 0.7
TTX-R INa inactivation		
Nf1+/+	-29.0 ± 2.4	5.0 ± 0.5
Nf1+/-	-20.8 ± 1.5 *	4.6 ± 0.3

*: represents a statistically significant difference between *Nf1+/+* and *Nf1+/-* sensory neurons using a t-test ($P < 0.05$).

5. Few cells exhibit the characteristics of TTX-S INa in *Nf1+/+* and *Nf1+/-* neurons with 30 mM extracellular sodium concentration and Cs-aspartate based intracellular solution.

Given the information that TTX-S INa has a strong link with the neuronal sensitization during inflammation and nerve injury (Black et al., 1999; Black et al., 2004; Dib-Hajj et al., 1996), I investigated whether the TTX-S INa in *Nf1+/-* and *Nf1+/+* neurons was different under the condition with reduced extracellular sodium concentration (30 mM) and Cs-aspartate based intracellular solution. TTX-S INa was obtained by digital subtraction of the current traces recorded before and after treatment with TTX by using the same voltage protocol for total INa. Surprisingly, under our experimental condition, few neurons exhibited the characteristics of TTX-S INa. For example, in 6 *Nf1+/+* neurons, only 3 cells had the TTX-S components. The average peak TTX-S INa was -511.3 ± 149.2 pA (-37.5 ± 11.2 pA/pF) for a step to -10 mV. In contrast to *Nf1+/+* cells, in 6 *Nf1+/-* neurons, only one cell exhibited TTX-S INa (peak INa was -289.9 pA for a step to -10 mV). As illustrated in Figure 35D, in both genotypes, the peak INa before and after TTX were not significantly different.

TTX-S INa with large amplitudes have been observed in small diameter sensory neurons (Cummins et al., 2001). Under my experimental condition, few cells had TTX-S components. This indicates that my experimental condition, i.e. 30 mM extracellular sodium concentration and Cs-aspartate based intracellular solution, was not ideal for investigating TTX-S INa in mouse sensory neurons.

Therefore, in the sections described below, recordings for INa were performed using full extracellular sodium (110 mM) and a CsF based pipette solution.

6. The total INa in neurons of either genotype exhibits two phenotypes with full extracellular sodium (110 mM) and a CsF based pipette solution.

To optimize the recording conditions to measure TTX-S INa, a full extracellular sodium solution and CsF based pipette solution was used. Because CsF caused a left-ward shift in the I-V relationship of INa (Coste et al., 2004), the protocols to record INa were modified in order to record total INa and TTX-R INa in the same neuron rapidly. In my experiments, the recording for total INa and TTX-R INa were finished in 6 min. In this short time-frame, the I-V curve was not significantly shifted by CsF, thus ensuring the successful isolation of TTX-S INa by digital subtraction of the currents recorded before and after applying TTX. In addition, the time at which the recordings were obtained was consistent. For example, the recordings for total INa were performed 2 min after establishing the whole-cell configuration, whereas all TTX-R currents were recorded 5 min after establishing the whole-cell configuration.

The detailed description of the protocol used to record INa under full sodium extracellular solution and CsF based pipette solution can be found in the Materials and Methods. Briefly, the membrane voltage was held at -100 mV after establishing the whole-cell configuration. Activation of INa was determined by voltage steps that were 30 ms in duration, which were applied at 10 s intervals in +5 mV increments from -80 to +60 mV. A 5 s interval separated each prepulse

sweep whose holding voltage was -100 mV. Using the recording conditions with 110 mM extracellular sodium and the CsF based pipette solution, the total INa clearly exhibited two phenotypes in both *Nf1*+/+ and *Nf1*+/- neurons: one was dominated by the fast activating and inactivating, TTX-S-like currents (type I, Figure 36A), the other was dominated by slow activating and inactivating, TTX-R-like currents (type II, Figure 36C). After type I neurons were treated with TTX, there was a dramatic decrease in the peak current in (Figure 36B). In contrast, in type II neurons, the peak current was not significantly altered by TTX (Figure 36D). In ten *Nf1*+/- neurons, four neurons belonged to the type I group and six neurons belonged to the type II group, whereas in the *Nf1*+/+ neurons, eight cells belonged to the type I group (Figure 36D). Because Type I neurons typically had a large peak TTX-S-like INa, the larger proportion of type I neurons in *Nf1*+/+ cells results a larger total currents. Consequently, the difference in total INa between genotypes was diminished when observed under the condition with reduced extracellular sodium (30 mM) and a Cs-aspartate based pipette solution. The average peak value of total INa in *Nf1*+/+ neurons was -10897.8 ± 1534.8 pA (n=5, for the step to -15 mV), which was not different from *Nf1*+/- neurons (-10390.3 ± 1346.3 pA, n=7, for the steps to -15 mV). To minimize the variance of the currents obtained from cells of different sizes, currents were normalized to cell surface area and expressed as current density (pA/pF). The current density-voltage relation for the total INa in *Nf1*+/+ and *Nf1*+/- neurons is illustrated in Figure 37B. Again, the peak current density of INa in *Nf1*+/+ neurons was not significantly different from the value in *Nf1*+/- neurons (-730.8 ± 148.0 pA/pF, n=5

versus -878.2 ± 145.5 pA/pF, n=7 for *Nf1*+/+ and *Nf1*+/- neurons, respectively, for the steps to -15 mV). Figure 37C shows the conductance-voltage relation obtained from *Nf1*+/+ and *Nf1*+/- sensory neurons. Activation of total INa in *Nf1*+/- neurons appeared to be unaltered from that in *Nf1*+/+ neurons. The values of $V_{0.5}$ and k in *Nf1*+/+ neurons were not different from those measured in *Nf1*+/- neurons. The values for $V_{0.5}$ and k are provided in Table 4. This result is contradictory to my previous observation that the total INa was augmented in *Nf1*+/- neurons using the reduced extracellular sodium solution and Cs-aspartate based pipette solution. Under the condition with 30 mM sodium in extracellular solution and with CsF based pipette solution, the total INa was dominated by TTX-R INa. This raised the question as to whether TTX-R INa was augmented in *Nf1*+/- neurons. Therefore, the TTX-R INa was isolated and compared in neurons isolated from the two genotypes.

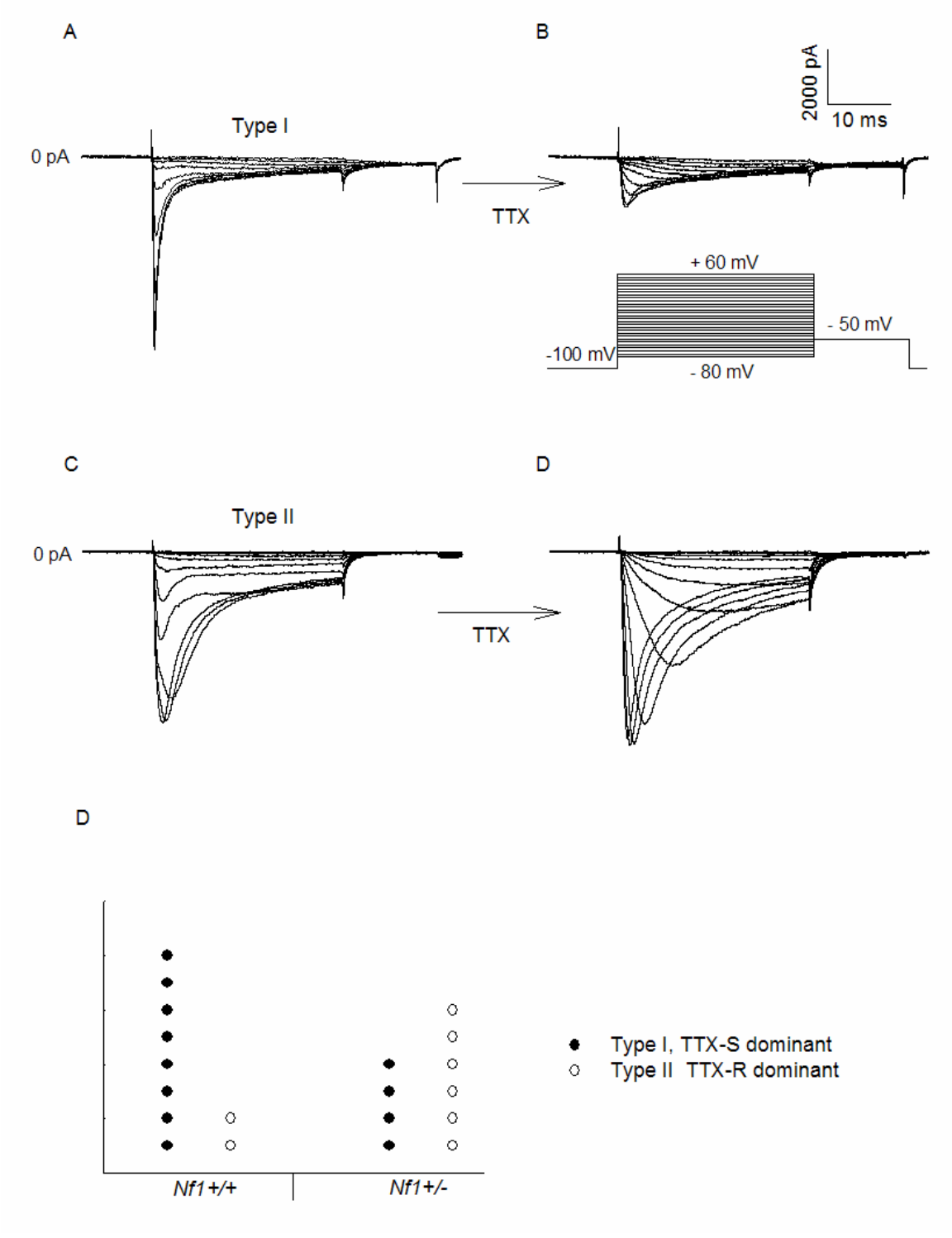

Figure 36. (Legend see next page).

Figure 36. The total INa exhibits two phenotypes in small diameter, nociceptive-like sensory neurons. The recordings of total INa evoked from either a type I neuron (A) or a type II neuron (C). B: The TTX-R INa in type I neuron. The lower part of panel B shows the protocol to elicit INa. The membrane potential was held at -100 mV, the voltage steps were from -80 mV to +60 mV with + 5 mV increments and 30 ms in duration. D: The TTX-R INa in type II neurons. E: left part of the Figure shows the phenotypes of total INa in 10 *Nf1+/+* neurons, whereas the right shows that of 10 *Nf1+/-* neurons. It is highly possible that the percentage of type I neurons whose total INa are dominated by TTX-S INa is decreased in *Nf1+/-* neurons. For clarity purposes, the INa presented in A and B only show the traces whose holding potential was from -60 mV to -15 mV, whereas the currents in C and D presents those whose holding potential was from -60 mV to -5 mV (the voltage-range from beginning to activate the current to maximum activate INa).

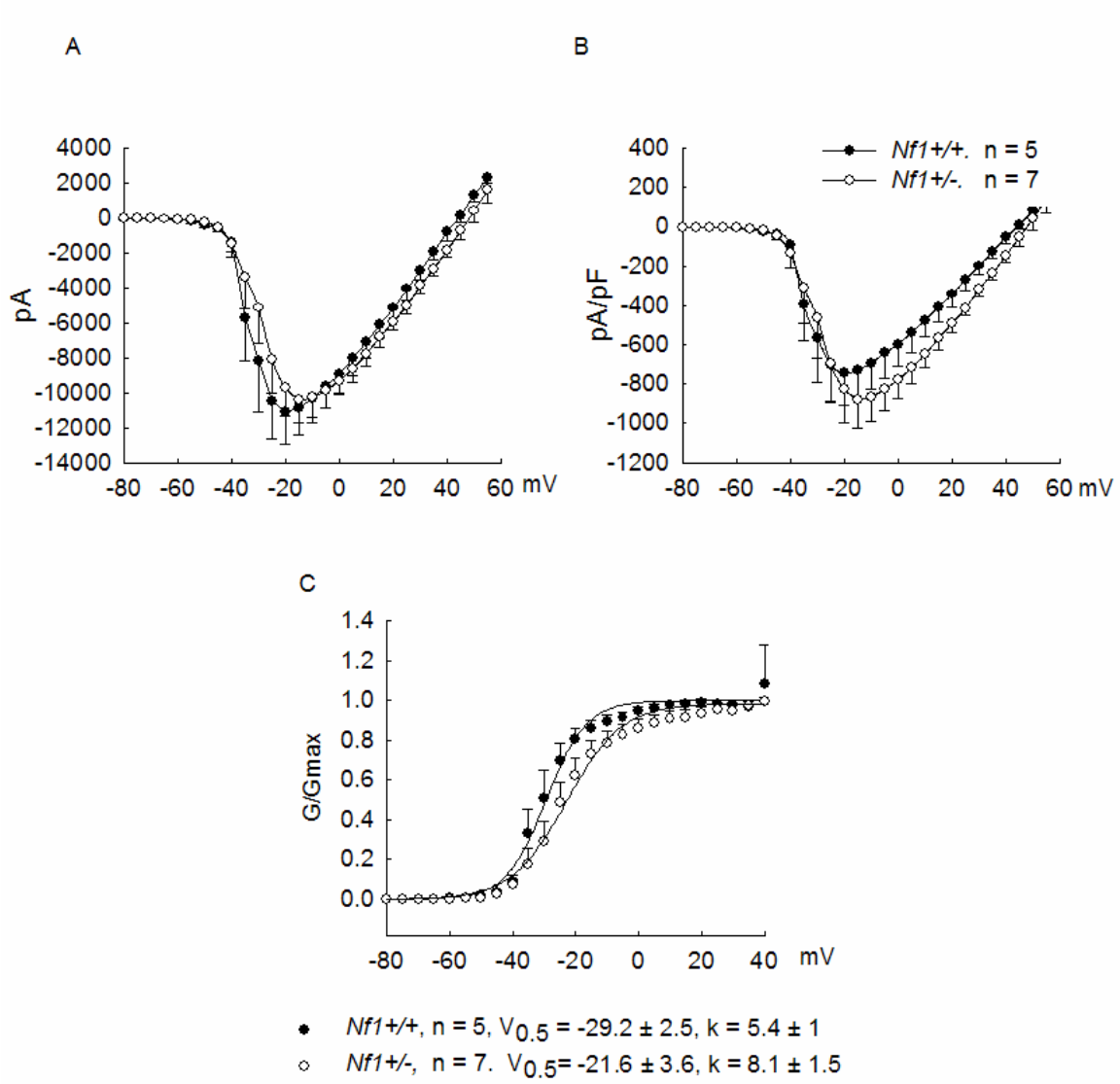

Figure 37. Total INa in *Nf1*+/+ and *Nf1*+/- neurons is not significantly different under full sodium extracellular solution and CsF based pipette solution. Panel A summarizes the current-voltage relation of total INa in both genotypes. The values of the currents were collected at the peak of each recorded trace. The currents were evoked by using the protocols described in Figure 35 legend. Panel B illustrates the current density-voltage relations of total INa in both genotypes. The values in each panel are from the same 5 *Nf1*+/+ and 7 *Nf1*+/- neurons. C: the conductance was normalized to Gmax, which was determined by fitting conductance-voltage curves obtained from each neuron using the Boltzmann relation. The voltage dependence for activation of total INa was determined by fitting the G/Gmax-voltage curve by Boltzmann relation and their corresponding Boltzmann fits are demonstrated in Table 4.

Table 4. Boltzmann parameters for the activation of total INa in *Nf1+/+* and *Nf1+/-* sensory neurons.

	$V_{0.5}$ (mV)	k (mV)
Total INa activation		
Nf1+/+ (n=5)	-29.2 ± 2.5	5.4 ± 1.0
Nf1+/- (n=7)	-21.6 ± 3.6	8.1 ± 1.5

7. The TTX-R INa is augmented in *Nf1*+/- neurons with full extracellular sodium (110 mM) and a CsF based pipette solution.

The TTX-R INa was obtained by using the same voltage protocol to evoke total INa in the presence of 500 nM TTX in the bath solution. The TTX-R INa in *Nf1*+/- neurons was significantly larger compared to *Nf1*+/+ neurons under the condition with full extracellular sodium and the CsF-based pipette solution. As illustrated in Figure 38A, the average peak value of TTX-R INa in *Nf1*+/- neurons was -6788.0 ± 1627.5 pA (n=6, for the step to -10 mV), which was significantly larger than the TTX-R INa in the *Nf1*+/+ neurons (-3149.9 ± 846.7 pA, n=4, for the step to -10 mV, Mann-Whitney Rank Sum Test). The current density-voltage relation of TTX-R INa in *Nf1*+/+ and *Nf1*+/- neurons is illustrated in Figure 38B. The peak current density of INa in *Nf1*+/- neurons was significantly larger than that in *Nf1*+/+ neurons. For example, for the step to -10 mV, the average peak current density of TTX-R INa in *Nf1*+/- neurons was -503.0 ± 71.8 pA/pF (n=6), which was significantly larger than that in *Nf1*+/+ neurons (-227.2 ± 72.3 pA/pF, n=4). Figure 38C represents the conductance-voltage relation of *Nf1*+/+ and *Nf1*+/- sensory neurons. Similar to the results obtained using low extracellular sodium and Cs-aspartate based pipette solution, the activation of TTX-R INa in *Nf1*+/- neurons appears to be unaltered compared to wild-type neurons. $V_{0.5}$ and k are provided in Table 5. Based on the experimental results using either full extracellular sodium and the CsF-based pipette solution or low extracellular sodium and Cs-aspartate-based pipette solution, it is clear that *Nf1*+/- neurons

have augmented TTX-R INa that could contribute to the enhanced excitability observed in *Nf1+/-* neurons.

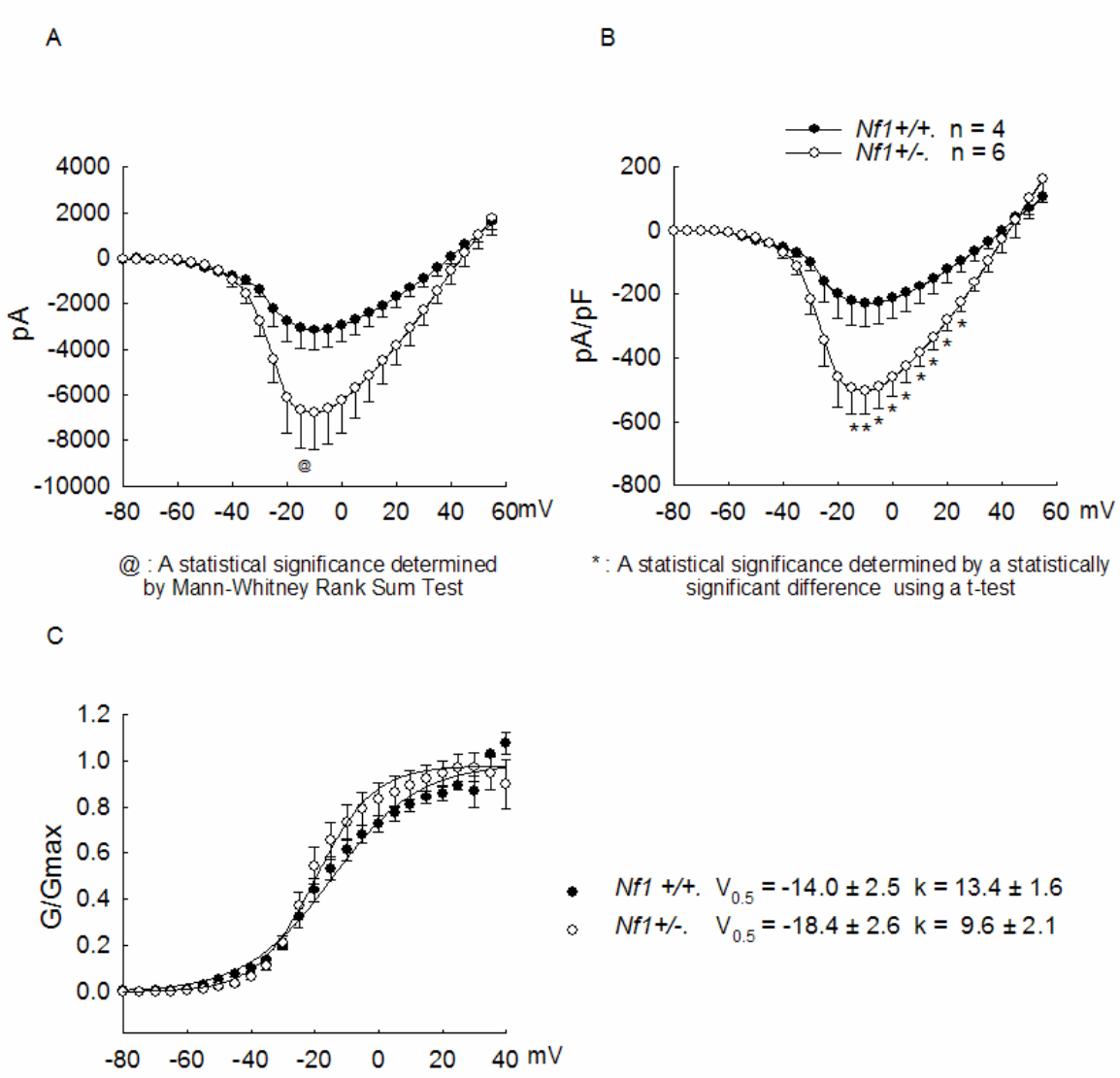

Figure 38. TTX-R INa in *Nf1*+/- neurons is significantly larger compared to *Nf1*+/+ neurons under full sodium extracellular solution and CsF based pipette solution. Panel A summarizes the current-voltage relation of TTX-R INa in both genotypes. The values of the currents were collected at the peak of each recorded trace. The currents were evoked by using the protocols described in Figure 35 legend and with 500 nM TTX in extracellular solution. Panel B illustrates the current density-voltage relations of TTX-R INa in both genotypes. The values in each panel are from the same 4 *Nf1*+/+ and 6 *Nf1*+/- neurons. C: the conductance was normalized to Gmax, which were determined by fitting conductance-voltage curves obtained from each neuron using the Boltzmann relation. The voltage dependence for activation of TTX-R INa was determined by fitting the G/Gmax-voltage curve using Boltzmann relation and their corresponding Boltzmann fits are demonstrated in Table 5. @: represent a statistically significant difference between genotypes using Mann-Whitney Rank Sum Test. *: represent a statistically significant difference between genotypes using a t-test.

Table 5. Boltzmann parameters for the activation of TTX-R INa in *Nf1+/+* and *Nf1+/-* sensory neurons

	$V_{0.5}$ (mV)	k (mV)
Total INa activation		
Nf1+/+ (n=5)	-14.0 ± 2.5	13.4 ± 1.6
Nf1+/- (n=7)	-18.4 ± 2.6	9.6 ± 2.1

8. The TTX-S INa is larger in *Nf1*+/- neurons with full extracellular sodium (110 mM) and a CsF based pipette solution.

This series of experiments was designed to investigate the TTX-S INa in *Nf1*+/- and *Nf1*+/+ neurons under the condition of full extracellular sodium solution and CsF-based pipette solution. After obtaining the total INa, the superfusate was changed to Ringer's solution containing 500 nM TTX and cells were superfused for the appropriate times. TTX-S INa (Figure 39C) was obtained by digital subtraction of the current traces recorded before (Figure 39A) and after TTX treatment (Figure 39B). As illustrated in Figure 39D, the TTX-S INa in *Nf1*+/- neurons was not significantly larger compared to the current obtained from *Nf1*+/+ neurons (-11230 ± 1126 pA versus -8299 ± 1057 pA, n=3, for the steps to -20 mV). However, the average peak current density in *Nf1*+/- neurons was -969 ± 72 pA/pF (n=3) and was significantly larger compared to *Nf1*+/+ neurons (-546 ± 92 pA/pF, n=3, for the steps to -20 mV) as demonstrated in Figure 39E. Figure 39F represents the conductance-voltage relation of *Nf1*+/+ and *Nf1*+/- sensory neurons. Similar to TTX-R INa, the activation of TTX-S INa in *Nf1*+/- neurons appears to be unaltered compared to that in *Nf1*+/+ neurons. $V_{0.5}$ and k are provided in Table 6.

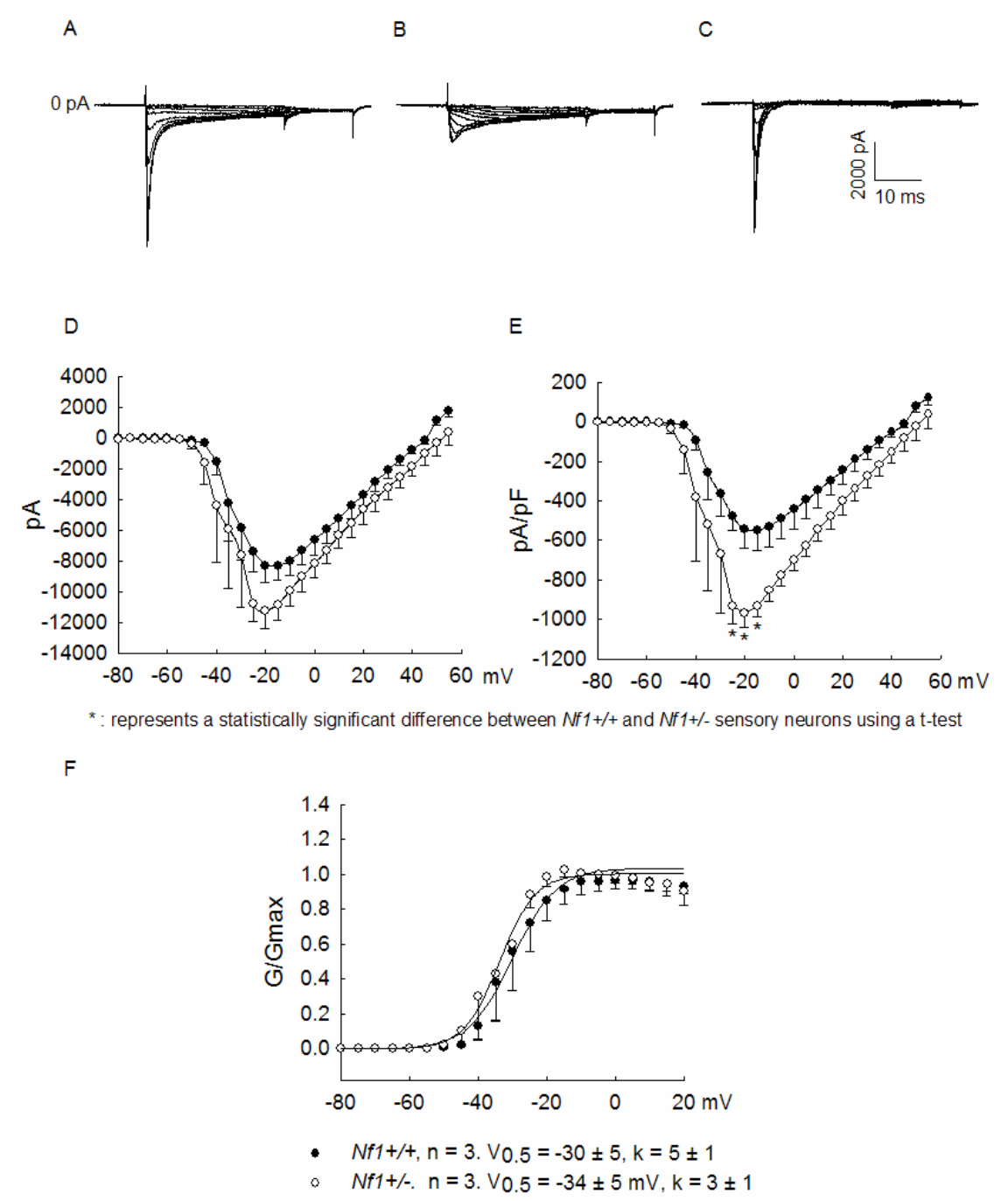

Figure 39. (legend see next page).

Figure 39. The current density of TTX-S INa in *Nf1+/-* neurons is significantly larger compared to *Nf1+/+* neurons under full sodium extracellular solution and CsF based pipette solution. A: Total INa. B: TTX-R INa. C: TTX-S INa obtained by digital subtraction (A-B). A-C: the membrane potential was hold at -100 mV. The INa was evoked by applying voltage steps of 30ms at 10 s intervals in +5 mV increments from -80 to +40 mV. The traces in A-C only show the currents whose command potential was from -60 mV to -15 mV. Panel D summarizes the current-voltage relation of TTX-S INa in both genotypes. The values of the currents were collected at the peak of each recorded trace. Panel E illustrates the current density-voltage relations of TTX-S INa in both genotypes. The values in each panel are from the same 3 *Nf1+/+* and 3 *Nf1+/-* neurons. F: the conductance was normalized with Gmax, which were determined by fitting conductance-voltage curves obtained from each neuron using the Boltzmann relation. The voltage dependence for activation of TTX-S INa was determined by fitting the G/Gmax-voltage curve using Boltzmann relation and their corresponding Boltzmann fits are demonstrated in Table 6. The asterisks represent a statistically significant difference between genotypes using a t-test.

Table 6. Boltzmann parameters for the activation of TTX-S INa in *Nf1*+/+ and *Nf1*+/- sensory neurons

	$V_{0.5}$ (mV)	k (mV)
Total INa activation		
Nf1+/+ (n=5)	-30 ± 5	5 ± 1
Nf1+/- (n=7)	-34 ± 5	5 ±1

IV. DISCUSSION

A. The sensory neurons with a heterozygous mutation of the *Nf1* gene have augmented neuronal excitability

In this thesis, I have demonstrated that small-diameter, capsaicin-sensitive sensory neurons with a heterozygous mutation of the *Nf1* gene have augmented excitability compared with wild-type neurons. The protein product of *Nf1* gene is neurofibromin, which is a GAP that catalyzes the hydrolysis of active Ras-GTP to inactive Ras-GDP and, thereby, reduces the activation of downstream cascades (Li et al., 1992; Martin et al., 1990; Wallace et al., 1990). Because *Nf1+/-* neurons have only one functional copy of the *Nf1* gene, the protein product of this gene should be expressed in a lower level in the cell. Neurofibromin is expressed most abundantly in the nervous system, in such cell types as neurons, Schwann cells and oligodendrocytes (Daston et al., 1992). The high incidence of developmental retardation, learning difficulties as well as exaggerated painful response of those people with NF1 (Creange et al., 1999; Trovo-Marqui et al., 2005) indicates that the single active NF1 allele does not generate enough neurofibromin to fulfill its normal biological function in the nervous system. The decrease of neurofibromin levels frequently results in both basal and cytokine-stimulated Ras activity in many cell types, including sensory neurons (Guha et al., 1996; Ingram et al., 2001; Klesse and Parada, 1998; Sherman et al., 2000; Vogel et al., 1995). Therefore, it is reasonable to infer that the *Nf1+/-* neurons have augmented levels of Ras-GTP. The enhanced neuronal excitability of *Nf1+/-*

neurons suggests that the activation of the Ras transduction cascade modulates the function of ion channels that regulate the capacity of sensory neurons to fire APs. However, the idea that the augmentation of intracellular Ras-GTP activity in *Nf1+/-* neurons enhances neuronal excitability is complicated because there are several isoforms of Ras that may have distinct functions in a variety of cell types. For example, H-Ras, another Ras isoform, was reported to suppress the expression of sodium and calcium channels in differentiated BC3H1 myocytes (Caffrey et al., 1987). In addition, Estacion (1990) reported that voltage-dependent INa was not observed in three cell lines containing activated H-Ras. Since INa is critical for the firing of an AP, the inhibition of the expression for sodium channels suggests that H-Ras may decrease neuronal excitability. Based on the augmented excitability of *Nf1+/-* neurons, it is less likely that the activity of H-Ras is enhanced by the *Nf1* mutation. Interestingly, evidence suggests that another Ras isoform, K-Ras, is the primary target of the GAP activity of neurofibromin. For example, K-Ras, but not H-Ras, is activated in astrocytes isolated from *Nf1+/-* and *Nf1-/-* mice, and could account for the fast proliferation and the abnormal actin cytoskeleton in these cells (Dasgupta et al., 2005). Since DRG neurons may express different isoforms of Ras with distinct functions, it should be very informative to investigate the expression of different Ras isoforms as well as their role in modulating channel activity, and thereby controlling the state of excitability.

Once Ras-GTP recruits the kinase, Raf, to the cell membrane, a cascade of downstream effectors is activated, such as the MAPK and PI-3K pathway (The

assumption here is that the augmented Ras-GTP level correlates with enhanced Ras activity). In many types of cells, the mutation of the *Nf1* gene decreased the intracellular GAP activity and led to an increase in cellular levels of Ras-GTP and its downstream effectors, like pERK, and pAkt, both at rest and when cells were exposed to growth factors that activate Ras (Guha et al., 1996; Ingram et al., 2001; Klesse and Parada, 1998; Sherman et al., 2000; Vogel et al., 2000). The enhanced activation of Ras and its downstream effectors in sensory neurons frequently correlate with hyperalgesia and neuronal sensitization. The hyperalgesia induced by TNFα and epinephrine was greatly attenuated by blockers of MEK, SB202190 and UO126 (Aley et al., 2001; Jin and Gereau, 2006). Likewise, blockade of MAPK activity by expressing a dominant negative MEK exclusively in sensory neurons of adult mice significantly reduced the pain behavior compared to wild-type controls in formalin-induced inflammation (Karim et al., 2006). Furthermore, applying the MEK inhibitors, PD98059 and U0126 significantly suppressed the firing of dorsal horn neurons elicited by electrical currents (Hu and Gereau, 2003). Based on the evidence above, it is possible that the activation of MAPK, as a consequence of the decreased GAP activity in *Nf1+/-* neurons, leads to the augmentation of excitability of *Nf1+/-* sensory neurons.

Few studies have investigated the role of the PI-3K pathway, another intracellular signaling cascades activated by Ras, in the modulation of neuronal excitability. Recent evidence shows that the PI-3K pathway is involved with neuronal sensitization. By mutating the tyrosine residue in TrkA (Y760) that is

involved in the activation of PI-3K, the sensitization produced by NGF was significantly attenuated (Zhang et al., 2005). To support the notion that PI-3K led to neuronal sensitization, Zhuang et al., (2004) demonstrated that the PI-3K inhibitors, LY294002 and wortmannin, successfully blocked the activation of ERK in primary rat sensory neurons and attenuated the capsaicin- and NGF-induced heat hyperalgesia. These findings suggest that PI-3K may lead to activation of ERK and could contribute to neuronal sensitization and inflammatory pain. Since the activity of PI-3K could also be augmented in *Nf1+/-* neurons by elevated level of Ras-GTP, it would be important to examine whether the activity of PI-3K is augmented in *Nf1+/-* neurons and contributes to the enhanced excitability.

Based on the current literature, it is poorly understood whether neurofibromin has other functions in addition to its capacity as a GAP for Ras. However, several investigations suggest that neurofibromin may interact with PKA and PKC, whose activation leads to neuronal sensitization (Ahlgren and Levine, 1994; Evans et al., 1999). It was reported that neurofibromin was phosphorylated constitutively by PKA (Izawa et al., 1996; Tokuo et al., 2001), indicating PKA might modulate the function of neurofibromin. Likewise, The et al., (1997) demonstrated that the expression of PKA rescued the size defect of a *Drosophila* mutant (reduction in size of larvae, pupae, and adults) that results from homozygous mutation of an NF1 homolog, suggesting that NF1 and PKA interacted to control the growth of *Drosophila*. The biological significance of the phosphorylation of neurofibromin or the interaction between PKA and neurofibromin is not clear at present, but I speculate that neurofibromin may

serve as a linker between two major intracellular pathways, the Ras and PKA signaling cascade, and the heterozygous mutation of the *Nf1* gene may alter the activity of PKA, a well documented protein kinase whose activation leads to neuronal sensitization (Aley and Levine, 1999; England et al., 1996; Evans et al., 1999; Lopshire and Nicol, 1998; Taiwo et al., 1989).

Besides PKA, neurofibromin was also reported to interact with other signaling molecules, like PKC. Mangoura et al., (2006) showed that PKC modulated the function of neurofibromin because the Ras-GAP activity of neurofibromin was diminished when PKCα (an isoform of PKC) was downregulated. PKC is another protein kinase that leads to neuronal sensitization (Ahlgren and Levine, 1994; Baker, 2005; Hucho et al., 2005; Vellani et al., 2001). Based on the close interaction between neurofibromin and PKC/PKA, it is possible that the heterozygous mutation of *Nf1* gene alters the activity of PKA and PKC, and contributes to neuronal sensitization. It will be interesting to study the activity of PKA or PKC in *Nf1+/-* neurons and determine whether there is an aberrant activity of PKA or PKC, whose activation could lead to the augmented excitability in *Nf1+/-* neurons.

The augmented neuronal firing in *Nf1+/-* neurons involves the activity of ion channels in the cell membrane. Previous evidence suggests that the Ras transduction cascade can modulate the activity of ion channels. For example, Fitzgerald and Dolphin (1997) demonstrated that microinjection of activated K-Ras enhanced the voltage-gated calcium current in DRG neurons isolated from

neonatal rats. This augmentation of calcium currents by K-Ras was not associated with any significant changes in either activation or inactivation of the current. In support of the notion that Ras modulates the activity of these calcium channels, the blockage of intracellular Ras activity decreased calcium currents. This was accomplished by two approaches, one used a Ras-neutralizing antibody, the other used a peptide that inhibited the interaction of Ras with the TrkA-Src complex (Fitzgerald and Dolphin, 1997). Besides affecting calcium channels, the activation of Ras may modulate other types of ion channels. The inward-rectifying potassium currents (IKir) in HEK cells coexpressed with constitutively active Ras are significantly smaller compared to the IKir in cells when IKir is expressed alone. These results suggest that Ras inhibits IKir (Giovannardi et al., 2002). Both the suppression of IK and the augmentation of calcium currents can lead to the augmentation of neuronal excitability. Therefore, these data support the idea that increased Ras activation leads to enhanced neuronal excitability in isolated *Nf1+/-* sensory neurons by modulating the activity of ion channels.

The downstream effectors of Ras were also shown to modulate channels. MAPK, a downstream effector of Ras-GTP, was reported to modulate multiple membrane currents. Jin and Gereau (2006) reported that the TNFα-induced augmentation of TTX-R INa was dramatically reduced by the blocker of MAPK, SB 202190 in DRG neurons isolated from adult mice.

In mouse sensory neurons, the ERK-dependent suppression of an A-type IK was significantly reduced when these neurons expressed a dominant negative MEK (Karim et al., 2006). Also, Kv4.2, one type of potassium channel exhibiting IA properties, was shown to be the substrate of MAPK by direct phosphorylation of the pore-forming alpha subunit (Adams et al., 2000; Schrader et al., 2006). Furthermore, Fitzgerald (2000) reported that voltage-gated calcium currents were significantly enlarged by activating Ras-MEK-MAPK pathway. Taken together, these investigations strongly suggest that the activation of MAPK leads to neuronal sensitization by modulating multiple membrane currents.

The augmentation of INa and suppression of IK could lead to enhanced neuronal excitability (Evans et al., 1999; Leffler et al., 2002; Waxman et al., 1999; Zhang et al., 2002). However, there was no difference in the resting membrane potential or the input resistance between *Nf1*+/+ and *Nf1*+/- neurons, suggesting that the potassium channels that maintain the resting membrane potential and resistance appear to be unaffected by the mutation in *Nf1*+/- cells. Consistent with this observation, neither the delayed rectifier types of IK nor IA were suppressed in *Nf1*+/- neurons (see section F for detailed discussion). Therefore, it is less likely that this mutation alters IK in mouse sensory neurons. Based on the augmented excitability of *Nf1*+/- neurons, we hypothesized that INa in *Nf1*+/- neurons was somehow modified by the mutation and contribute to the enhanced excitability of *Nf1*+/- neurons. To elucidate the specific channels that are modulated by the *Nf1* mutation and contribute to the augmented excitability of

Nf1+/- neurons, we performed voltage-clamp studies for INa (see G about the detailed discussion about INa).

B. NGF in the culture media for 4-12 hours causes neuronal sensitization in *Nf1+/+* neurons.

Much evidence suggests that NGF causes hyperalgesia and neuronal sensitization (Fjell et al., 1999a; Ji et al., 2002; Lewin and Mendell, 1993; Lewin et al., 1993; Woolf et al., 1994; Zhang et al., 2005; Zhang and Nicol, 2004; Zhang et al., 2002). My investigation demonstrates that when NGF is added to the culture media for 4-12 hours the neuronal excitability of wild-type sensory neurons is significantly augmented. The direct sensitizing effect of NGF on sensory neurons was also observed in other studies. For example, NGF enhanced the neuronal firing of isolated sensory neurons in response to electrical stimuli (Zhang et al., 2002) as well as augmented the capsaicin-evoked inward current (Shu and Mendell, 1999). Several investigations demonstrated that the Ras-MEK-MAPK pathway and the downstream effectors of this pathway could underlie the NGF-induced neuronal sensitization. The injection of NGF into the rat hind paw produced a profound thermal hyperalgesia in these animals (Lewin et al., 1993; Woolf et al., 1994) as well as increased p-ERK labeling in TrkA-containing neurons in the DRG (Averill et al., 2001), suggesting that NGF could directly act on the peripheral terminal of sensory neurons to enhance ERK activity and thereby contribute to the augmented neuronal firing. In addition, during peripheral inflammation in which the local concentration of NGF was

enhanced, the level of phosphorylated p38 (another member of the mitogen-activated kinase family) in nociceptive sensory neurons was elevated (Ji et al., 2002). This increase in phosphorylated p38 was correlated with an increase in expression of TRPV1 in DRG neurons and elevated thermal hyperalgesia. All of these responses were blocked by treatment with antisera to NGF prior to the initiation of inflammation induced by CFA. It is possible that NGF enhanced the expression of TRPV1 by activating p38 and thereby contributing to the thermal hyperalgesia and neuronal sensitization. In addition, the expression of constitutively active Ras mimicked the action of NGF to increase TRPV1 expression in isolated sensory neurons and increased neuronal levels of pERK and pAkt (Bron et al., 2003). Moreover, treatment with the Mek inhibitor, PD98059, reduced the capsaicin sensitivity of neurons that were treated with NGF for 1 week (Ganju et al., 1998). These studies suggest that Ras modulates TRPV1. Although most of these investigations have focused on the role of the Ras transduction cascade in NGF-mediated changes of TRPV1 expression and capsaicin responses, they do not exclude the possibility of Ras-mediated changes in the excitability of nociceptive sensory neurons. To address this question, it will be important to examine whether the increased excitability induced by NGF can be suppressed by the approaches to reduce intracellular Ras-GTP levels, e.g., Ras-neutralizing antibodies and dominant-negative isoforms of Ras in sensory neurons.

In addition to stimulating intracellular signaling cascades, NGF can induce gene expression. In my experiments, NGF remained in the culture media for 4-

12 hours. The NGF-induced sensitization (under our condition) could involve acute as well as chronic sensitization that resulted from NGF-induced changes in gene expression. After treatment by NGF, a myriad of genes was induced in neurons and PC12 cells. Mandelzys et al. (1990) described that NGF strongly increased the expression of nicotinic receptors in nodose neurons from neonatal rats. Likewise, Toledo-Aral et al., (1995) found that exposure to NGF for 1 min was sufficient to increase the expression of functional sodium channels in PC12 cells. The induction of genes by NGF in PC12 cells was mimicked by expressing activated forms of Src, Ras or raf and was blocked by expression of a dominant-negative form of Ras (D'Arcangelo and Halegoua, 1993). These observations support the notion that NGF induces gene expression by activating downstream intracellular signaling molecules. Consistent with this idea, in sensory neurons, the mRNAs of several sodium channel subunits, such as Nav1.1, β1 and β2 were significantly upregulated in sensory neurons isolated from NGF-overexpressing transgenic mice (Fjell et al., 1999a). Likewise, Zur et al., (1995) reported similar observations that NGF increased the mRNA levels of Nav1.2 and β1 in neurons isolated from E16 rat embryos. The upregulation of sodium channel transcripts was often paralleled by the augmentation of INa in sensory neurons (Cummins and Waxman, 1997). Based on these observations, under my experimental condition wherein NGF is present in media for 4-12 hours, it is possible that the NGF-induced augmentation of neuronal firing also depends on the upregulation of the mRNA of sodium channels and other functional proteins that may enhance neuronal excitability.

IK is another membrane current suppressed by acute exposure to NGF in rat sensory neurons (Zhang et al., 2002). However, based on published studies, the idea that NGF regulates the expression levels of the mRNA for Kv channels is complicated by different results. In PC12 cells, (Sharma et al., 1993) reported that the mRNA for Kv2.1 was increased about 4 fold after exposure to NGF for 12 hours, and this elevation lasted for at least six days of continuous NGF treatment. Conversely, Lei et al., (2001) demonstrated that the amplitude of IK in adult sympathetic neurons were unchanged by exposure to a high concentration of NGF (200 ng/ml) in the culture media for more than 10 days. Likewise, Park et al. (2003) suggested that no significant change in the levels of mRNA for Kv1.1, 1.4 and 4.2 after treatment with NGF for 12-24 hours in sensory neurons isolated from adult rats. Based on my observation that neither the resting membrane potential nor the input resistance was significantly altered after exposure to NGF for 4-12 hours compared with neurons grown in the absence of NGF, it seems less likely that long-term exposure to NGF (4-12 hrs) alters the expression pattern of Kv channels. As a consequence, IK in adult mice sensory neurons may not be changed by long-term NGF treatment. In addition, my studies showed that neither the amplitude of total IK nor IA was suppressed in *Nf1*+/- neurons, suggesting that the activation of Ras-MEK-MAPK, either by long-term NGF treatment or by decreased Ras-GAP activity of neurofibromin, did not suppress IK in mouse sensory neurons. In general, the observations described above are consistent with our findings that NGF increased the excitability of wild-type mouse sensory neurons. NGF could augment neuronal firing either by

activating intracellular second messengers that modulate the activity of ion channels, or by the upregulation of the mRNA for sodium channels and other functional proteins that could augment neuronal excitability. It is important to establish the hierarchy of the signaling molecules following NGF stimulation, such as Ras, MAPK, ceramide and their role in modulating the activity of specific ion channels that contribute to the augmentation of neuronal firing. Such information can lead to the identification of novel therapeutic targets for the hyperalgesia associated with inflammation or the chronic painful conditions that arise from other ailments.

C. Exposure to NGF has little effect of *Nf1+/-* sensory neurons.

My results demonstrate that exposure of the *Nf1+/-* neurons to NGF has little effect on the neuronal excitability. It is possible that NGF did not further enhance the excitability of *Nf1+/-* neurons because the mutated neurons have already attained their maximum ability to fire APs when stimulated by electrical currents. Alternatively, it is possible that the pathway(s) activated by NGF may be chronically stimulated in the *Nf1+/-* neurons and not capable of further modulation. Interestingly, applying NGF acutely via bath perfusion did augment the number of evoked APs by the current ramp in 2 out of 6 *Nf1+/-* neurons. It is difficult to explain how NGF sensitized these 2 of 6 *Nf1+/-* neurons. One possibility is that, in a group of *Nf1+/-* neurons, NGF still increases neuronal excitability by enhancing the Ras-GTP levels and thereby augments neuronal excitability. However, it seems unlikely because NGF failed to sensitize other

Nf1+/- neurons (n=33) in my experiments. Based on my observations, I speculate that the augmentation of excitability in these two *Nf1+/-* neurons may be due to some unknown reasons other than to be sensitized by NGF. However, Hingtgen et al., (2006) reported that NGF increased the release of CGRP from *Nf1+/-* neurons in a concentration-responsive manner, indicating that these neurons can be further sensitized by NGF. This discrepancy between my results and Hingtgen et al., (2006) raises the question that the signaling cascades stimulated by NGF that augment neuronal firing may be different from the cascades modulating the release of neurotransmitters in sensory neurons. In addition, the different culture conditions could also contribute to the difference. Under my experimental condition, neurons were isolated from adult mice and stayed in culture for 4-12 hours, whereas the neurons in study by Hingtgen et al., (2006) remained in culture for 7 days before performing the release experiments. It is possible that the properties of these neurons may change after staying in culture for a long time and result in the different NGF-induced sensitization in these cells.

My data suggested that the pathway(s), such as the Ras-dependent pathways activated by NGF, which augment neuronal firing may be chronically stimulated in the *Nf1+/-* neurons. However, internal perfusion with the Ras-blocking antibody failed to suppress the augmented excitability in the *Nf1+/-* neurons. These results suggest that the effectors downstream of Ras have a key role in the NGF-induced augmentation of neuronal firing.

D. Y13-259 blocks the NGF-induced augmentation of neuronal firing in wild-type sensory neurons.

My study demonstrates that the acute NGF-induced sensitization (NGF 100 ng/ml via bath perfusion for five min) in wild-type neurons is suppressed by using a specific Ras-blocking antibody that binds directly to the amino acid residues of Ras that regulate its activity; this converts the active Ras back to its inactive form (Sigal et al., 1986). This loss of NGF-induced sensitization is not due to the non-specific effect of a high concentration of IgG inside the cell because these neurons can be sensitized by an acute 5 min exposure to NGF in the presence of 30 μg/ml IgG in the recording pipette. In addition, the non-specific actions of IgG do not alter basal neuronal excitability over the 20 min recording period. My investigation demonstrates that the activation of Ras is a critical step in the acute NGF-induced augmentation of neuronal excitability in mouse sensory neurons. Since the NGF-induced sensitization occurs on a rapid time scale (less than 5 min), the acute effect of NGF likely results from the activation of Ras and the downstream effectors of Ras that modulate channel activity (such as phosphorylation of channels), rather than the induction of gene expression.

The Ras-MEK-MAPK pathway can modulate many membrane currents such as TTX-R INa (Jin and Gereau, 2006), A-types of IK (Adams et al., 2000; Karim et al., 2006; Schrader et al., 2006) and voltage-gated calcium currents (Fitzgerald, 2000; Fitzgerald and Dolphin, 1997). It is possible that the NGF-mediated activation of Ras or its downstream effectors modulates the activity of

channels, and thereby enhances neuronal excitability. Based on my observation that NGF does not depolarize these *Nf1+/-* cells in the presence of IgG, Ras may not modulate IK that is a key player in setting the resting membrane potential. However, Zhang et al., (2002) demonstrated that NGF depolarized sensory neurons isolated from adult rats as well as suppressed IK. This inconsistency between my observation and Zhang et al., (2002) leads to the speculation that NGF may modulate the activity of different ion channels in sensory neurons isolated from different species. Consistent with this idea, Woodbury et al., (2004) reported that mouse and rat exhibit different colocalization of TRPV1 and isolectin B4 (IB4) binding in small diameter sensory neurons. In this study, rat sensory neurons exhibited staining profiles where approximately 60% of the IB4 positive cells stained for TRPV1, however, only 2% of the IB4 positive mouse sensory neurons were TRPV1 positive. The TRPV1 positive and the majority of the IB4-positive neurons are highly likely to be heat-responsive nociceptors (Holzer, 1991; Molliver et al., 1997). The distinct pattern of colocalization of TRPV1 and IB4 may indicate that the signaling cascades whose activation can lead to modulation of channels and thereby augment neuronal excitability could be different between mouse and rat sensory neurons. Because neither the resting membrane potential nor the input resistance is changed by acute exposure to NGF in mouse sensory neurons, it is possible that the activation of Ras may not suppress IK in mouse neurons.

In summary, my data demonstrate that the acute NGF-induced augmentation of neuronal excitability is blocked by the Ras-blocking antibody,

suggesting that NGF enhances neuronal excitability via activation of Ras in wild-type neurons. The validity of this conclusion depends on how specific this Ras-blocking antibody is in its ability to neutralize Ras activity. Although it is less likely that this Ras-blocking antibody binds to other intracellular proteins modulating neuronal excitability with the exact same amino acid residues like those in Ras, additional experiments, like those examining NGF-induced sensitization in primary sensory neurons expressing a dominant negative or constitutively active Ras are necessary to resolve this question.

E. Y13-259 has little effect on the excitability of *Nf1+/-* neurons.

As established above, the activation of Ras appears to be a critical step in NGF-induced sensitization of wild-type neurons. Surprisingly, the Ras-blocking antibody has little effect on the parameters of excitability in *Nf1+/-* neurons. Several potential mechanisms could underlie the relative ineffectiveness of the Ras-blocking antibody in *Nf1+/-* neurons. First, although the activation of Ras could contribute to neuronal sensitization, it is not a direct modulator of ion channel activity. In this case, the downstream factors that directly phosphorylate channels have already been activated by the high level of Ras-GTP. Therefore, blockade of upstream Ras activity will have little effect on the downstream effectors and likely can not suppress the excitability. Second, since neurofibromin is a large protein that could interact with multiple signaling molecules, such as PKA and PKC (Izawa et al., 1996; Mangoura et al., 2006; The et al., 1997; Tokuo et al., 2001), the involvement of signaling cascades other

than Ras could produce the neuronal sensitization of *Nf1+/-* neurons. In this case, neutralizing Ras activity would not suppress the excitability of *Nf1+/-* neurons. Third, it is well documented that the activation of the Ras-MEK-MAPK pathway stimulates gene transcription. After treatment of cells with mitogens and growth factors for 1-5 min, ERK translocates from cytoplasm to the nucleus and phosphorylates TCF, the transcription factor that mediates *c-fos* induction (Gille et al., 1992). *c-fos* belongs to the family of immediate early genes that are activated in response to a wide variety of cellular stimuli and has many functions, such as serving as transcription factors or DNA binding proteins. The long term changes in gene transcription in *Nf1+/-* neurons can not be reversed by short-term Ras neutralization. Lastly, the compensatory mechanisms for the mutation of the *Nf1* gene may also contribute to the neuronal sensitization of *Nf1+/-* neurons. These compensatory mechanisms may change the expression of specific signaling molecules or functional channels, leading to the augmentation of neuronal excitability. Therefore, other approaches, such as using gene chips to examine the changes in the global expression patterns of genes in *Nf1+/-* neurons, could be important to identify the exact targets whose activity leads to the elevated neuronal firing and help to develop better therapeutic strategies for the elevated pain sensitivity in people with NF1.

F. IK does not contribute to the enhanced excitability of *Nf1*+/- neurons.

It is well established that the inhibition of IK by multiple inflammatory mediators led to the augmentation of neuronal excitability (Nicol et al., 1997; Zhang et al., 2002; Zhang et al., 2006b). However, my results indicate that neither the amplitude nor the activation kinetics of IK is altered in *Nf1*+/- neurons, suggesting the activation of Ras and its downstream effectors by the *Nf1* mutation does not modulate IK in mouse DRG neurons. However, evidence indicates that MAPK modulated the IA type of IK in dorsal horn neurons and COS-7 cells (Adams et al., 2000; Hu et al., 2003; Karim et al., 2006). The difference between my results and published studies could be explained by the variance of biological systems wherein these studies were conducted. In my experiments, many small-diameter mouse sensory neurons do not have apparent IA currents (in eleven wild-type sensory neurons, only five cells had IA; whereas in seven *Nf1*+/- neurons, three had IA components), suggesting that IA may not a major IK in some subsets (e.g. capsaicin-sensitive) of mouse sensory neurons. Since the expression of IA in different types of cells could have large diversities, the signaling cascades modulating the activity of these potassium channels may also be different. Based on my observations, it is less likely that the mutation of the *Nf1* gene and its consequent activation of Ras and its downstream effectors suppress IK in mouse sensory neurons.

To determine whether the kinetics of IK is changed in *Nf1*+/- neurons, the deactivation (the kinetic analysis of the current decay) of the potassium tail

currents is analyzed. The time constant for the IK tail (τ tail) reflects how fast the channels are closing. The longer the τ tail, the slower the channels are closed. Surprisingly, the τ tail in *Nf1*+/- neurons is much longer compared to *Nf1*+/+ neurons, indicating that the potassium channels are closing more slowly. If this result truly reflects the character of potassium channels in *Nf1*+/- neurons, larger IK should be observed (more potassium channels should be open due to the slow closing of channels). In addition, the opening of more potassium channels during the firing of an AP can lead to more effective repolarization in the falling phase, resulting in a narrower AP. However, none of the above phenomena was observed in *Nf1*+/- neurons. It is possible that the slower deactivation kinetics of potassium tail currents in *Nf1*+/- neurons results from biological variability of these sensory neurons.

The suppression of IK can lead to increased neuronal excitability (Zhang et al., 2002). However, based on my results, neither IK nor IA was suppressed in *Nf1*+/- neurons. Thus, the augmented neuronal firing of *Nf1*+/- neurons did not result from the modulation of IK. It is less likely those signaling cascades stimulated by the mutation of the *Nf1* gene modulate the activity of potassium channels.

G. Augmented INa could contribute to the enhanced excitability in *Nf1+/-* neurons

My investigation demonstrates that both TTX-R and TTX-S INa are significantly augmented in *Nf1+/-* neurons, suggesting the increased excitability of *Nf1+/-* neurons could result from larger INa. Although the augmentation of INa during neuronal sensitization is well documented (England et al., 1996; Gold et al., 1996a; Gold et al., 2002; Jeftinija, 1994; Rush and Waxman, 2004; Waxman et al., 1994; Zhang et al., 2002), the cellular mechanisms that give rise to enlarged INa in sensory neurons are poorly understood. Interestingly, multiple inflammatory mediators enhancing INa, like NGF and TNFα, were also reported to activate the MAPK pathway. It is possible that the activation of MAPK modulates the activity of sodium channels. Indeed, Jin and Gereau (2006) reported that the augmentation of TTX-R INa by acutely applying TNFα on mouse sensory neurons was dramatically suppressed by a blocker of MEK, SB 202190. Thus, it is logical to speculate that the activation of MAPK augments INa in *Nf1+/-* neurons or in wild-type sensory neurons upon stimulation with inflammatory mediators and this leads to neuronal sensitization. It would be interesting to examine whether the augmented INa in *Nf1+/-* neurons could be suppressed by MEK inhibitors.

In addition to augmented TTX-R INa, my results demonstrate that the TTX-S INa in *Nf1+/-* neurons is significantly larger than that in wild-type neurons. Interestingly, the TTX-S INa is much larger when a CsF-based pipette solution is

used compared to the currents obtained by using a Cs-aspartate-based pipette solution. This obvious difference in the amplitude of TTX-S INa using different pipette solutions leads to the speculation whether CsF functions as an activator of TTX-S INa in small diameter, capsaicin-sensitive sensory neurons. One possibility is that the F^- binds to the Al^{+3} released from the glass of the pipette, forming a complex able to activate G proteins that may increase the amplitude of TTX-S INa (Saab et al., 2003). However, Saab et al., (2003) reported that the peak INa was not altered by inclusion of an aluminum chelator in the pipette solution, suggesting that the fluoride-aluminum complex did not augment INa. It is unlikely that the augmentation of TTX-S INa in *Nf1+/-* neurons results from including F^- in pipette solution. Consistent with this idea, Black et al., (2004) demonstrated that TTX-S INa in DRG neurons was augmented following carrageenan-induced inflammation when a CsF-based pipette solution was used. In addition, many reports demonstrated that multiple inflammatory mediators were able to augment TTX-R INa when CsF was in the pipette (Cardenas et al., 1997; Cardenas et al., 2001; England et al., 1996; Gold et al., 1996a; Rush and Waxman, 2004; Tanaka et al., 1998; Zhang et al., 2006a; Zhang et al., 2002). These investigations suggest that CsF in the pipette is not a confounding variable in studying the manipulation of INa by multiple inflammatory mediators. Based on my observation that the amplitudes of both TTX-R and TTX-S INa are increased in *Nf1+/-* neurons that exhibit augmented excitability, it is possible that the larger INa contributes to the augmented excitability in *Nf1+/-* neurons. The

enlarged INa may have resulted from these pathways that are chronically activated in *Nf1*+/- neurons, like Ras and MAPK.

In addition to a larger INa, the gating properties of INa in *Nf1*+/- neurons are different from that in *Nf1*+/+ neurons. Voltage-dependent activation of INa in *Nf1*+/- neurons appears to be unaltered because the $V_{0.5}$ was not different than that measured in wild-type neurons. Interestingly, multiple inflammatory mediators, such as PGE_2, NGF and endothelin, do cause a hyperpolarized shift in the voltage-dependent activation of INa in rat sensory neurons (England et al., 1996; Gold et al., 1996a; Gold et al., 2002; Kwong and Lee, 2005; Zhang et al., 2002; Zhou et al., 2002). This inconsistency could result from species difference (mouse vs. rat). Alternatively, the signaling cascades activated by these inflammatory mediators other than Ras and MAPK, such as cyclic AMP-PKA pathway, could cause the hyperpolarized shift in the voltage-dependent activation of INa.

However, there is a significant depolarizing shift in the $V_{0.5}$ of the steady-state inactivation for total INa in *Nf1*+/- neurons. At the voltage range of -50 mV to +10 mV (during this voltage range, sodium channels have the possibility to open), the depolarizing shift in $V_{0.5}$ indicates that fewer sodium channels are inactivated, resulting in a greater number of sodium channels that are available to open, and thereby augmenting window currents. The window current is represented by the area created by the overlap of the activation and inactivation functions of the sodium channel. The opening of the non-inactivated sodium

channels (known as persistent INa) could augment window currents. It is possible that the *Nf1* mutation somehow increases the expression of more persistent INa, or shifts the inactivation of more sodium channels to a depolarized potential.

Augmented INa could lead to higher overshoot of the AP. However, in my experiments, the overshoot of the APs evoked from *Nf1+/-* neurons is not significantly different from wild-type neurons. This lack of difference in the shape of APs may due to the electronic design of my amplifier (both Axon 200 B and EPC-7 amplifier), which can generate a voltage error in current-clamp mode that distorts the recorded signal (Magistretti et al., 1996). Thus, in order to record APs with negligible distortions, a classical microelectrode amplifier is preferred in future current-clamp experiments.

Interestingly, the morphology of total INa traces in mouse sensory neurons is different. Two classes of neurons were identified based on the morphology of total INa: type I neurons were dominated by the fast inactivating TTX-S INa, whereas type II neurons exhibited mostly the slow inactivating TTX-R INa. After treatment by TTX, the majority of INa evoked from type I neurons was diminished. In contrast, in type II neurons, there was little decrease in the peak currents observed after TTX. The distribution of type I and type II neurons between genotypes is different. There are more type II neurons in *Nf1+/-* sensory neurons compared to wild-type neurons. In my study, eight out of ten wild-type sensory neurons were type I neurons, whereas in *Nf1+/-* neurons, only four of the ten

were type I neurons. In *Nf1+/-* neurons, there is an increase in the percentage of type II neurons. This could indicate that the expression of sodium channel transcripts may be different compared to wild-types. Indeed, in mammalian sensory neurons, multiple sodium channel transcripts are detected: $Na_v1.1$-1.4, $Na_v1.6$-1.7 are TTX- S sodium channels, whereas $Na_v1.5$, $Na_v1.8$ and Na_v 1.9 are recognized as TTX-R sodium channels (Wood et al., 2004). The enhanced percentage of type II neurons leads to the speculation that the subtypes encoding TTX-R sodium channels are upregulated in *Nf1+/-* neurons. The upregulation of TTX-R sodium channel transcripts can be induced by multiple inflammatory mediators, such as NGF. For example, Rudy et al., (1987) demonstrated that NGF increased the number of functional sodium channels and induced the expression of TTX-R sodium channels in PC12 cells. In addition, Fjell et al., (1999b) showed that the deprivation of NGF in vivo suppressed the expression of $Na_v1.8$, the transcript of a TTX-R sodium channel in small diameter sensory neurons. Furthermore, delivery of NGF to the transected sciatic nerve up-regulated the mRNA of Na_v 1.8 and augmented the TTX-R INa in small diameter sensory neurons (Dib-Hajj et al., 1998). Based on the observation that more type II neurons in neurons isolated from *Nf1+/-* mouse, it is possible that the mRNA transcripts for TTX-R sodium channels in these *Nf1+/-* neurons were upregulated. It is reasonable to speculate that the Ras-MEK-MAPK pathway, which could be activated either by decreased activity of neurofibromin or stimulation of NGF, upregulates the mRNA transcripts for TTX-R sodium

channels. Therefore, the mRNA levels of multiple sodium channel subtypes in *Nf1*+/+ and *Nf1*+/- sensory neurons should be examined in future experiments.

Interestingly, Breese et al., (2005) reported that the percentage of IB4-positive mouse sensory neurons that were TRPV1-immunoreactive was elevated after CFA-induced inflammation. The IB4-positive neurons typically have larger TTX-R INa (Stucky and Lewin, 1999). In my study, the high percentage of type II, capsaicin-sensitive *Nf1*+/- neurons may suggest that the heterozygous mutation of the NF1 gene somehow increases the percentage of IB4-positive neurons that are TRPV1-immunoreactive. Further experiments, like these to examine the colocalization of IB4 and TRPV1 on sensory neurons of both genotypes, should be performed in future investigations.

The opening of sodium channels can lead to other functional changes of sensory neurons, such as the release of neurotransmitter from nerve terminals. Bouron and Reuter (1996) demonstrated that an elevated intracellular concentration of sodium ions entering the cell following AP firing caused an increase in glutamate release and accelerated the turnover rate of the vesicular pool in cultured rat hippocampal neurons. In addition, a selective activator of voltage-gated sodium channels, brevetoxin-3, significantly augmented neurotransmitter release from the neuromuscular junction (Meunier et al., 1997). To further support the notion that augmented INa leads to the enhanced release of neurotransmitters, Hingtgen et al., (2006) reported that *Nf1*+/- neurons released more CGRP when stimulated by capsaicin and high potassium. How

this augmented INa influences the release machinery in sensory neurons remains poorly understood. It is possible that augmented INa produces longer depolarization of the membrane potential during the firing of an AP, and facilitates calcium ions entering the cell via voltage-gated calcium channels, thereby increasing the release of neurotransmitters.

In summary, my data clearly suggest that neurofibromin can play a key role in modulating the excitability of small-diameter, capsaicin-sensitive sensory neurons by augmenting both TTX-R and TTX-S INa. However, much evidence suggests that Ras modulates calcium currents and TRPV1 (Bron et al., 2003; Fitzgerald and Dolphin, 1997). My data do not rule out the possibility that other channels, such as calcium channel and TRPV1 channels may also contribute to the augmented neuronal firing of *Nf1*+/- neurons. A clearer understanding of the mechanisms underlying the enhanced neuronal excitability in sensory neurons with the *Nf1* mutation, similar to the human disorder NF1, and how this sensitization may be modified in inflammation or injury could lead to better therapies for the painful conditions associated with NF1 or chronic painful conditions that arise from other ailments.

REFERENCES

- Adams, J. P., Anderson, A. E., Varga, A. W., Dineley, K. T., Cook, R. G., Pfaffinger, P. J., and Sweatt, J. D. (2000). The A-type potassium channel Kv4.2 is a substrate for the mitogen-activated protein kinase ERK. J Neurochem *75*, 2277-2287.

- Ahlgren, S. C., and Levine, J. D. (1994). Protein kinase C inhibitors decrease hyperalgesia and C-fiber hyperexcitability in the streptozotocin-diabetic rat. J Neurophysiol *72*, 684-692.

- Aley, K. O., and Levine, J. D. (1999). Role of protein kinase A in the maintenance of inflammatory pain. J Neurosci *19*, 2181-2186.

- Aley, K. O., Martin, A., McMahon, T., Mok, J., Levine, J. D., and Messing, R. O. (2001). Nociceptor sensitization by extracellular signal-regulated kinases. J Neurosci *21*, 6933-6939.

- Averill, S., Delcroix, J. D., Michael, G. J., Tomlinson, D. R., Fernyhough, P., and Priestley, J. V. (2001). Nerve growth factor modulates the activation status and fast axonal transport of ERK 1/2 in adult nociceptive neurones. Mol Cell Neurosci *18*, 183-196.

- Baker, M. D. (2005). Protein kinase C mediates up-regulation of tetrodotoxin-resistant, persistent Na+ current in rat and mouse sensory neurones. J Physiol *567*, 851-867.

- Becker, E. B., Howell, J., Kodama, Y., Barker, P. A., and Bonni, A. (2004). Characterization of the c-Jun N-terminal kinase-BimEL signaling pathway in neuronal apoptosis. J Neurosci *24*, 8762-8770.

- Beloeil, H., Ji, R. R., and Berde, C. B. (2006). Effects of bupivacaine and tetrodotoxin on carrageenan-induced hind paw inflammation in rats (Part 2): cytokines and p38 mitogen-activated protein kinases in dorsal root ganglia and spinal cord. Anesthesiology *105*, 139-145.

- Bergstroem, S., Danielsson, H., Klenberg, D., and Samuelsson, B. (1964). The Enzymatic Conversion of Essential Fatty Acids into Prostaglandins. J Biol Chem *239*, PC4006-4008.

- Bielefeldt, K., Ozaki, N., and Gebhart, G. F. (2002). Experimental ulcers alter voltage-sensitive sodium currents in rat gastric sensory neurons. Gastroenterology *122*, 394-405.

- Bilderback, T. R., Gazula, V. R., and Dobrowsky, R. T. (2001). Phosphoinositide 3-kinase regulates crosstalk between Trk A tyrosine kinase and p75(NTR)-dependent sphingolipid signaling pathways. J Neurochem *76*, 1540-1551.

- Birinyi-Strachan, L. C., Gunning, S. J., Lewis, R. J., and Nicholson, G. M. (2005). Block of voltage-gated potassium channels by Pacific ciguatoxin-1 contributes to increased neuronal excitability in rat sensory neurons. Toxicol Appl Pharmacol *204*, 175-186.

- Black, J. A., Cummins, T. R., Plumpton, C., Chen, Y. H., Hormuzdiar, W., Clare, J. J., and Waxman, S. G. (1999). Upregulation of a silent sodium channel after peripheral, but not central, nerve injury in DRG neurons. J Neurophysiol *82*, 2776-2785.

- Black, J. A., Liu, S., Tanaka, M., Cummins, T. R., and Waxman, S. G. (2004). Changes in the expression of tetrodotoxin-sensitive sodium channels within dorsal root ganglia neurons in inflammatory pain. Pain *108*, 237-247.

- Blochl, A., Blumenstein, L., and Ahmadian, M. R. (2004). Inactivation and activation of Ras by the neurotrophin receptor p75. Eur J Neurosci *20*, 2321-2335.

- Bouron, A., and Reuter, H. (1996). A role of intracellular Na+ in the regulation of synaptic transmission and turnover of the vesicular pool in cultured hippocampal cells. Neuron *17*, 969-978.

- Breese, N. M., George, A. C., Pauers, L. E., and Stucky, C. L. (2005). Peripheral inflammation selectively increases TRPV1 function in IB4-positive sensory neurons from adult mouse. Pain *115*, 37-49.

- Bron, R., Klesse, L. J., Shah, K., Parada, L. F., and Winter, J. (2003). Activation of Ras is necessary and sufficient for upregulation of vanilloid receptor type 1 in sensory neurons by neurotrophic factors. Mol Cell Neurosci *22*, 118-132.

- Caffrey, J. M., Brown, A. M., and Schneider, M. D. (1987). Mitogens and oncogenes can block the induction of specific voltage-gated ion channels. Science *236*, 570-573.

- Cardenas, C. G., Del Mar, L. P., Cooper, B. Y., and Scroggs, R. S. (1997). 5HT4 receptors couple positively to tetrodotoxin-insensitive sodium channels in a subpopulation of capsaicin-sensitive rat sensory neurons. J Neurosci *17*, 7181-7189.

- Cardenas, L. M., Cardenas, C. G., and Scroggs, R. S. (2001). 5HT increases excitability of nociceptor-like rat dorsal root ganglion neurons via cAMP-coupled TTX-resistant Na(+) channels. J Neurophysiol *86*, 241-248.

- Carter, B. D., Kaltschmidt, C., Kaltschmidt, B., Offenhauser, N., Bohm-Matthaei, R., Baeuerle, P. A., and Barde, Y. A. (1996). Selective activation of NF-kappa B by nerve growth factor through the neurotrophin receptor p75. Science *272*, 542-545.

- Catterall, W. A. (2000). From ionic currents to molecular mechanisms: the structure and function of voltage-gated sodium channels. Neuron *26*, 13-25.

- Cesare, P., Dekker, L. V., Sardini, A., Parker, P. J., and McNaughton, P. A. (1999). Specific involvement of PKC-epsilon in sensitization of the neuronal response to painful heat. Neuron *23*, 617-624.

- Chandy, K. G., and Gutman, G. A. (1993). Nomenclature for mammalian potassium channel genes. Trends Pharmacol Sci *14*, 434.

- Cherkas, P. S., Huang, T. Y., Pannicke, T., Tal, M., Reichenbach, A., and Hanani, M. (2004). The effects of axotomy on neurons and satellite glial cells in mouse trigeminal ganglion. Pain *110*, 290-298.

- Chien, U. H., Lai, M., Shih, T. Y., Verma, I. M., Scolnick, E. M., Roy-Burman, P., and Davidson, N. (1979). Heteroduplex analysis of the sequence relationships between the genomes of Kirsten and Harvey sarcoma viruses, their respective parental murine leukemia viruses, and the rat endogenous 30S RNA. J Virol *31*, 752-760.

- Christie, M. J., North, R. A., Osborne, P. B., Douglass, J., and Adelman, J. P. (1990). Heteropolymeric potassium channels expressed in Xenopus oocytes from cloned subunits. Neuron *4*, 405-411.

- Chuang, H. H., Prescott, E. D., Kong, H., Shields, S., Jordt, S. E., Basbaum, A. I., Chao, M. V., and Julius, D. (2001). Bradykinin and nerve growth factor release the capsaicin receptor from PtdIns(4,5)P2-mediated inhibition. Nature *411*, 957-962.

- Connor, J. A. (1978). Slow repetitive activity from fast conductance changes in neurons. Fed Proc *37*, 2139-2145.

- Connor, J. A., and Stevens, C. F. (1971). Prediction of repetitive firing behaviour from voltage clamp data on an isolated neurone soma. J Physiol *213*, 31-53.

- Corbett, K. D., and Alber, T. (2001). The many faces of Ras: recognition of small GTP-binding proteins. Trends Biochem Sci *26*, 710-716.

- Coste, B., Osorio, N., Padilla, F., Crest, M., and Delmas, P. (2004). Gating and modulation of presumptive NaV1.9 channels in enteric and spinal sensory neurons. Mol Cell Neurosci *26*, 123-134.

- Creange, A., Zeller, J., Rostaing-Rigattieri, S., Brugieres, P., Degos, J. D., Revuz, J., and Wolkenstein, P. (1999). Neurological complications of neurofibromatosis type 1 in adulthood. Brain *122 (Pt 3)*, 473-481.

- Cuello, A. C. (1987). Peptides as neuromodulators in primary sensory neurons. Neuropharmacology *26*, 971-979.

- Cummins, T. R., Aglieco, F., Renganathan, M., Herzog, R. I., Dib-Hajj, S. D., and Waxman, S. G. (2001). Nav1.3 sodium channels: rapid repriming and slow closed-state inactivation display quantitative differences after expression in a mammalian cell line and in spinal sensory neurons. J Neurosci *21*, 5952-5961.

- Cummins, T. R., Dib-Hajj, S. D., and Waxman, S. G. (2004). Electrophysiological properties of mutant Nav1.7 sodium channels in a painful inherited neuropathy. J Neurosci *24*, 8232-8236.

- Cummins, T. R., and Waxman, S. G. (1997). Downregulation of tetrodotoxin-resistant sodium currents and upregulation of a rapidly repriming tetrodotoxin-sensitive sodium current in small spinal sensory neurons after nerve injury. J Neurosci *17*, 3503-3514.

- D'Arcangelo, G., and Halegoua, S. (1993). A branched signaling pathway for nerve growth factor is revealed by Src-, Ras-, and Raf-mediated gene inductions. Mol Cell Biol *13*, 3146-3155.

- Dai, Y., Iwata, K., Fukuoka, T., Kondo, E., Tokunaga, A., Yamanaka, H., Tachibana, T., Liu, Y., and Noguchi, K. (2002). Phosphorylation of extracellular signal-regulated kinase in primary afferent neurons by noxious stimuli and its involvement in peripheral sensitization. J Neurosci *22*, 7737-7745.

- Dasgupta, B., Li, W., Perry, A., and Gutmann, D. H. (2005). Glioma formation in neurofibromatosis 1 reflects preferential activation of K-RAS in astrocytes. Cancer Res *65*, 236-245.

- Daston, M. M., Scrable, H., Nordlund, M., Sturbaum, A. K., Nissen, L. M., and Ratner, N. (1992). The protein product of the neurofibromatosis type 1 gene is expressed at highest abundance in neurons, Schwann cells, and oligodendrocytes. Neuron *8*, 415-428.

- Datta, S. R., Dudek, H., Tao, X., Masters, S., Fu, H., Gotoh, Y., and Greenberg, M. E. (1997). Akt phosphorylation of BAD couples survival signals to the cell-intrinsic death machinery. Cell *91*, 231-241.

- Dib-Hajj, S., Black, J. A., Felts, P., and Waxman, S. G. (1996). Down-regulation of transcripts for Na channel alpha-SNS in spinal sensory neurons following axotomy. Proc Natl Acad Sci U S A *93*, 14950-14954.

- Dib-Hajj, S. D., Black, J. A., Cummins, T. R., Kenney, A. M., Kocsis, J. D., and Waxman, S. G. (1998). Rescue of alpha-SNS sodium channel expression in small dorsal root ganglion neurons after axotomy by nerve growth factor in vivo. J Neurophysiol *79*, 2668-2676.

- Dib-Hajj, S. D., Fjell, J., Cummins, T. R., Zheng, Z., Fried, K., LaMotte, R., Black, J. A., and Waxman, S. G. (1999). Plasticity of sodium channel expression in DRG neurons in the chronic constriction injury model of neuropathic pain. Pain *83*, 591-600.

- Djouhri, L., Dawbarn, D., Robertson, A., Newton, R., and Lawson, S. N. (2001). Time course and nerve growth factor dependence of inflammation-induced alterations in electrophysiological membrane properties in nociceptive primary afferent neurons. J Neurosci *21*, 8722-8733.

- Dobrowsky, R. T., Werner, M. H., Castellino, A. M., Chao, M. V., and Hannun, Y. A. (1994). Activation of the sphingomyelin cycle through the low-affinity neurotrophin receptor. Science *265*, 1596-1599.

- Eichler, M. E., and Rich, K. M. (1989). Death of sensory ganglion neurons after acute withdrawal of nerve growth factor in dissociated cell cultures. Brain Res *482*, 340-346.

- Elliott, A. A., and Elliott, J. R. (1993). Characterization of TTX-sensitive and TTX-resistant sodium currents in small cells from adult rat dorsal root ganglia. J Physiol *463*, 39-56.

- England, S., Bevan, S., and Docherty, R. J. (1996). PGE2 modulates the tetrodotoxin-resistant sodium current in neonatal rat dorsal root ganglion neurones via the cyclic AMP-protein kinase A cascade. J Physiol *495 (Pt 2)*, 429-440.

- Epa, W. R., Markovska, K., and Barrett, G. L. (2004). The p75 neurotrophin receptor enhances TrkA signalling by binding to Shc and augmenting its phosphorylation. J Neurochem *89*, 344-353.

- Esposito, D., Patel, P., Stephens, R. M., Perez, P., Chao, M. V., Kaplan, D. R., and Hempstead, B. L. (2001). The cytoplasmic and transmembrane domains of the p75 and Trk A receptors regulate high affinity binding to nerve growth factor. J Biol Chem *276*, 32687-32695.

- Estacion, M. (1990). Inhibition of voltage-dependent Na+ current in cell-fusion hybrids containing activated c-Ha-ras. J Membr Biol *113*, 169-175.

- Evans, A. R., Vasko, M. R., and Nicol, G. D. (1999). The cAMP transduction cascade mediates the PGE2-induced inhibition of potassium currents in rat sensory neurones. J Physiol *516 (Pt 1)*, 163-178.

- Ferreira, S. H., Nakamura, M., and de Abreu Castro, M. S. (1978). The hyperalgesic effects of prostacyclin and prostaglandin E2. Prostaglandins *16*, 31-37.

- Fitzgerald, E. M. (2000). Regulation of voltage-dependent calcium channels in rat sensory neurones involves a Ras-mitogen-activated protein kinase pathway. J Physiol *527 Pt 3*, 433-444.

- Fitzgerald, E. M., and Dolphin, A. C. (1997). Regulation of rat neuronal voltage-dependent calcium channels by endogenous p21-ras. Eur J Neurosci *9*, 1252-1261.

- Fjell, J., Cummins, T. R., Davis, B. M., Albers, K. M., Fried, K., Waxman, S. G., and Black, J. A. (1999a). Sodium channel expression in NGF-overexpressing transgenic mice. J Neurosci Res *57*, 39-47.

- Fjell, J., Cummins, T. R., Fried, K., Black, J. A., and Waxman, S. G. (1999b). In vivo NGF deprivation reduces SNS expression and TTX-R sodium currents in IB4-negative DRG neurons. J Neurophysiol *81*, 803-810.

- Galoyan, S. M., Petruska, J. C., and Mendell, L. M. (2003). Mechanisms of sensitization of the response of single dorsal root ganglion cells from adult rat to noxious heat. Eur J Neurosci *18*, 535-541.

- Ganju, P., O'Bryan, J. P., Der, C., Winter, J., and James, I. F. (1998). Differential regulation of SHC proteins by nerve growth factor in sensory neurons and PC12 cells. Eur J Neurosci *10*, 1995-2008.

- Gille, H., Sharrocks, A. D., and Shaw, P. E. (1992). Phosphorylation of transcription factor p62TCF by MAP kinase stimulates ternary complex formation at c-fos promoter. Nature *358*, 414-417.

- Giovannardi, S., Forlani, G., Balestrini, M., Bossi, E., Tonini, R., Sturani, E., Peres, A., and Zippel, R. (2002). Modulation of the inward rectifier potassium channel IRK1 by the Ras signaling pathway. J Biol Chem *277*, 12158-12163.

- Gold, M. S. (1999). Inflammatory mediator-induced modulation of TTX-R INa: an underlying mechanism of inflammatory hyperalgesia. Proc West Pharmacol Soc *42*, 111-112.

- Gold, M. S., and Flake, N. M. (2005). Inflammation-mediated hyperexcitability of sensory neurons. Neurosignals *14*, 147-157.

- Gold, M. S., Reichling, D. B., Shuster, M. J., and Levine, J. D. (1996a). Hyperalgesic agents increase a tetrodotoxin-resistant Na+ current in nociceptors. Proc Natl Acad Sci U S A *93*, 1108-1112.

- Gold, M. S., Shuster, M. J., and Levine, J. D. (1996b). Characterization of six voltage-gated K+ currents in adult rat sensory neurons. J Neurophysiol *75*, 2629-2646.

- Gold, M. S., Zhang, L., Wrigley, D. L., and Traub, R. J. (2002). Prostaglandin E(2) modulates TTX-R I(Na) in rat colonic sensory neurons. J Neurophysiol *88*, 1512-1522.

- Grewal, S. S., York, R. D., and Stork, P. J. (1999). Extracellular-signal-regulated kinase signalling in neurons. Curr Opin Neurobiol *9*, 544-553.

- Guha, A., Lau, N., Huvar, I., Gutmann, D., Provias, J., Pawson, T., and Boss, G. (1996). Ras-GTP levels are elevated in human NF1 peripheral nerve tumors. Oncogene *12*, 507-513.

- Guy, H. R., and Seetharamulu, P. (1986). Molecular model of the action potential sodium channel. Proc Natl Acad Sci U S A *83*, 508-512.

- Hamill, O. P., Marty, A., Neher, E., Sakmann, B., and Sigworth, F. J. (1981). Improved patch-clamp techniques for high-resolution current recording from cells and cell-free membrane patches. Pflugers Arch *391*, 85-100.

- Harper, A. A., and Lawson, S. N. (1985). Conduction velocity is related to morphological cell type in rat dorsal root ganglion neurones. J Physiol *359*, 31-46.

- Hawkins, R. D., Abrams, T. W., Carew, T. J., and Kandel, E. R. (1983). A cellular mechanism of classical conditioning in Aplysia: activity-dependent amplification of presynaptic facilitation. Science *219*, 400-405.

- Hida, H., Takeda, M., and Soliven, B. (1998). Ceramide inhibits inwardly rectifying K+ currents via a Ras- and Raf-1-dependent pathway in cultured oligodendrocytes. J Neurosci *18*, 8712-8719.

- Higgs, G. A., Moncada, S., and Vane, J. R. (1984). Eicosanoids in inflammation. Ann Clin Res *16*, 287-299.

- Hille, B. (2001). Ion Channels of Excitable Membranes

- Hingtgen, C. M., Roy, S. L., and Clapp, D. W. (2006). Stimulus-evoked release of neuropeptides is enhanced in sensory neurons from mice with a heterozygous mutation of the Nf1 gene. Neuroscience *137*, 637-645.

- Hingtgen, C. M., and Vasko, M. R. (1994). Prostacyclin enhances the evoked-release of substance P and calcitonin gene-related peptide from rat sensory neurons. Brain Res *655*, 51-60.

- Hodgkin, A. L., and B.Katz (1949). The effect of sodium ions on the electrical activity of the giant axon of the squid. . J Physiol (Lond) *108*, 37-77.

- Holzer, P. (1991). Capsaicin as a tool for studying sensory neuron functions. Adv Exp Med Biol *298*, 3-16.

- Hu, H. J., and Gereau, R. W. t. (2003). ERK integrates PKA and PKC signaling in superficial dorsal horn neurons. II. Modulation of neuronal excitability. J Neurophysiol *90*, 1680-1688.

- Hu, H. J., Glauner, K. S., and Gereau, R. W. t. (2003). ERK integrates PKA and PKC signaling in superficial dorsal horn neurons. I. Modulation of A-type K+ currents. J Neurophysiol *90*, 1671-1679.

- Huang, E. J., and Reichardt, L. F. (2003). Trk receptors: roles in neuronal signal transduction. Annu Rev Biochem *72*, 609-642.

- Hucho, T. B., Dina, O. A., and Levine, J. D. (2005). Epac mediates a cAMP-to-PKC signaling in inflammatory pain: an isolectin B4(+) neuron-specific mechanism. J Neurosci *25*, 6119-6126.

- Hwang, S. W., Cho, H., Kwak, J., Lee, S. Y., Kang, C. J., Jung, J., Cho, S., Min, K. H., Suh, Y. G., Kim, D., and Oh, U. (2000). Direct activation of capsaicin receptors by products of lipoxygenases: endogenous capsaicin-like substances. Proc Natl Acad Sci U S A *97*, 6155-6160.

- Ingram, D. A., Hiatt, K., King, A. J., Fisher, L., Shivakumar, R., Derstine, C., Wenning, M. J., Diaz, B., Travers, J. B., Hood, A., et al. (2001). Hyperactivation of p21(ras) and the hematopoietic-specific Rho GTPase, Rac2, cooperate to alter the proliferation of neurofibromin-deficient mast cells in vivo and in vitro. J Exp Med *194*, 57-69.

- Isacoff, E. Y., Jan, Y. N., and Jan, L. Y. (1990). Evidence for the formation of heteromultimeric potassium channels in Xenopus oocytes. Nature *345*, 530-534.

- Isom, L. L. (2001). Sodium channel beta subunits: anything but auxiliary. Neuroscientist *7*, 42-54.

- Izawa, I., Tamaki, N., and Saya, H. (1996). Phosphorylation of neurofibromatosis type 1 gene product (neurofibromin) by cAMP-dependent protein kinase. FEBS Lett *382*, 53-59.

- Jacks, T., Shih, T. S., Schmitt, E. M., Bronson, R. T., Bernards, A., and Weinberg, R. A. (1994). Tumour predisposition in mice heterozygous for a targeted mutation in Nf1. Nat Genet *7*, 353-361.

- Jeftinija, S. (1994). Bradykinin excites tetrodotoxin-resistant primary afferent fibers. Brain Res *665*, 69-76.

- Ji, R. R., Samad, T. A., Jin, S. X., Schmoll, R., and Woolf, C. J. (2002). p38 MAPK activation by NGF in primary sensory neurons after inflammation increases TRPV1 levels and maintains heat hyperalgesia. Neuron *36*, 57-68.

- Jin, X., and Gereau, R. W. t. (2006). Acute p38-mediated modulation of tetrodotoxin-resistant sodium channels in mouse sensory neurons by tumor necrosis factor-alpha. J Neurosci *26*, 246-255.

- Johnson, E. M., Jr., Osborne, P. A., and Taniuchi, M. (1989). Destruction of sympathetic and sensory neurons in the developing rat by a monoclonal antibody against the nerve growth factor (NGF) receptor. Brain Res *478*, 166-170.

- Kaplan, D. R., and Stephens, R. M. (1994). Neurotrophin signal transduction by the Trk receptor. J Neurobiol *25*, 1404-1417.

- Karim, F., Hu, H. J., Adwanikar, H., Kaplan, D. R., and Gereau, R. W. t. (2006). Impaired Inflammatory Pain and Thermal Hyperalgesia in Mice Expressing Neuron-Specific Dominant Negative Mitogen Activated Protein Kinase Kinase (MEK). Mol Pain *2*, 2.

- Katz, E. J., and Gold, M. S. (2006). Inflammatory hyperalgesia: a role for the C-fiber sensory neuron cell body? J Pain *7*, 170-178.

- Kawamura, M., Kuraishi, Y., Minami, M., and Satoh, M. (1989). Antinociceptive effect of intrathecally administered antiserum against calcitonin gene-related peptide on thermal and mechanical noxious stimuli in experimental hyperalgesic rats. Brain Res *497*, 199-203.

- Kim, U. H., Fink, D., Jr., Kim, H. S., Park, D. J., Contreras, M. L., Guroff, G., and Rhee, S. G. (1991). Nerve growth factor stimulates phosphorylation of phospholipase C-gamma in PC12 cells. J Biol Chem *266*, 1359-1362.

- Kirstein, M., and Farinas, I. (2002). Sensing life: regulation of sensory neuron survival by neurotrophins. Cell Mol Life Sci *59*, 1787-1802.

- Klesse, L. J., and Parada, L. F. (1998). p21 ras and phosphatidylinositol-3 kinase are required for survival of wild-type and NF1 mutant sensory neurons. J Neurosci *18*, 10420-10428.

- Kostyuk, P. G., Veselovsky, N. S., and Tsyndrenko, A. Y. (1981). Ionic currents in the somatic membrane of rat dorsal root ganglion neurons-I. Sodium currents. Neuroscience *6*, 2423-2430.

- Kwong, K., and Lee, L. Y. (2005). Prostaglandin E2 potentiates a TTX-resistant sodium current in rat capsaicin-sensitive vagal pulmonary sensory neurones. J Physiol *564*, 437-450.

- Lai, J., Gold, M. S., Kim, C. S., Bian, D., Ossipov, M. H., Hunter, J. C., and Porreca, F. (2002). Inhibition of neuropathic pain by decreased expression of the tetrodotoxin-resistant sodium channel, NaV1.8. Pain *95*, 143-152.

- Lakkis, M. M., and Tennekoon, G. I. (2000). Neurofibromatosis type 1. I. General overview. J Neurosci Res *62*, 755-763.

- Largaespada, D. A., Brannan, C. I., Jenkins, N. A., and Copeland, N. G. (1996). Nf1 deficiency causes Ras-mediated granulocyte/macrophage colony stimulating factor hypersensitivity and chronic myeloid leukaemia. Nat Genet *12*, 137-143.

- Le Good, J. A., Ziegler, W. H., Parekh, D. B., Alessi, D. R., Cohen, P., and Parker, P. J. (1998). Protein kinase C isotypes controlled by phosphoinositide 3-kinase through the protein kinase PDK1. Science *281*, 2042-2045.

- Lee, S. B., and Rhee, S. G. (1995). Significance of PIP2 hydrolysis and regulation of phospholipase C isozymes. Curr Opin Cell Biol *7*, 183-189.

- Lee, Y., Takami, K., Kawai, Y., Girgis, S., Hillyard, C. J., MacIntyre, I., Emson, P. C., and Tohyama, M. (1985). Distribution of calcitonin gene-related peptide in the rat peripheral nervous system with reference to its coexistence with substance P. Neuroscience *15*, 1227-1237.

- Leffler, A., Cummins, T. R., Dib-Hajj, S. D., Hormuzdiar, W. N., Black, J. A., and Waxman, S. G. (2002). GDNF and NGF reverse changes in repriming of TTX-sensitive Na(+) currents following axotomy of dorsal root ganglion neurons. J Neurophysiol *88*, 650-658.

- Lei, S., Dryden, W. F., and Smith, P. A. (2001). Nerve growth factor regulates sodium but not potassium channel currents in sympathetic B neurons of adult bullfrogs. J Neurophysiol *86*, 641-650.

- Leuchtag, H. R. (1994). Long-range interactions, voltage sensitivity, and ion conduction in S4 segments of excitable channels. Biophys J *66*, 217-224.

- Levi-Montalcini, R. (1952). Effects of mouse tumor transplantation on the nervous system. Ann N Y Acad Sci *55*, 330-344.

- Levi-Montalcini, R., and Hamburger, V. (1951). Selective growth stimulating effects of mouse sarcoma on the sensory and sympathetic nervous system of the chick embryo. J Exp Zool *116*, 321-361.

- Lewin, G. R., and Mendell, L. M. (1993). Nerve growth factor and nociception. Trends Neurosci *16*, 353-359.

- Lewin, G. R., Ritter, A. M., and Mendell, L. M. (1993). Nerve growth factor-induced hyperalgesia in the neonatal and adult rat. J Neurosci *13*, 2136-2148.

- Li, J., McRoberts, J. A., Ennes, H. S., Trevisani, M., Nicoletti, P., Mittal, Y., and Mayer, E. A. (2006). Experimental colitis modulates the functional properties of NMDA receptors in dorsal root ganglia neurons. Am J Physiol Gastrointest Liver Physiol.

- Li, Y., Bollag, G., Clark, R., Stevens, J., Conroy, L., Fults, D., Ward, K., Friedman, E., Samowitz, W., Robertson, M., and et al. (1992). Somatic mutations in the neurofibromatosis 1 gene in human tumors. Cell *69*, 275-281.

- Liman, E. R., Hess, P., Weaver, F., and Koren, G. (1991). Voltage-sensing residues in the S4 region of a mammalian K+ channel. Nature *353*, 752-756.

- Lindsay, R. M. (1988). Nerve growth factors (NGF, BDNF) enhance axonal regeneration but are not required for survival of adult sensory neurons. J Neurosci *8*, 2394-2405.

- Linhart, O., Obreja, O., and Kress, M. (2003). The inflammatory mediators serotonin, prostaglandin E2 and bradykinin evoke calcium influx in rat sensory neurons. Neuroscience *118*, 69-74.

- Liu, C. N., Raber, P., Ziv-Sefer, S., and Devor, M. (2001). Hyperexcitability in sensory neurons of rats selected for high versus low neuropathic pain phenotype. Neuroscience *105*, 265-275.

- Long, S. B., Campbell, E. B., and Mackinnon, R. (2005). Crystal structure of a mammalian voltage-dependent Shaker family K+ channel. Science *309*, 897-903.

- Lopshire, J. C., and Nicol, G. D. (1998). The cAMP transduction cascade mediates the prostaglandin E2 enhancement of the capsaicin-elicited current in rat sensory neurons: whole-cell and single-channel studies. J Neurosci *18*, 6081-6092.

- MacKinnon, R. (1991a). Determination of the subunit stoichiometry of a voltage-activated potassium channel. Nature *350*, 232-235.

- MacKinnon, R. (1991b). New insights into the structure and function of potassium channels. Curr Opin Neurobiol *1*, 14-19.

- Magistretti, J., Mantegazza, M., Guatteo, E., and Wanke, E. (1996). Action potentials recorded with patch-clamp amplifiers: are they genuine? Trends Neurosci *19*, 530-534.

- Malcangio, M., Garrett, N. E., and Tomlinson, D. R. (1997). Nerve growth factor treatment increases stimulus-evoked release of sensory neuropeptides in the rat spinal cord. Eur J Neurosci *9*, 1101-1104.

- Mandelzys, A., Cooper, E., Verge, V. M., and Richardson, P. M. (1990). Nerve growth factor induces functional nicotinic acetylcholine receptors on rat sensory neurons in culture. Neuroscience *37*, 523-530.

- Mangoura, D., Sun, Y., Li, C., Singh, D., Gutmann, D. H., Flores, A., Ahmed, M., and Vallianatos, G. (2006). Phosphorylation of neurofibromin by PKC is a possible molecular switch in EGF receptor signaling in neural cells. Oncogene *25*, 735-745.

- Marshall, C. J. (1995). Specificity of receptor tyrosine kinase signaling: transient versus sustained extracellular signal-regulated kinase activation. Cell *80*, 179-185.

- Martin, G. A., Viskochil, D., Bollag, G., McCabe, P. C., Crosier, W. J., Haubruck, H., Conroy, L., Clark, R., O'Connell, P., Cawthon, R. M., and et al. (1990). The GAP-related domain of the neurofibromatosis type 1 gene product interacts with ras p21. Cell *63*, 843-849.

- Marzella, P. L., and Gillespie, L. N. (2002). Role of trophic factors in the development, survival and repair of primary auditory neurons. Clin Exp Pharmacol Physiol *29*, 363-371.

- McCarthy, P. W., and Lawson, S. N. (1990). Cell type and conduction velocity of rat primary sensory neurons with calcitonin gene-related peptide-like immunoreactivity. Neuroscience *34*, 623-632.

- McFarlane, S., and Cooper, E. (1991). Kinetics and voltage dependence of A-type currents on neonatal rat sensory neurons. J Neurophysiol *66*, 1380-1391.

- McMahon, S. B., Bennett, D. L., Priestley, J. V., and Shelton, D. L. (1995). The biological effects of endogenous nerve growth factor on adult sensory neurons revealed by a trkA-IgG fusion molecule. Nat Med *1*, 774-780.

- Meakin, S. O., and Shooter, E. M. (1992). The nerve growth factor family of receptors. Trends Neurosci *15*, 323-331.

- Meunier, F. A., Colasante, C., and Molgo, J. (1997). Sodium-dependent increase in quantal secretion induced by brevetoxin-3 in Ca2+-free medium is associated with depletion of synaptic vesicles and swelling of motor nerve terminals in situ. Neuroscience *78*, 883-893.

- Molliver, D. C., Wright, D. E., Leitner, M. L., Parsadanian, A. S., Doster, K., Wen, D., Yan, Q., and Snider, W. D. (1997). IB4-binding DRG neurons switch from NGF to GDNF dependence in early postnatal life. Neuron *19*, 849-861.

- Neher, E., and Sakmann, B. (1976). Single-channel currents recorded from membrane of denervated frog muscle fibres. Nature *260*, 799-802.

- Neumcke, B. (1990). Diversity of sodium channels in adult and cultured cells, in oocytes and in lipid bilayers. Rev Physiol Biochem Pharmacol *115*, 1-49.

- Nicol, G. D., and Cui, M. (1994). Enhancement by prostaglandin E2 of bradykinin activation of embryonic rat sensory neurones. J Physiol *480 (Pt 3)*, 485-492.

- Nicol, G. D., Vasko, M. R., and Evans, A. R. (1997). Prostaglandins suppress an outward potassium current in embryonic rat sensory neurons. J Neurophysiol *77*, 167-176.

- Noda, M., Shimizu, S., Tanabe, T., Takai, T., Kayano, T., Ikeda, T., Takahashi, H., Nakayama, H., Kanaoka, Y., Minamino, N., and et al. (1984). Primary structure of Electrophorus electricus sodium channel deduced from cDNA sequence. Nature *312*, 121-127.

- Park, S. Y., Choi, J. Y., Kim, R. U., Lee, Y. S., Cho, H. J., and Kim, D. S. (2003). Downregulation of voltage-gated potassium channel alpha gene expression by axotomy and neurotrophins in rat dorsal root ganglia. Mol Cells *16*, 256-259.

- Philpott, K. L., McCarthy, M. J., Klippel, A., and Rubin, L. L. (1997). Activated phosphatidylinositol 3-kinase and Akt kinase promote survival of superior cervical neurons. J Cell Biol *139*, 809-815.

- Pusch, M., and Neher, E. (1988). Rates of diffusional exchange between small cells and a measuring patch pipette. Pflugers Arch *411*, 204-211.

- Rhee, S. G., and Choi, K. D. (1992). Multiple forms of phospholipase C isozymes and their activation mechanisms. Adv Second Messenger Phosphoprotein Res *26*, 35-61.

- Rizzo, M. A., Kocsis, J. D., and Waxman, S. G. (1995). Selective loss of slow and enhancement of fast Na+ currents in cutaneous afferent dorsal root ganglion neurones following axotomy. Neurobiol Dis *2*, 87-96.

- Rodriguez-Viciana, P., Warne, P. H., Vanhaesebroeck, B., Waterfield, M. D., and Downward, J. (1996). Activation of phosphoinositide 3-kinase by interaction with Ras and by point mutation. Embo J *15*, 2442-2451.

- Roy, M. L., and Narahashi, T. (1992). Differential properties of tetrodotoxin-sensitive and tetrodotoxin-resistant sodium channels in rat dorsal root ganglion neurons. J Neurosci *12*, 2104-2111.

- Rudy, B., Kirschenbaum, B., Rukenstein, A., and Greene, L. A. (1987). Nerve growth factor increases the number of functional Na channels and induces TTX-resistant Na channels in PC12 pheochromocytoma cells. J Neurosci *7*, 1613-1625.

- Rush, A. M., and Waxman, S. G. (2004). PGE2 increases the tetrodotoxin-resistant Nav1.9 sodium current in mouse DRG neurons via G-proteins. Brain Res *1023*, 264-271.

- Saab, C. Y., Cummins, T. R., and Waxman, S. G. (2003). GTP gamma S increases Nav1.8 current in small-diameter dorsal root ganglia neurons. Exp Brain Res *152*, 415-419.

- Salvarezza, S. B., Lopez, H. S., and Masco, D. H. (2003). The same cellular signaling pathways mediate survival in sensory neurons that switch their trophic requirements during development. J Neurochem *85*, 1347-1358.

- Samuelsson, B. (1972). The synthesis and biological role of prostaglandins. Biochem J *128*, 4P.

- Schlessinger, J. (1993). How receptor tyrosine kinases activate Ras. Trends Biochem Sci *18*, 273-275.

- Schrader, L. A., Birnbaum, S. G., Nadin, B. M., Ren, Y., Bui, D., Anderson, A. E., and Sweatt, J. D. (2006). ERK/MAPK regulates the Kv4.2 potassium channel by direct phosphorylation of the pore-forming subunit. Am J Physiol Cell Physiol *290*, C852-861.

- Sharma, N., D'Arcangelo, G., Kleinlaus, A., Halegoua, S., and Trimmer, J. S. (1993). Nerve growth factor regulates the abundance and distribution of K+ channels in PC12 cells. J Cell Biol *123*, 1835-1843.

- Sherman, L. S., Atit, R., Rosenbaum, T., Cox, A. D., and Ratner, N. (2000). Single cell Ras-GTP analysis reveals altered Ras activity in a subpopulation of neurofibroma Schwann cells but not fibroblasts. J Biol Chem *275*, 30740-30745.

- Shieh, C.-C., Coghlan, M., Sullivan, J. P., and Gopalakrishnan, M. (2000). Potassium Channels: Molecular Defects, Diseases, and Therapeutic Opportunities. Pharmacol Rev *52*, 557-594.

- Shu, X., and Mendell, L. M. (1999). Nerve growth factor acutely sensitizes the response of adult rat sensory neurons to capsaicin. Neurosci Lett *274*, 159-162.

- Sigal, I. S., Gibbs, J. B., D'Alonzo, J. S., and Scolnick, E. M. (1986). Identification of effector residues and a neutralizing epitope of Ha-ras-encoded p21. Proc Natl Acad Sci U S A *83*, 4725-4729.

- Sleeper, A. A., Cummins, T. R., Dib-Hajj, S. D., Hormuzdiar, W., Tyrrell, L., Waxman, S. G., and Black, J. A. (2000). Changes in expression of two tetrodotoxin-resistant sodium channels and their currents in dorsal root ganglion neurons after sciatic nerve injury but not rhizotomy. J Neurosci *20*, 7279-7289.

- Smith, C. A., Farrah, T., and Goodwin, R. G. (1994). The TNF receptor superfamily of cellular and viral proteins: activation, costimulation, and death. Cell *76*, 959-962.

- Souza, A. L., Moreira, F. A., Almeida, K. R., Bertollo, C. M., Costa, K. A., and Coelho, M. M. (2002). In vivo evidence for a role of protein kinase C in peripheral nociceptive processing. Br J Pharmacol *135*, 239-247.

- Stucky, C. L., and Lewin, G. R. (1999). Isolectin B(4)-positive and -negative nociceptors are functionally distinct. J Neurosci *19*, 6497-6505.

- Stuhmer, W., Ruppersberg, J. P., Schroter, K. H., Sakmann, B., Stocker, M., Giese, K. P., Perschke, A., Baumann, A., and Pongs, O. (1989). Molecular basis of functional diversity of voltage-gated potassium channels in mammalian brain. Embo J *8*, 3235-3244.

- Susen, K., Heumann, R., and Blochl, A. (1999). Nerve growth factor stimulates MAPK via the low affinity receptor p75(LNTR). FEBS Lett *463*, 231-234.

- Taiwo, Y. O., Bjerknes, L. K., Goetzl, E. J., and Levine, J. D. (1989). Mediation of primary afferent peripheral hyperalgesia by the cAMP second messenger system. Neuroscience *32*, 577-580.

- Tanaka, M., Cummins, T. R., Ishikawa, K., Dib-Hajj, S. D., Black, J. A., and Waxman, S. G. (1998). SNS Na+ channel expression increases in dorsal root ganglion neurons in the carrageenan inflammatory pain model. Neuroreport *9*, 967-972.

- The, I., Hannigan, G. E., Cowley, G. S., Reginald, S., Zhong, Y., Gusella, J. F., Hariharan, I. K., and Bernards, A. (1997). Rescue of a Drosophila NF1 mutant phenotype by protein kinase A. Science *276*, 791-794.

- Tokuo, H., Yunoue, S., Feng, L., Kimoto, M., Tsuji, H., Ono, T., Saya, H., and Araki, N. (2001). Phosphorylation of neurofibromin by cAMP-dependent protein kinase is regulated via a cellular association of N(G),N(G)-dimethylarginine dimethylaminohydrolase. FEBS Lett *494*, 48-53.

- Toledo-Aral, J. J., Brehm, P., Halegoua, S., and Mandel, G. (1995). A single pulse of nerve growth factor triggers long-term neuronal excitability through sodium channel gene induction. Neuron *14*, 607-611.

- Trovo-Marqui, A. B., Goloni-Bertollo, E. M., Valerio, N. I., Pavarino-Bertelli, E. C., Muniz, M. P., Teixeira, M. F., Antonio, J. R., and Tajara, E. H. (2005). High frequencies of plexiform neurofibromas, mental retardation, learning difficulties, and scoliosis in Brazilian patients with neurofibromatosis type 1. Braz J Med Biol Res *38*, 1441-1447.

- Twiss, J. L., Wada, H. G., Fok, K. S., Chan, S. D., Verity, A. N., Baxter, G. T., Shooter, E. M., and Sussman, H. H. (1998). Duration and magnitude of nerve growth factor signaling depend on the ratio of p75LNTR to TrkA. J Neurosci Res *51*, 442-453.

- Tytgat, J., Nakazawa, K., Gross, A., and Hess, P. (1993). Pursuing the voltage sensor of a voltage-gated mammalian potassium channel. J Biol Chem *268*, 23777-23779.

- Vellani, V., Mapplebeck, S., Moriondo, A., Davis, J. B., and McNaughton, P. A. (2001). Protein kinase C activation potentiates gating of the vanilloid receptor VR1 by capsaicin, protons, heat and anandamide. J Physiol *534*, 813-825.

- Vetter, M. L., Martin-Zanca, D., Parada, L. F., Bishop, J. M., and Kaplan, D. R. (1991). Nerve growth factor rapidly stimulates tyrosine phosphorylation of phospholipase C-gamma 1 by a kinase activity associated with the product of the trk protooncogene. Proc Natl Acad Sci U S A *88*, 5650-5654.

- Vogel, K. S., Brannan, C. I., Jenkins, N. A., Copeland, N. G., and Parada, L. F. (1995). Loss of neurofibromin results in neurotrophin-independent survival of embryonic sensory and sympathetic neurons. Cell *82*, 733-742.

- Vogel, K. S., El-Afandi, M., and Parada, L. F. (2000). Neurofibromin negatively regulates neurotrophin signaling through p21ras in embryonic sensory neurons. Mol Cell Neurosci *15*, 398-407.

- Wallace, M. R., Marchuk, D. A., Andersen, L. B., Letcher, R., Odeh, H. M., Saulino, A. M., Fountain, J. W., Brereton, A., Nicholson, J., Mitchell, A. L., and et al. (1990). Type 1 neurofibromatosis gene: identification of a large transcript disrupted in three NF1 patients. Science *249*, 181-186.

- Wang, Y., Nicol, G. D., Clapp, D. W., and Hingtgen, C. M. (2005). Sensory neurons from Nf1 haploinsufficient mice exhibit increased excitability. J Neurophysiol *94*, 3670-3676.

- Waxman, S. G., Cummins, T. R., Dib-Hajj, S., Fjell, J., and Black, J. A. (1999). Sodium channels, excitability of primary sensory neurons, and the molecular basis of pain. Muscle Nerve *22*, 1177-1187.

- Waxman, S. G., Kocsis, J. D., and Black, J. A. (1994). Type III sodium channel mRNA is expressed in embryonic but not adult spinal sensory neurons, and is reexpressed following axotomy. J Neurophysiol *72*, 466-470.

- Wei, A., Covarrubias, M., Butler, A., Baker, K., Pak, M., and Salkoff, L. (1990). K+ current diversity is produced by an extended gene family conserved in Drosophila and mouse. Science *248*, 599-603.

- Willis, A. L., and Cornelsen, M. (1973). Repeated injection of prostaglandin E2 in rat paws induces chronic swelling and a marked decrease in pain threshold. Prostaglandins *3*, 353-357.

- Wolkenstein, P., Zeller, J., Revuz, J., Ecosse, E., and Leplege, A. (2001). Quality-of-life impairment in neurofibromatosis type 1: a cross-sectional study of 128 cases. Arch Dermatol *137*, 1421-1425.

- Wood, J. N., Boorman, J. P., Okuse, K., and Baker, M. D. (2004). Voltage-gated sodium channels and pain pathways. J Neurobiol *61*, 55-71.

- Woodbury, C. J., Zwick, M., Wang, S., Lawson, J. J., Caterina, M. J., Koltzenburg, M., Albers, K. M., Koerber, H. R., and Davis, B. M. (2004). Nociceptors lacking TRPV1 and TRPV2 have normal heat responses. J Neurosci *24*, 6410-6415.

- Woolf, C. J., Safieh-Garabedian, B., Ma, Q. P., Crilly, P., and Winter, J. (1994). Nerve growth factor contributes to the generation of inflammatory sensory hypersensitivity. Neuroscience *62*, 327-331.

- Yang, N., and Horn, R. (1995). Evidence for voltage-dependent S4 movement in sodium channels. Neuron *15*, 213-218.

- Yoon, S. O., Casaccia-Bonnefil, P., Carter, B., and Chao, M. V. (1998). Competitive signaling between TrkA and p75 nerve growth factor receptors determines cell survival. J Neurosci *18*, 3273-3281.

- Yu, F. H., and Catterall, W. A. (2003). Overview of the voltage-gated sodium channel family. Genome Biol *4*, 207.

- Yuan, J., and Yankner, B. A. (2000). Apoptosis in the nervous system. Nature *407*, 802-809.

- Zhang, X., Huang, J., and McNaughton, P. A. (2005). NGF rapidly increases membrane expression of TRPV1 heat-gated ion channels. Embo J *24*, 4211-4223.

- Zhang, Y., Fehrenbacher, J. C., Vasko, M. R., and Nicol, G. D. (2006a). Sphingosine-1-phosphate via activation of a G protein-coupled receptor(s) enhances the excitability of rat sensory neurons. J Neurophysiol.

- Zhang, Y. H., and Nicol, G. D. (2004). NGF-mediated sensitization of the excitability of rat sensory neurons is prevented by a blocking antibody to the p75 neurotrophin receptor. Neurosci Lett *366*, 187-192.

- Zhang, Y. H., Vasko, M. R., and Nicol, G. D. (2002). Ceramide, a putative second messenger for nerve growth factor, modulates the TTX-resistant Na(+) current and delayed rectifier K(+) current in rat sensory neurons. J Physiol *544*, 385-402.

- Zhang, Y. H., Vasko, M. R., and Nicol, G. D. (2006b). Intracellular sphingosine 1-phosphate mediates the increased excitability produced by nerve growth factor in rat sensory neurons. J Physiol *575*, 101-113.

- Zhou, Y., Zhou, Z. S., and Zhao, Z. Q. (2001). PKC regulates capsaicin-induced currents of dorsal root ganglion neurons in rats. Neuropharmacology *41*, 601-608.

- Zhou, Z., Davar, G., and Strichartz, G. (2002). Endothelin-1 (ET-1) selectively enhances the activation gating of slowly inactivating tetrodotoxin-resistant sodium currents in rat sensory neurons: a mechanism for the pain-inducing actions of ET-1. J Neurosci *22*, 6325-6330.

- Zhuang, Z. Y., Gerner, P., Woolf, C. J., and Ji, R. R. (2005). ERK is sequentially activated in neurons, microglia, and astrocytes by spinal nerve ligation and contributes to mechanical allodynia in this neuropathic pain model. Pain *114*, 149-159.

- Zhuang, Z. Y., Xu, H., Clapham, D. E., and Ji, R. R. (2004). Phosphatidylinositol 3-kinase activates ERK in primary sensory neurons and mediates inflammatory heat hyperalgesia through TRPV1 sensitization. J Neurosci *24*, 8300-8309.

- Zur, K. B., Oh, Y., Waxman, S. G., and Black, J. A. (1995). Differential up-regulation of sodium channel alpha- and beta 1-subunit mRNAs in cultured embryonic DRG neurons following exposure to NGF. Brain Res Mol Brain Res *30*, 97-105.

CURRICULUM VITAE

NAME: Yue Wang

EDUCATION

- 2001-current
  Indiana University, Indianapolis, Indiana
  Department of Pharmacology and Toxicology
  Doctor of Philosophy

- 1997.9-2000.7
  Harbin Medical University, Harbin, China
  Pharmacology Department
  Master of Pharmacology

- 1991.9-1994.7
  Harbin Medical University, Harbin, China
  Department of Clinical Medicine
  Associates of Clinical Medicine

PROFESSIONAL MEMBERSHIPS

- **Society for Neuroscience**

PUBLICATIONS

1. Wang,Y.; Hingtgen, C. M.; Nicol, G. D., Augmented sodium currents contribute to the enhanced excitability of sensory neurons in *Nf1+/-* mice. Society for Neuroscience 2006 Annual Meeting, 245.8 (Atlanta, GA. 2006).

2. Wang, Y.; Nicol, G. D.; Clapp, D. W.; Hingtgen, C. M., Sensory neurons from *Nf1* haploinsufficient mice exhibit increased excitability. Journal of Neurophysiology, 94(6):3670-6 (2005).

3. Wang, Y.; Roy, S.L.; Nicol, G.D.; Hingtgen, C.M., Sensory neurons from *Nf1* heterozygous mutant mice exhibit increased excitability and capsaicin-evoked release of neuropeptide. Society for Neuroscience 2004 Annual Meeting, 290.20 (San Diego, CA, 2004).

4. Liu, Y.; Wang, Y.; Ma, M. L.; Zhang, Y.; Li, H. W.; Chen, Q. W. and Yang, B. F., Cardiac-hemodynamic effects of M3 receptor agonist on rat and rabbit hearts, Yao Xue Xue Bao, 36:84-87 (2001).

5. Ai,J.; Gao H.; Wang, Y.; Liu, Y.; He, S.; Yang, B. F., The effect of matrine on the intracellular calcium concentration of freshly isolated ventricular myocytes from guinea pig. Transaction of Harbin Medical University, 34(4): 235-236 (2000).

6. Xing, Y.; Wang, Y., Quality research on indigenous reagent for primary screening testing the HIV antidody. Commenorative Transactions for the 10 Years Promulgation of the Frontier Sanitation Quarantine Law by the People's Republic of China, People's Sanitation Press, 12:5-7 (1996).

HONORS & SCHOLARSHIPS

1. **Academic Scholarship,** Department of Pharmacology and Toxicology Scholarship for supporting the research of graduate student, 07/01/2005-11/30/2006.

2. **Annual Direct Award**, Agency: NIH. Supplement to 5R01CA074177-07, the research project title is: *Nf1+/-* Mast Cells Promote Inflammation and Angiogenesis. (Section PI, Hingtgen, Overall PI, DW Clapp). This study is collaboration of investigators studying the actions of *Nf1* haploinsufficient mast cells on other cell types. The aims of Dr. Hingtgen's section are to investigate the effects of *Nf1* haploinsufficient mast cells on sensory neuron excitability. My role: as a graduate student, my goal in this project is to study the excitability of sensory neurons from wild type or Nf1 heterozygous mice. 07/01/2003-06/30/2005.

3. **Academic Scholarship,** Department of Pharmacology and Toxicology Scholarship for supporting the research of graduate student, 07/01/2002-06/30/2003.

4. **IUPUI Graduate Fellowship.** Indiana University School of Medicine, 07/01/2001-06/30/2002.

5. **Academic Scholarship.** Department of Pharmacology and Toxicology Scholarship for supporting the research of graduate student, 11/01/2000-07/01/2001.

6. **HMU Scholarship**, Harbin Medical university, 1992, 1993, 1994.

7. **HMU Outstanding Student**, Harbin Medical University, 1991, 1992, 1993, 1994.